UNIVERSITY OF SOUTHAMPTON

HEAD AND HELMET MOTION DURING RUNNING, JUMPING AND EXPOSURE TO WHOLE-BODY VIBRATION

M REUBEN PECKHAM

MASTER OF PHILOSOPHY

FACULTY OF ENGINEERING AND APPLIED SCIENCE
INSTITUTE OF SOUND AND VIBRATION RESEARCH

MARCH 2000

UNIVERSITY OF SOUTHAMPTON

ABSTRACT

FACULTY OF ENGINEERING AND APPLIED SCIENCE
INSTITUTE OF SOUND AND VIBRATION RESEARCH

Master of Philosophy

HEAD AND HELMET MOTION DURING RUNNING, JUMPING AND EXPOSURE TO WHOLE-BODY VIBRATION

by M Reuben Peckham

An understanding of the mechanical responses of the head and helmet is important to minimise adverse effects of helmet motion on health and comfort. Little is known of the interaction between head and helmet when running or jumping and during exposure to whole-body vibration. This study was conducted to investigate the frequency, magnitude and dominant directions of motion occurring at the head and helmet under these conditions and to gain an understanding of the mechanical relationship between head and helmet based upon their modal characteristics.

Three experiments were conducted to measure the frequency response of the head and helmet whilst running, jumping and during exposure to whole-body vibration. The experiments showed that both translational and rotational motion of the head and helmet can occur whilst running or jumping and when exposed to whole-body vibration, with the dominant motion occurring in the mid-sagittal plane. When running and jumping the greatest amount of motion, in all directions of motion, occurred at the excitation frequency. In these conditions the head and helmet moved together in the vertical direction at the excitation frequencies. In the fore-aft direction relative motion was observed between head and helmet at the excitation frequencies when running and jumping.

The effect of helmet mass and distribution of mass on the helmet was investigated during exposure to whole-body vibration. The study showed that at frequencies between 3 and 5 Hz motion of the head was reduced when a helmet was placed on the head. This occurred in all directions of motion in the mid-sagittal plane. Seat-to-head transmissibilities, in all directions, decreased further as helmet mass increased. The seat-to-head transmissibility was also influenced by the distribution of mass on the helmet. Seat-to-head fore-aft and vertical transmissibilities decreased as additional helmet mass was moved lower and further forward on the helmet.

An experimental modal analysis identified three modes of vibration of the neck-head system and four modes of vibration of the neck-head-helmet system. A finite element lumped parameter model of the neck-head-helmet system was also developed and predicted the four dominant mode shapes that were obtained in the experimental modal analysis.

The variability in seat-to-head and seat-to-helmet transmissibilities was thought to be attributable to resonance behaviour of the system. The extra mode of vibration obtained in the neck-head-helmet system was a pitch mode of the helmet on the head. Its natural frequency was controlled by helmet mass and the stiffness of the skin coupling at the fore-head. This implies that this mode was an independent mode of the helmet on the head.

CONTENTS

ACKNOWLEDGEMENTS

This research was sponsored by the Defence Clothing and Textiles Authority, Colchester, England.

I would like to express my deepest gratitude to Professor Mike Griffin for his support, encouragement and unwavering advice during the production of this thesis.

I would also like to thank other ex-colleagues and friends at the Human Factors Research Unit, particularly Dr. Chris Lewis, Dr. Gurmail Paddan, Dr. Neil Mansfield, Mr. Colin Littler and Mr. Gary Parker.

I must express thanks to my subjects for participating in the experiments. Without them this work could not have gone ahead.

Finally I would like to thank my partner, Nicola Collings, not just for spending three-and-a half weeks out of the country this Summer which enabled me to proceed with this thesis without distraction but also for her support and encouragement over the last two years!

LIST OF SYMBOLS

A_{x1}	*acceleration in the fore-aft direction at point 1*
r_x	roll acceleration
r_y	pitch acceleration
r_z	yaw acceleration
d_y	displacement in the y axis
T1	1^{ST} thoracic vertebra
Z..	acceleration in vertical direction
x..	acceleration in fore-aft direction
y..	acceleration in lateral direction
C1	1^{st} cervical vertebra
L1	1^{st} Lumbar vertebra
$Ktheta_n$	Rotational spring stiffness
K_n	Translation spring stiffness

CHAPTER 1 INTRODUCTION

Helmets are worn by a varied cross-section of the community as they go about their daily lives. The helmeted schoolboy on his pedal cycle, the racing driver and the motorcyclist are common everyday sights.

In the future, technological developments may increase the use of helmet-mounted displays and other helmet attachments. The performance of a helmet-mounted visual display is limited by the relative motion between head and helmet (Wells and Griffin, 1984). The need for extra attachments to the helmet will invariably increase the helmet mass which could increase the relative motion between head and helmet (Woodman, 1995a).

In the battlefield, combat helmets are worn for long periods of time in a variety of dynamic situations. These include walking, running, jumping and riding in vehicles. It would be desirable to learn more about the relative motion between head and helmet, how the helmet moves on the head and how head motion is affected by the presence of a helmet under dynamic conditions. This would enable the helmet designer to develop a helmet with additional life support aids and an effective head-up display without causing discomfort to the user due to additional helmet mass or excessive relative motion between head and helmet. Understanding the dynamic response of the human head and helmet system will also help in avoiding spinal injuries by providing helmet designers with the necessary information to design a helmet which is optimised to provide the minimum amount of relative motion with an appropriate amount of mass.

There have been some studies investigating the mechanical response of the human neck and head but very few investigating the change in response due to a helmet or the interaction between head and helmet. This research was conducted to understand the dynamics and interaction of the head and helmet system.

The objectives of this study were to gain an understanding of the dynamic response of the head-helmet system. This has involved quantifying how the head and helmet move when running, jumping and while exposed to whole-body vibration. Particular attention has been applied to understanding the frequency, magnitude and direction of motion. It

was also considered necessary to investigate the modal response of the head-helmet system and the effect of helmet mass and other variables upon the natural modes of vibration of the system. The final objective was to produce a mathematical model of the head-helmet system, partly as a qualitative guide to understanding, but with the ultimate aim that such a model could be an aid for helmet designers, allowing optimisation of helmet design without undue effects upon the wearer.

This thesis is divided into seven chapters. Chapter 2 presents a review of the literature on measurement and modelling of human vibration and particularly the head and helmet system to summarise current known information. Chapters 3 and 4 contain experimental work conducted to determine the response of the head and helmet whilst running and jumping respectively. The experiment in Chapter 5 investigated the response of the head and helmet while exposed to whole-body vibration. An experimental modal analysis was carried out on some of the measured data to determine the mode shapes and frequencies of the head-helmet system. The effect of helmet mass and distribution of mass on the helmet was also investigated. In Chapter 6 a model of the neck-head-helmet system was developed and compared the natural frequencies and the vibration mode shapes of the model with the measurements. Chapter 7 describes the general conclusions and recommendations.

CHAPTER 2 LITERATURE REVIEW

2.1 INTRODUCTION

The literature review is divided into five main areas of study. The first is a review of studies which have investigated the relationship between helmet design and head and helmet motion. It reviews research into the interface between head and helmet that occurs at the scalp and the corresponding effect on motion of the head and helmet. The effect of helmet mass and moment of inertia on the head/helmet interaction is also reviewed. The second area of study identifies and explains techniques for the measurement and analysis of human vibration. The third section reviews previous work which has investigated motion of the neck, head or helmet to provide an insight into the known dynamics of the neck-head-helmet system. The basic anatomy of the human neck and head is described in the fourth area of study. The fifth study area reviews work concerned with biodynamic modelling of the human body. As well as including various areas of the body for modelling (spine, neck-head, head-helmet etc.) it also reviews the modelling techniques necessary for this type of application.

2.2 VARIABLES AFFECTING HEAD AND HELMET MOTION

2.2.1 Introduction

There are a number of external parameters which may affect the motion of the head and helmet under dynamic conditions. For example, when walking the type of footwear and the surface can affect the motion of the head and consequently the helmet (Woodman, 1995a). It is documented that head motion is affected by the helmet mass and distribution of mass on the helmet (Woodman and Griffin, 1995). In high g scenarios this potentially could lead to neck injury (Huston and Sears, 1981). The scalp coupling between head and helmet is also known to influence motion of the helmet on the head (Woodman, 1995b). When exposed to vertical whole-body vibration, head motion can be influenced by a variety of parameters such as posture and muscle stiffness etc. (Griffin, 1990).

This section of Chapter 2 reviews some studies which have investigated these variables and their effect upon head and helmet motion.

2.2.2 Extrinsic variables

2.2.2.1 *Effect of footwear*

High magnitude shocks are generated when walking and running and might be of pathological importance. For example, the shock at the tibia has been claimed to overload the knee, causing wearing of the joint and resulting in osteoarthritis (Voloshin and Wosk, 1982). In a later study Johnson (1986) reported that Sorbothane shoe inserts reduced shock loading by up to 20%.

Lafortune (1991) measured three-dimensional acceleration using bone-mounted accelerometers on the tibia. One subject walked at 1.5m/s while barefoot and when wearing leather-soled shoes. The average peak positive axial acceleration was 3.3g when barefoot and 1.71g when shod.

Rao and Jones (1975) measured the effect of footwear on the motion of the head and shoulders of twelve male subjects walking a distance of 6m on a concrete floor. The overall mean peak-to-peak acceleration at the head and shoulders without shoes was greater than with shoes. The mean peak-to-peak accelerations at the head shod and barefoot were 0.65 and 0.84g respectively.

Light *et al.* (1979) investigated the effect of footwear, of both conventional shoes and shock absorbing shoes, on the vertical motions at the shoe heel, tibia and head. The impulse at the head was greatest when barefoot and the impulse measured at the head was less when the shock absorbing shoes were worn than when conventional shoes were worn.

Woodman (1995a) conducted a small study to investigate the effect of footwear on the motion of the head whilst walking. A single subject walked at six different speeds when barefoot and when wearing Army Combat Assault boots and socks. The motions of the head and helmet were measured in six axes. This showed the magnitude of the peaks of

pitch motion at the head to be less when boots were worn than when the subject walked barefoot. However, the roll motion of the head was greater with the subject wearing boots than when barefoot. The transmission of pitch motion from the head to the helmet when walking was unaffected by footwear.

2.2.2.2 *Effect of helmet mass and moment of inertia*

The helmet design emphasis on the prevention of cranial injury may result in deficiencies in other areas. The helmet mass, placement of the mass and the shape of a helmet are important factors in reducing the probability and severity of neck injuries (Frievalds and McCauley, 1990).

Research has been conducted to investigate the effect of helmet mass and/or moment of inertia on the loading of the spine, the risk of injury and the wearer's comfort and performance etc.

Particular practical applications in which helmets are worn and could cause injury are in ejections from fighter aircraft. Anton (1987) reported that the risk of sustaining a neck fracture on ejection is between 1 and 2%. Increasing the mass on the head particularly in association with forward shifts of the centre of gravity could increase the incidence of fracture.

These findings were confirmed by Settecerri *et al.* (1987). A study was carried out investigating the effect of varying the mass properties of aviator helmets upon the forces and moments occurring in the head and neck during impact events. A Hybrid III anthropomorphic manikin head was used in the tests. The results showed that large changes in the centre of gravity and moment of inertia of the helmet can lead to considerable increases in the forces and moments in the head and neck.

Hoek Van Dijke *et al.* (1993) made measurements of neck and head acceleration in four simulated flights. Muscle forces and joint reaction forces in the neck were estimated and calculations made to investigate the influence of the helmet, helmet-mounted devices and a counter-weight fitted to the helmet. The following four situations were analysed; with the head unloaded (no helmet), the head loaded by a normal helmet, the head

loaded by a normal helmet fitted with a helmet-mounted device and a helmet with an additional counter weight of 0.44kg mass added at the dorsal side of the helmet. The additional weight of the helmet caused the joint reaction forces in the neck to increase by a factor of 1.4 on average. This increased to 1.7 with the addition of helmet-mounted devices. The addition of the counterweight partly compensated for the influence of the helmet-mounted devices, and the joint reaction forces in the neck decreased to 1.6.

A similar set of calculations were made to investigate the influence of helmet mass and the position of the mass on the helmet. It was observed that shifting the centre of mass posteriorly (behind the atlanto-occipital joint) reduced the mean joint load on the cervical spine to 0.9 times the load when the pilot wore a standard helmet.

Frievalds and McCauley (1990) used the Articulated Total Body Model to investigate the effects of helmet and assembly mass, head/helmet centre of gravity, and initial head-rest position on pilot injury under high G_z loads (pilot ejection). The study indicated that additional helmet mass had very little effect on head injury under pilot ejection conditions. However, any combination of helmet centre-of-gravity offset or initial head-rest position that causes the combined head and helmet assembly centre of gravity to be anterior of the atlanto-occipital joint would result in a significant head rotation. It was concluded that the location of the helmet centre-of-gravity is the crucial parameter when designing an aviator's helmet.

Woodman and Griffin (1993) studied the relationship between helmet mass and the transmission of fore-and-aft seat vibration to the head and helmet. An excitation frequency range of 0 to 20 Hz was used and helmet mass was varied from 0 to 4.2kg. Measurements of head and helmet motion were made in the mid-sagittal plane and transfer functions determined from the fore-and-aft motion of the seat to each of the directions of movement on the head and helmet. Although the results presented errors due to large amounts of inter-subject variability it was still possible to conclude that placing a helmet on the head reduced the fore-and-aft frequencies measured at the head. Placing a helmet on the head also reduced the pitch movement that occurred on the head at 5Hz. A mode of vibration, containing both pitch head and pitch helmet motion, decreased from 10Hz to 5Hz as the helmet mass increased from 1.4 to 4.2kg.

Woodman and Griffin (1995), in continuation of this work, conducted an experiment to determine the effect of helmet mass and moment of inertia on pitch head to pitch helmet transmissibility. In the experiment whole-body vertical vibration was presented to twelve male subjects in the frequency range between 0 and 20Hz. Pitch motion was measured at the head and at the helmet and the transmissibility calculated between the two. The results showed that at 4Hz the transmission of pitch head motion to pitch motion of the helmet increased with each increase in helmet mass. There was also a decrease from approximately 10 Hz to 5 Hz in the resonance frequency showing the transmissibility between pitch head motion and pitch helmet motion as the helmet mass increased. Figure 2.1 shows the head to helmet pitch transmissibility with helmets of varying masses. At frequencies between 2 and 12 Hz the magnitude of the head to helmet transmissibility generally decreased as the helmet mass increased.

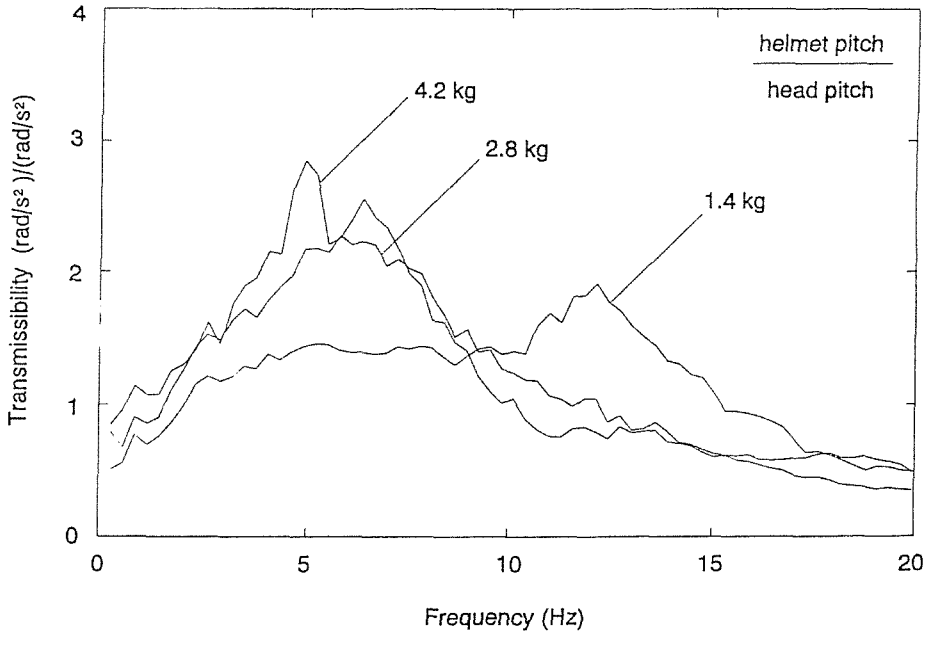

Figure 2.1 Median transmissibilities of 12 subjects from head pitch motion to helmet pitch motion, during vertical seat vibration. (From Woodman and Griffin (1995))

2.2.2.3 *Forehead skin and helmet coupling*

The relative motion of a helmet on the head may be influenced by motion of skin or by motion of the internal fittings of the helmet (Woodman, 1995b). The contact area

between a helmet and a head will vary between different designs of helmet and may alter the dynamic properties of the skin on the head.

Neary *et al.* (1993) investigated helmet slippage and suggested that the helmet can move on the head due to looseness of skin during voluntary head movements. The r.m.s. helmet slippage was measured and shown to be a function of head motion. It was also observed that slippage increased linearly with increasing r.m.s. head motion.

The effect of the contact area on the stiffness of forehead skin was studied by Woodman (1995b) to evaluate whether the contact area with the forehead influenced the relative head and helmet motion. The study consisted of two parts. The first calculated the static skin stiffness by measuring the skin displacement after a certain mass was applied. The results indicated that the forehead shear skin stiffness varied over the twelve subjects tested from 300 to 650N/m. The second part of the study measured the dynamic response of the head and the helmet to vertical seat acceleration for each subject. Transmissibilities were calculated between head pitch and helmet pitch motion. The results showed a large amount of intersubject variability. There was, however, a marginally significant correlation between median forehead static skin stiffness and the frequency of the peak in the transmission of pitch motion from the head to the helmet for each subject.

2.2.3 Intrinsic variables

2.2.3.1 *Intersubject variability*

Intersubject variability is the variability in results that can occur across a sample of subjects. The nature of the human race dictates that no two people are the same. All have a different, physical, genetical and anatomical structure. This can cause problems when conducting experiments with human subjects. For this reason, studies investigating the human response to vibration usually make use of a sample of subjects, the number depending upon the nature of the experiment. Results from the sample of people are generally analysed using statistical methods and displayed to provide conclusions which are representative of a sample of the relevant population.

Paddan and Griffin (1988) conducted a study into the effect of intersubject variability on the transmission of translational seat vibration to the head. Twelve male subjects participated in the experiment, (aged 18-34 years) with a reasonable cross-section of weight and height. The results showed large differences in the transmissibilities between subjects, particularly in the vertical seat-to-head transmissibility curves, with one subject having a seat-to-head transmissibility of 0.1 at 6.5Hz and another subject having a transmissibility value of 1.6. The authors suggested that this scatter, as well as being caused by individual experimental differences between subjects such as posture and voluntary movements of the head, could be caused by physical differences between subjects (weight, age, height, hip size, leg size etc). The effect of the subject relying on a backrest is also another significant factor in producing large amounts of intersubject variability.

2.2.3.2 *Intrasubject variability*

Intrasubject variability is the variability between the test results of one subject, when experiencing the same experimental conditions at differing times.

The causes of intrasubject variability are due to uncontrollable changes in the experiment and are mostly caused by changes in posture and lack of careful observance of the subject by the experimenter.

Paddan and Griffin's experiments (1988) also investigated the effect of intrasubject variability in the transmission of vertical seat vibration to the head. These results indicated a high repeatability in transmissibility compared to the changes caused by different seating conditions and those associated with inter-subject variability. A possible explanation given for this was that the subject repeated the experiment over a short period during which he was able to recall the precise form of his sitting posture.

2.2.3.3 *Effect of posture in vertical whole-body vibration transmitted to the head*

Coermann (1962) investigated the effect of posture on the transmissibility from seat vertical acceleration to vertical head acceleration. One subject was exposed to vertical sinusoidal vibration with a magnitude of 0.1g, in the frequency range from 1 to 20 Hz, in erect and relaxed postures. The erect posture increased the first resonance frequency

from 4.6Hz in the relaxed posture to about 5.2Hz and produced another resonance at about 3.2Hz. The second frequency peak with a relaxed posture at about 10 Hz increased to 11Hz when an erect posture was adopted. A third resonance at 15 Hz with an erect posture was not seen when the posture was relaxed. The erect posture also decreased the transmissibility at frequencies below 5.2Hz but increased the transmissibility above 5.2 Hz.

Griffin (1975) exposed twelve subjects to vertical discrete sinusoidal vibration in the frequency range from 7 to 75 Hz with six magnitudes from 0.2 to 4.0 m/s^2 r.m.s. Each subject adopted the most and least severe posture in a sitting position. Acceleration at the head in the vertical, fore-and-aft, lateral and pitch directions was measured and the transmissibilities from seat to head were calculated and compared between the two postures. It was found that the transmissibility to the head vertical and lateral directions in the most severe posture was reduced when the least severe posture was adopted at all the frequencies measured. The effect of posture on the transmissibility to the fore-and-aft and pitch motion of the head was small.

2.2.3.4 *Effect of muscle tension*

Griffin *et al.* (1978) measured the transmissibility of vertical seat acceleration to vertical head motion of a subject with the muscles tensed as much as possible and with the muscles relaxed. The subject kept a normal sitting posture in both conditions. It was found that the tensed muscles increased the transmissibility at most frequencies upto 100Hz with the largest increment from 1.0 to 1.4 at 5Hz. The first resonance at about 4 Hz with relaxed muscles shifted to about 5Hz when the muscles were tensed. However, the effect of muscle tension appeared smaller than the effects of changing posture.

2.2.3.5 *Effect of backrest in vertical whole-body vibration*

Paddan and Griffin's study (1988) into the transmission of vertical seat vibration to the head showed the transmissibility to the head in the fore-and-aft direction to be greater when a backrest was used in the experiment (in the frequency range between 4 and 8Hz). Using a backrest resulted in approximately 60% more motion of the head in the vertical direction at the main resonance frequency of 6Hz. Removing the backrest decreased the frequency and magnitude of the main resonance peak and the point of

minimum response decreased from 13 to 8Hz when the backrest was removed. The changes in transmissibility when contact is made with the seat backrest arise partly from the additional transmission path for vibration. However, it was also suggested that leaning against the backrest may alter the dynamic response of the body by providing additional stiffness, hence increasing some resonance frequencies.

2.2.3.3 *Effect of bite-bar mass and grip when measuring whole-body vibration*

Paddan and Griffin's study (1988) showed that bite-bar grip does not have a significant effect upon the transmission of vibration from seat to head. However, it was observed that increasing the mass of the bite-bar from 135 to 375g increased the pitch motion of the head at 7Hz by approximately 18%.

2.3 MEASUREMENT AND ANALYSIS TECHNIQUES OF HUMAN VIBRATION

2.3.1 Introduction

This section introduces and explains some of the more commonly used techniques that have been used by previous authors in experiments concerning the measurement and analysis of human vibration.

2.3.2 Transmissibility

Transmissibility is the non-dimensional ratio of the response amplitude of a linear system in steady-state forced vibration to the excitation amplitude expressed as a function of the vibration frequency. The ratio may be one of forces, displacements, velocities or accelerations (Griffin, 1990). Transmissibility measurements can therefore for be used to quantify the amount of acceleration travelling through the body, from one point to another.

2.3.3 Six axis bite-bar

Paddan (1984) first used a six-axis bite bar to measure rigid-body motion of the head. Many researchers have since used a similar bar in subsequent studies. The instrumented bar consists of six translational accelerometers to measure six axes of motion of the head and helmet. Rotational accelerations are determined from signals

provided by pairs of translational accelerometers. The bite bar is shown in Figure 2.2. Translational accelerations are taken as those measured by three mutually perpendicular accelerometers on block 3 (i.e. A_{x1} for x-axis, A_{y1} for y-axis and A_{z1} for z-axis motion at the head or helmet). The signals A_{z1} and A_{z2} and the separation between the blocks 2 and 3 enable the roll accelerations to be calculated, A_{z1} and A_{z3} together with the separation between the blocks 1 and 3 are used to calculate pitch acceleration. Yaw motion is calculated using A_{x1}, A_{x2} and the separation between blocks 2 and 3.

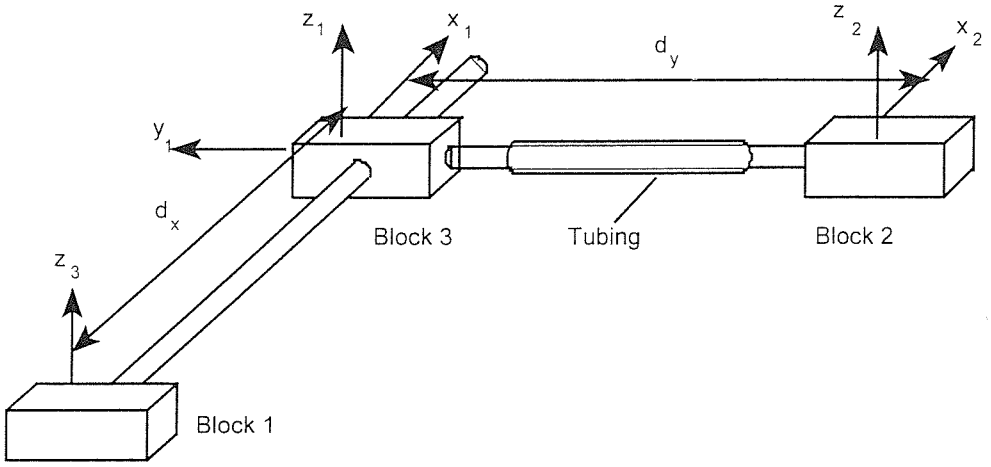

x_1 x_2	- axes of fore-and-aft accelerometers
y_1	- axis of lateral accelerometer
z_1 z_2 z_3	- axes of vertical accelerometers

Figure 2.2 Six axis bite-bar with accelerometer positions, mounting blocks and sterilised tubing to bite.

The equations required to calculate the rotational accelerations are:

roll acceleration $r_x = \dfrac{A_{z2} - A_{z1}}{d_y}$

pitch acceleration $r_y = \dfrac{A_{z3} - A_{z1}}{d_y}$

yaw acceleration $r_z = \frac{A_{x2} - A_{x1}}{d_y}$

2.3.4 Apparent mass

Apparent mass is the complex ratio of force to acceleration during vibration measured in a linear system under simple harmonic motion or random vibration. It has the advantage that it can be measured directly from signals provided by accelerometers and force transducers. When the human body is rigid (for example at low frequencies) the apparent mass of the body is equal to its static mass, and force and acceleration are proportional and inverse with each other. As the excitation frequency increases, passing through one or more resonances there is an increasing phase difference between force and acceleration. At higher frequencies the upper parts of the body are only loosely coupled, the force is dominated by the mass and the apparent mass falls.

2.3.5 Experimental Modal Analysis

Experimental modal analysis is a method used to characterise the dynamic behaviour of a structure. When using experimental modal analysis it is assumed that the structure behaves in a linear manner with hysteretic damping. The technique relies on the assumption that the dynamic behaviour of a structure may be described in terms of its modal properties of natural frequencies, mode shapes and damping. Experimental modal analysis seeks to extract modal information from measured data, generally transfer functions, based on a mathematical model formulated in terms of modal properties and presents the results in the form of natural frequencies and mode shapes.

Kitazaki (1992) conducted a pilot study to investigate the application of experimental modal analysis on data measured at the vertebrae T1, T6, T11, L3 and S2, front pelvis, torso-wall and at the head of one subject who was exposed to vertical whole-body vibration. The effect of local skin vibration was eliminated, using a procedure to take into account the relative motion between the vertebrae and the accelerometers.

Acceleration transfer functions between the vertical input at the seat and each measurement point were used in the experimental modal analysis. Although there was

heavy damping of the human body, the experimental modal analysis technique was found to be applicable to human whole-body vibration.

2.3.6 Coherency

Coherency is an expression of the proportion of the output of a system that is related to the input. All transfer function measurements (including transmissibility and apparent mass) should be used with coherency measurements to ensure reliable data.. It is used to gain confidence in the measured data and to ensure that noise or linearity issues do not compromise the quality of the transfer function data.

2.4 MEASUREMENTS OF HEAD AND/OR HELMET MOTION

2.4.1 Introduction

The transmission of vibration through the body may reduce comfort or have an adverse affect on health. Vibration of the head may impair vision and difficulties can be encountered in controlling a vehicle or when performing some other task. The vibration of a helmet mounted on the head may produce discomfort, fatigue, a reduction in task performance efficiency and potentially the risk of spinal injury to the wearer.

This section reviews known circumstances in which helmets are worn and measurements of head and/or helmet motion have been made. This includes laboratory conditions, when head /helmet motion has been provoked by shakers, ambulatory conditions and in-vehicle measurements made in the field.

2.4.2 Walking and running

Compared with whole-body vertical vibration whilst seated, the motions occurring during running and walking are complex (Sandover, 1975). The pelvis oscillates in the *xz* and *xy* planes with alternate steps to a marked degree, and the abdominal muscles are probably under greater tension.

No studies have been found which quantify the effect of a helmet on head motion or report on the nature of the motion that occurs at the head and helmet when running. It has, however, been shown that the levels of whole-body vibration present when running

are greater than the maximum vibration levels permitted from agricultural and industrial machinery and vehicles.

Sandover (1975) measured the vertical head motion of 8 subjects whilst walking and running and compared these data with those occurring at the head during externally applied whole-body vibration. Using an iterative trial and error method it was possible to match head acceleration with seat input for both ambulation conditions. It was concluded that the level of whole-body vibration induced whilst running can be much greater than the levels considered unacceptable by I.S.O 2631 (1974) at a shaker platform.

Cappozzo (1982) expanded upon the idea of self-generated vibration further by conducting acceleration measurements at the head, shoulders and pelvis of five healthy male subjects when walking. It was concluded that the acceleration components to which the upper part of the body is subjected combine so as to give rise to a smooth and well co-ordinated pattern of ambulation; both in time and in space. It was also observed that vertical acceleration of the head shifted towards higher frequencies as walking speed increased and was 'considerably' greater in magnitude than the horizontal components. Figure 2.3 below shows a sample of the measured time-histories whilst walking at 1.63 m/s.

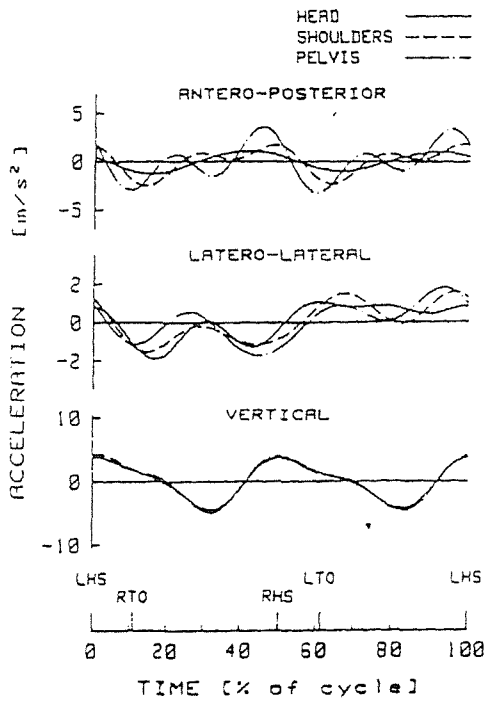

Figure 2.3 Acceleration time histories measured on a single subject when walking at 1.63 m/s (Capozzo, 1982).

It has been shown that a helmet can increase motion of the head in certain conditions and at certain frequencies and consequently it is hypothesised that the addition of a helmet, of known mass and moment of inertia could increase the levels of self-induced whole-body vibration.

Some studies have been conducted which quantify the motion of the head when running. These are explained below.

Gunther (1969) conducted a study to investigate the effect of impact vibrations at the head, pelvis and heel when walking and running on an elastic floor, concrete surface and a lawn. In walking, average accelerations were shown, for men at the heel to be 3.0g, at the pelvis 1.3g and at the head 0.6g. This provided an indication of the attenuation of the acceleration as it is transmitted through the body. It was also concluded that there is no connection between the magnitude of the acceleration and the magnitude of the body weight of the subject.

Simic (1970) explored the theory that human tolerance to externally applied vibration is closely linked with the self-induced accelerations and frequencies which occur during walking. He employed a total of 73 subjects ambulating at speeds varying between slow walking and running and measured the corresponding acceleration in the head *x* and *z* directions and at waist level in the *x, y* and *z* directions. He concluded that the accelerations in the vertical directions are greatest for all subjects and deduced the following 'rule of thumb' for the ratio of acceleration in the three directions.

Z: x: y 1: 0.8: 0.5

Walters *et al.* (1973) conducted a more academic study into human locomotion. Translational acceleration and displacement of the head and trunk at different walking speeds was measured. Fore-aft displacement of the head was sinusoidal. The head and trunk moved faster than the stepping rate (fore-aft direction) in the first 31% of the step cycle and this increase in velocity started at 90% of the previous step cycle. At all other times in the cycle the head moved at a slower rate than the stepping rate in the fore-aft direction. Maximum downward (-z) displacement of the head occurred at 17% of the step cycle when the head was centred between both feet in a double stance. It was observed that the maximum amplitude of vertical head displacement was 4.2cm. This occurred 68% of the way through the cycle when the feet rise over the fixed stance extremity. It was also observed that increased vertical head displacement occurred as walking rate increased.

Acceleration of the head in the fore-aft and vertical directions was also measured for each step. Forward acceleration of the head began at 60% of the step cycle and continued to 10% of the next step cycle. This relates to push-off, deceleration of the swing limb and downward movement of the head and trunk. It was observed that as walking speed increased the magnitude of forward and backward acceleration of the head increased. Vertical acceleration of the head was maximum at 9% of the stepping cycle and averaged 0.31g. The minimum acceleration (-z) occurred at 50% of the cycle averaged 0.08g. As walking speeds increased the magnitude of vertical acceleration of the head increased. The overall process of head and trunk movement when walking is

believed to conserve energy between successive steps by providing a smooth transfer of energy.

Rao and Jones (1975) conducted a study on the human response to walking and obtained some basic spectral information at the head and shoulders of a sample of 29 male subjects when walking. They showed that the head vertical response during walking shows the behaviour of a two degree of freedom viscoelastic system, whilst the shoulder response shows the behaviour of a single degree of freedom system. The results identified three frequency regions during the walking process, a head response at 1.2-2.0Hz- the range of normal walking frequencies, a shoulder response of approximately 5Hz and a mean frequency response of the head of approximately 19Hz. Recommendations, based upon these results were made to restrict the magnitude of vibration occurring in vehicles.

Das, *et al.* (1995) conducted a study to investigate the effect of viewing a fixed target whilst walking upon rotational head motion. Whilst the majority of the conclusions made are not relevant in the context of this thesis some useful information was supplied. In particular a comparison was made between normal walking and treadmill walking which showed head motion in the pitch direction to occur at very similar frequencies but to have a substantially greater peak velocity during natural walking.
Woodman (1995a) measured acceleration at the heads of 12 subjects in translational and rotational axes whilst walking at speeds of between 1 and 2.25 steps per second. The effect of wearing a 1.3kg helmet was also investigated. Power spectral densities of the acceleration at the head showed that increases in walking speed increased the magnitude of dominant vertical and pitch head acceleration which occurred at the stepping frequency. Acceleration measured in the fore-and-aft axis of the head was greatest at the lowest walking speeds. Wearing the helmet tended to reduce head accelerations in the frequency range between 2 and 5Hz.

2.4.3 Jumping

Jumping conditions introduce shocks and impulses into the body and skeletal system rather than the periodic-type of signal seen when walking or running. It could be hypothesised that the response at the head and helmet (if worn) would show greater

acceleration and displacement under jumping conditions than in any of the other ambulation conditions. It is therefore suprising to find little relevant literature on the subject.

Work has, however, been conducted on the overall body human to jumping excitation. Bhattacharya *et al.* (1980) measured accelerations in the vertical direction at three points on the body: the ankle, the lumbosacral region of the back and at the forehead. Endevco piezo-resistive accelerometers, placed in plexi-glass holders to maintain orientation in the vertical axis were taped to the skin to measure the acceleration at each point. Measurements were made during trampoline jumping at four heights of 18, 37, 75 and 100 cm while the subjects jumped for a duration of five minutes at each height. Eight male subjects were used in the experiment. When the results were normalised to take into account body weight, the peak accelerations increased progressively with increased jumping height at all three body locations.

Figure 2.4 shows typical time histories of the acceleration of a single subject whilst jumping on a trampoline. It can be seen that the accelerations at all three sites on the body during jumping were similar, indicating that impact forces were transmitted throughout the body with little attenuation.

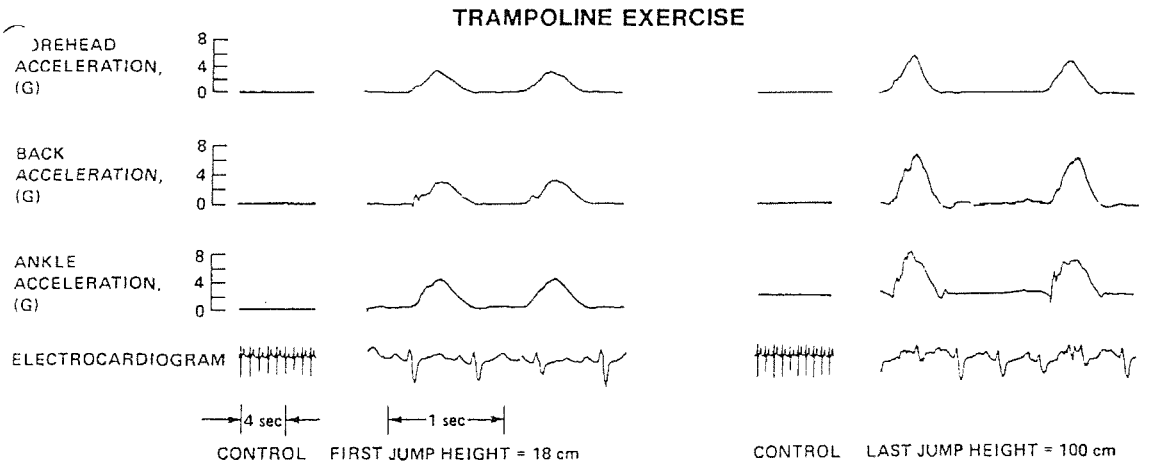

Figure 2.4 Typical records of the forehead, back and ankle acceleration waveforms during trampoline jumping for one subject (Bhattacharya *et al.*, 1980)

Pernica (1990) conducted a study to measure the dynamic load factors for pedestrian movements and rhythmic exercises. As part of the study the floor response was measured with a subject 'stride jumping'. Figure 2.5 shows the time-history and spectra of that event, showing repeatable sinusoidal motion and a well defined frequency spectrum with fundamental and harmonics.

Other studies have been conducted to investigate the human response to jumping, although these have not measured head motion. Ozguven and Berme (1988) conducted a study of the impact forces during human jumping and developed a two-degree of freedom model showing that the human could be modelled to simulate jumping from a different height and predict ground reaction forces. Berme *et al.* (1984) conducted a study to investigate the compressive loading of the spine whilst jumping from height and concluded that spinal loading when jumping is approximately equal to that occurring when running.

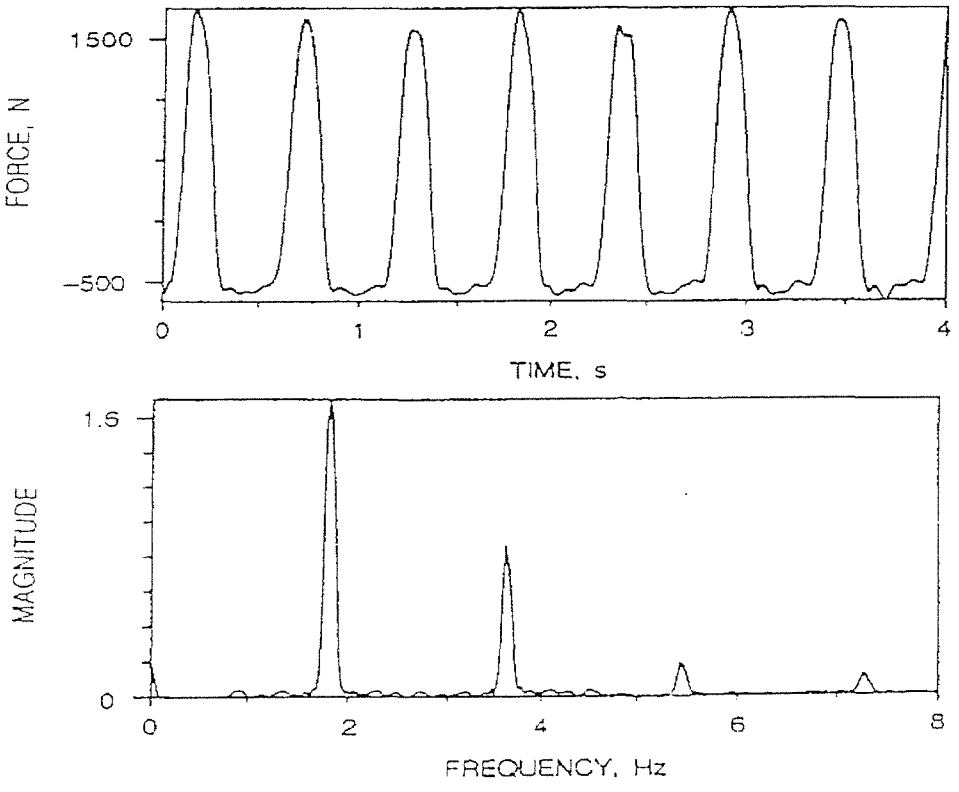

Figure 2.5 Time history and spectrum of ground forces produced by one person stride jumping at 1.8m/s, Pernica (1990).

2.4.4 From whole-body vibration

Paddan (1986) measured the transmissibility of seat-to-head vibration in an armoured fighting vehicle driven over a rough cross-country course. Vibration recorded at the head and seat in the mid-sagittal plane and the mid-coronal plane were analysed using transmissibilities, partial coherencies and conditioned power spectral densities. It was shown that fore-aft, vertical and pitch motion of the head were mostly affected by vertical motion of the seat. Pitch axis seat motion had no effect on motion in the three axes at the head.

In Paddan and Griffin's study (1988) vibration was measured in three translational and three rotational axes of the head during exposure to whole-body random vertical vibration. The excitation was provided by a 1m one-stroke electro hydraulic vertical vibrator and the response measured using a six axis bite-bar. Participants in the experiment were subjected to the same Gaussian random vibration, presented for 60 seconds at 1.75 $\pm$0.05m.s^{-2} r.m.s. at frequencies between 0.2 and 31.5Hz. Twelve subjects were used in the experiment and asked to maintain a 'comfortable upright posture' throughout the experiment and avoid voluntary movements of the head. Seat-to-head transfer functions were calculated for motion occurring 100mm to the left of the mid-sagittal plane at mouth level and calculated using the 'cross spectral density function method'. The study provided valuable information into the effect of backrests, bite-bar grip strength and inter and intra subject variability, results of which are discussed in Section 2.2 of the literature review.

Paddan (1990) made transmissibility measurements for a single subject of vertical seat to vertical head and vertical seat to fore-and-aft head motion. This experimental work identified three main resonances, providing information about the dynamics of the head. The first, at approximately 3Hz showed mostly *x*-axis motion at the chin, falling steadily towards the crown. The second mode occurred at around 4.5 Hz and showed a large amount of *x*-axis motion at the chin and a large amount of *z*-axis motion at the back of the head, which decreased steadily towards the front of the head. The third mode occurred at around 6.5 Hz. In the *z*-axis there was a lot of motion at the front of the head and at the crown of the head in the x-axis, decreasing steadily towards the chin.

Paddan and Griffin (1992) measured head motion in six axes of twelve subjects exposed to vertical whole-body vibration in the frequency range between 0.5 and 25 Hz. Translational acceleration was calculated at various locations on the head from the measured data and seat-to-head transmissibilities were calculated at each location in each translational axis. It was discovered that the translational motion of the head was most affected by head pitch motion. This caused variations in fore-and-aft motion with position along the vertical axis of the head and variations in vertical motion with position along the fore-and-aft axis of the head. Individual subject data allowed the identification of various modes of vibration and showed that seat-to-head transmissibility is greatly affected by pitch modes of the head and neck as shown in Figure 2.6.

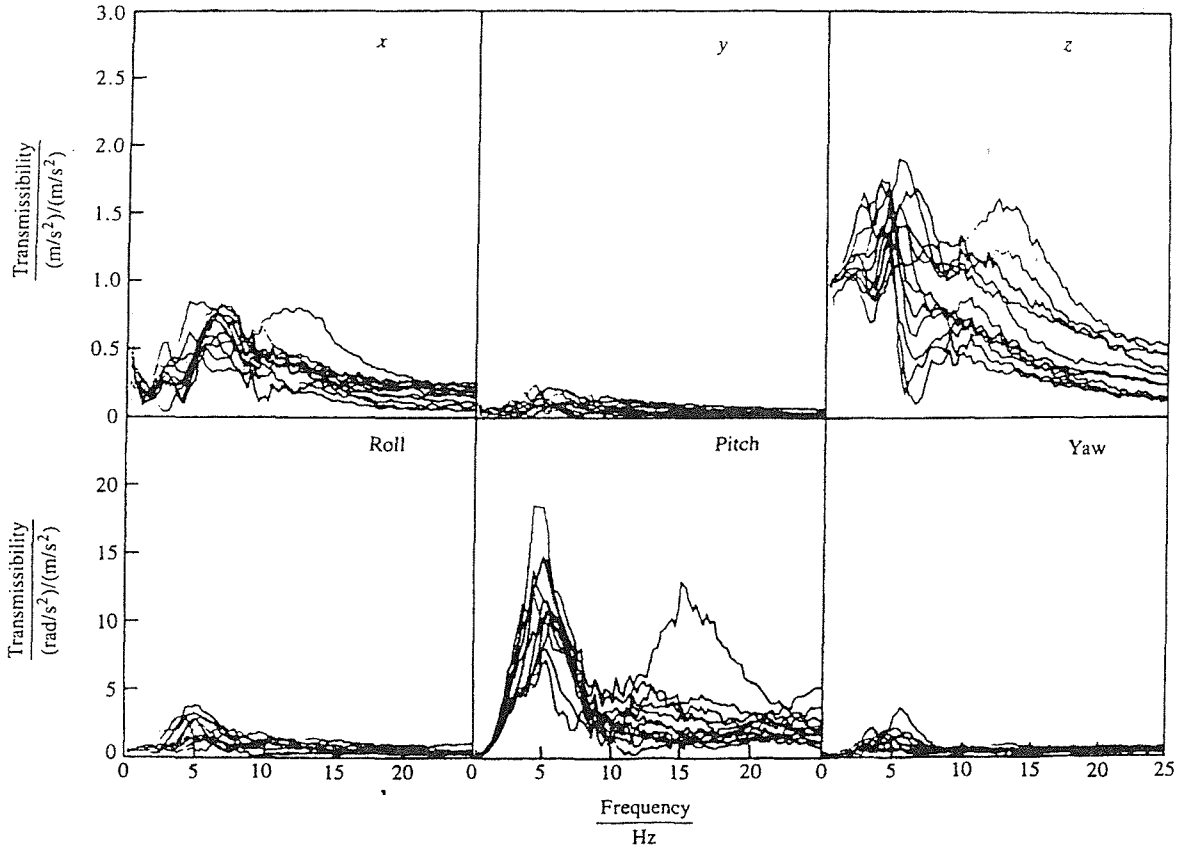

Figure 2.6 Transmissibilities for 12 subjects in a back-off posture during vertical seat motion, from Paddan and Griffin (1992)

Kitazaki and Griffin, (1998) conducted a series of experiments to identify the resonance behaviour of the seated human body. Experimental modal analysis was applied to data

measured under whole-body vertical vibration with three seated postures. Motions of the spine, pelvis and viscera, in the mid-sagittal plane, were derived from skin-mounted accelerometers and head responses were measured using a bite-bar.
Eight modes of vibration were extracted from the mean transfer functions of eight subjects at frequencies below 10 Hz. These are summarised in Table 2.1 above and shown in Figure 2.7. Natural frequencies were also extracted from the mean apparent mass. The first principal resonance occurred at 4.9Hz and the second principal resonance occurred at 8.6Hz.

Table 2.1. Frequencies and mode shapes obtained from Kitazaki and Griffin (1997)

Mode No	Frequency	Mode shape description
1	1.1 Hz	Bending mode of the thoracic and cervical spine
2	2.2 Hz	Anterior-posterior motion of the head and pelvis (opposite phase)
3	3.4 Hz	Anterior-posterior motion of the head and pelvis (in phase)
4	4.9 Hz	Entire body mode- head, spinal column and pelvis moved vertically due to axial and phase with a vertical and visceral mode and a bending mode of the upper thoracic and cervical spine. (1^{st} Principal resonance)
5	5.6 Hz	Bending mode of the lumbar and the lower thoracic spine and vertical motion of the head.
6	8.1 Hz	Pitching modes of the pelvis with different locations of pivot- (associated with second principal resonance)
7	8.7 Hz	
8	9.3 Hz	2^{nd} visceral mode (associated with second principal resonance)

Wells (1982) conducted a study to investigate the acceleration levels occuring in a military helicopter and its occupants. In particular measurements were made of head and helmet pitch acceleration- both in the helicopter and in simulated flight conditions in the laboratory. It was observed that most energy in the head and helmet pitch directions

of motion occurred at frequencies below 10Hz. The transfer function of head pitch to helmet pitch acceleration was dominated by peaks representing the main rotor blade passing frequency (and associated harmonics). At frequencies between approximately 2 and 12 Hz the head to helmet pitch transmissibility was never less than one, indicating extra helmet pitch motion (relative to head pitch).

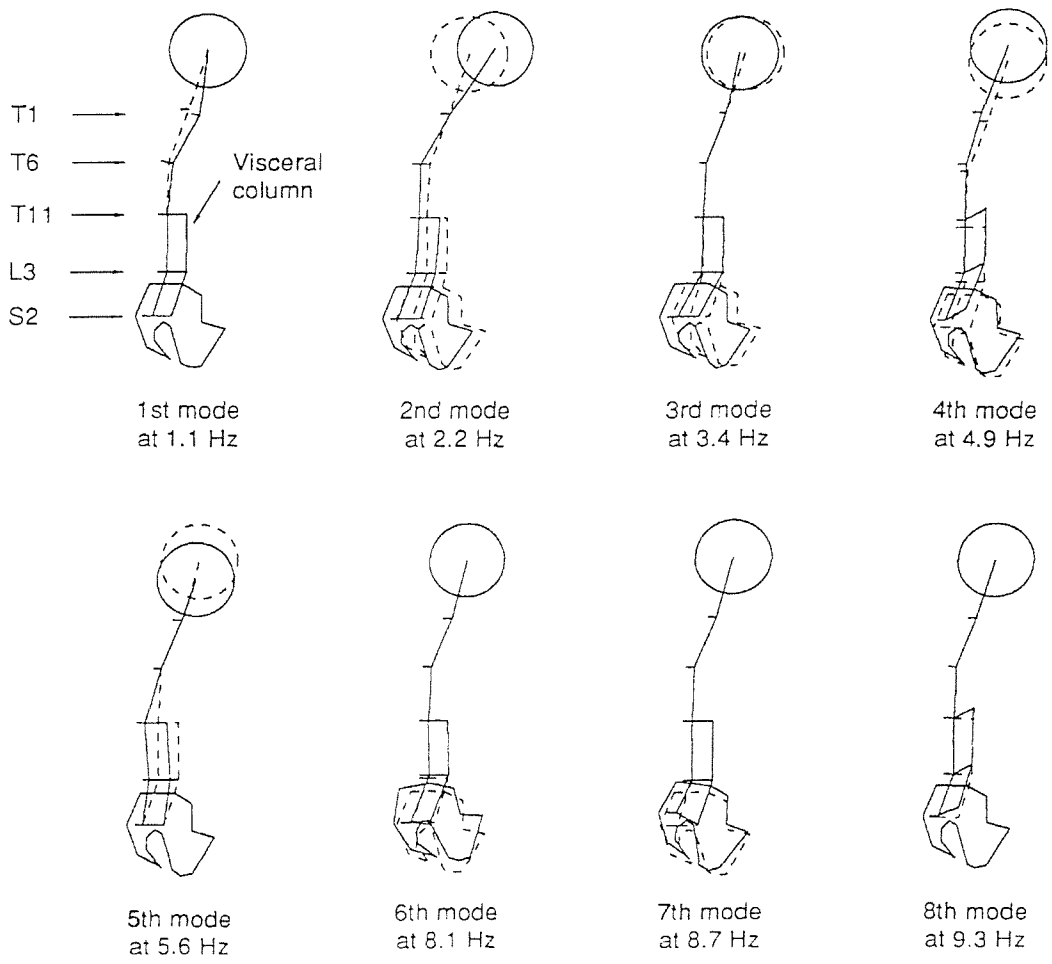

Figure 2.7 Vibration mode shapes in the normal posture extracted from the mean transfer functions of eight subjects below 10Hz, Kitazaki and Griffin (1998).

The study by Woodman and Griffin (1995) measured head and helmet motion under whole-body vertical vibration conditions to investigate the effect of helmet mass and moment of inertia. A peak in the transmissibility of pitch acceleration from head to helmet was observed and this varied from approximately 4.8Hz to 12Hz depending upon

helmet mass. The amplitude of each peak in transmissibility varied between approximately 2 and 3- indicating that there was considerably more helmet pitch acceleration than head pitch acceleration at this frequency.

2.5 THE ANATOMY OF THE HUMAN NECK AND HEAD

2.5.1 Structure of the skeletal system

The adult human skeleton consists of 206 named bones. These are grouped into the axial and appendicular skeleton. The axial skeleton contains the bones which lie around the longitudinal axis of the upper body such as the skull, vertebral column and the ribs. The appendicular division contains the bones of the upper and lower extremities (limbs) and the shoulder and pelvic girdles which connect the extremities to the axial skeleton.

2.5.2 The structure of the vertebral column

The vertebral column (spine), the sternum and ribs, constitute the skeleton or trunk of the body. The adult vertebral column consists of seven cervical vertebrae, twelve thoracic vertebrae and five lumbar vertebrae (24 in total). There are also five fused vertebrae that form the sacrum, and usually four fused vertebrae that form the coccyx. The vertebral column has the principle function of supporting the human body in the upright posture, protecting the spinal cord and allowing axial movement of the spine. Figure 2.8 shows an anterior and lateral view of the vertebral column.

2.5.3 Vertebral structure

2.5.3.1 *Introduction*

Although there are variations in the size, shape and detail in the vertebral structure in different regions of the vertebral column the vertebrae are essentially similar in structure. A typical vertebra consists of the vertebral body, vertebral arch and processes. The vertebral body is a bony, thick, disc-shaped anterior portion that is the load-bearing part of a vertebra. Its superior and inferior surfaces are roughened for the attachment of intervertebral disks. The vertebral arch extends posteriorly from the body. It is formed by two short and thick processes (the pedicles and the laminae). The space between the vertebral arch and the body is the vertebral foramen and this contains the spinal cord.

The vertebral foramina of all the vertebrae together form the vertebral (spinal) canal. A transverse process extends laterally on each side and a single spinous process projects posteriorly and inferiorly from the junction of the laminae. These three processes serve as points of attachment for the connective ligaments. The remaining four processes form joints with other vertebrae. The two superior articular processes articulate with the vertebra next to them. The articulating surfaces of the articular processes are referred to as facets.

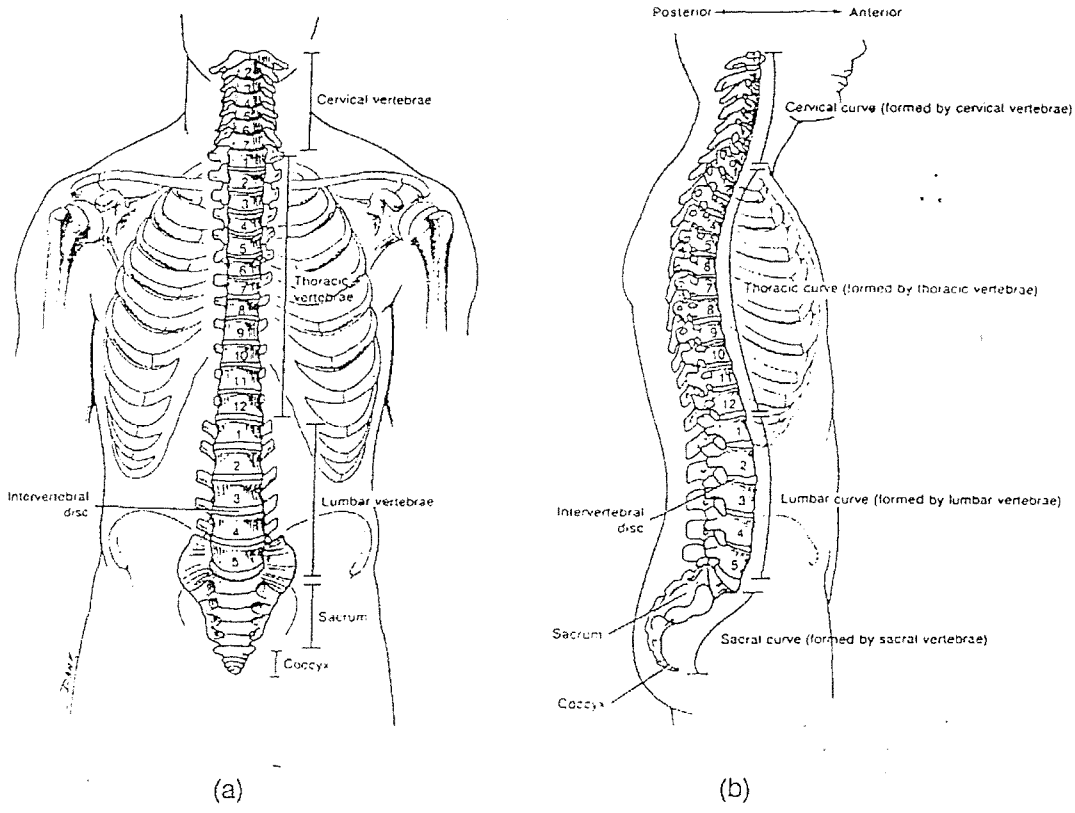

(a) (b)

Figure 2.8 Vertebral column: (a) anterior view; (b) right lateral view (from Tortora and Anagnostakos, 1990)

2.5.3.2 *Cervical vertebrae*

The bodies of the cervical vertebrae are smaller than those of the thoracic vertebrae. However, the vertebral arches are larger. The first two cervical vertebrae differ considerably from the others. The first cervical vertebra (the atlas) supports the head. The superior articular facet is linked to the occipital bone of the head and subsequently allows for the nodding (pitching of the head). The inferior articular facets are linked to the

second cervical vertebra (the axis vertebra). The structural pattern of the 3rd to 7th cervical vertebrae corresponds to that of a typical vertebra.

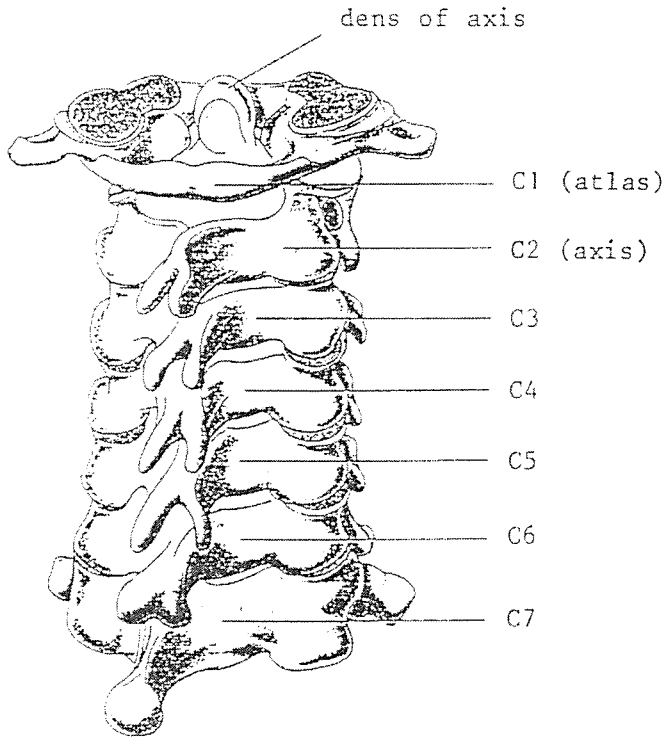

Figure 2.9 Basic Anatomy of the neck (cervical spine), (from Tortora and Anagostakos, 1990)

2.5.3.3 *Thoracic vertebrae*

The thoracic vertebrae are larger than the cervical vertebrae. The spinous processes are longer and directed inferiorly. The thoracic vertebrae also have longer and heavier transverse processes than the cervical vertebrae. With the exception of the eleventh and the twelfth thoracic vertebrae, the transverse processes have facets which articulate with the tubercles of the ribs, and the bodies have whole facets or half facets for articulating with the heads of the ribs.

2.5.3.4 *Lumbar vertebrae*

The lumbar vertebrae are the largest and strongest vertebrae in the spinal column. Their various projections are shorter and thicker than other vertebrae in the thoracic and cervical regions. The superior articular processes are directed medially instead of

superiorly and the inferior articular processes are directed laterally instead of inferiorly. The spinous processes are thick and broad and project almost posteriorly.

2.5.3.5 *Sacrum and coccyx*

The sacrum is a triangular bone formed by union of five fused sacral vertebrae. The sacrum serves as a strong foundation for the pelvic girdle. It is located at the posterior portion of the pelvic cavity between the two coaxial (hip) bones. The coccyx is also triangular in shape and is formed by fusion of coccygeal vertebrae, usually the last four. The coccyx articulates superiorly with the sacrum.

2.6 MODELS OF THE HUMAN NECK, HEAD AND HELMET

2.6.1 Introduction

This section of the literature review investigates previous research into biodynamic modelling of the human body. It also reviews the modelling techniques necessary for this type of application and details relevant previous models of the spine, neck, head and helmet.

Many applications of biodynamic modelling use finite element analysis to produce an accurate representation of the system. The finite element method is to divide the region in a model into as many subregions as possible. The subregions are rejoined by enforcing conditions that make each boundary compatible with each of its neighbours.

Finite element analysis is widely used to model the response of a structure to specific operating loads and conditions. In mechanical applications this is advantageous as it saves both time and money and often eliminates the need for prototype structures.

Biodynamic models have been developed using finite element analysis to predict the response of the human body under certain conditions. Thus biodynamic models have been written to predict the risk of injury to pilots when ejecting and, among others, to see how the body responds to whole-body vibration.

It is the aim of this chapter to review biodynamic models that have been developed to predict the effect of vibration upon the response of the spine, neck head and helmet.

2.6.2 Models of the human spine

Kim and Goel (1990) developed a three-dimensional non-linear finite element model of a half-intact L3-4 ligamentous lumbar motion segment. The model consisted of 436 three-dimensional elements and was used to compare disc bulge, loads across the facets and intradiscal pressure with measured data taken from a segment dissected from a human cadaver.

Toth (1966) developed an eight degree-of-freedom non-linear model of the thoracic and lumbar vertebrae and pelvis. Various acceleration waveform inputs were applied to the model and the force response was compared with the vertebra breaking strength. Consequently it was possible to define human tolerance to vertebral injury for various cephalad directed waveforms.

Orne and Liu (1971) developed a discrete parameter model of the human body using the spine as the main load-carrying element. The spine was modelled as a collection of elements with each element consisting of a rigid vertebra and a massless, deformable disc. Each rigid body had two translational and one rotational degree of freedom (in the midsagittal plane). An acceleration pulse (representing an ejection force) was applied at an angle to the midsagittal plane. The axial, shear, bending and displacement response of the spinal column was calculated and the effect of varying the angle of the applied ejection force was also investigated.

Prasad and King (1974) produced a spinal model with 24 vertebrae. The head and the pelvis were all modelled as rigid bodies with three degrees-of-freedom in the mid-sagittal plane. Mass and moment of inertia data were obtained for each vertebra by measuring cadaveric segments. The model was validated with experiments using three human cadavers by applying an acceleration input to the pelvis whilst the top of the head remained stress free. The force was measured between segments using an intervertebral force load cell.

2.6.3 Models of the human spine-neck-head (and helmet)

2.6.3.1 *Introduction*

There has been some development of biodynamic models to predict motion at the spine, neck and head. Belytschko *et al.* (1976) conducted a study into head-spine dynamics. The three dimensional model produced was the foundation for many later models, such as those developed and applied by Privitzer and Kaleps (1990) and Kitazaki (1991).

2.6.3.2 *Belytschko*

Belytschko *et al.* (1976) developed a three-dimensional discrete model of the human spine, torso and head for the primary purpose of evaluating mechanical response in pilot ejection. It was developed in sufficient generality to be applicable to the response of arbitrary loads on the head-spine system, with no restriction on the distribution or direction of applied loads on the measured responses.

The body's anatomy was modelled as a complex collection of rigid bodies representing the skeletal system (e.g. vertebrae, pelvis and head). These were interconnected by deformable elements representing ligaments, cartilaginous joints, viscera and other connective tissues. The complete model was highly complex, however, it was modular in format enabling various components to be omitted or replaced by simplified representations.
The model was constructed with rigid bodies, spring elements, beam elements and hydrodynamic elements and was the foundation for many future models. A brief description of each element used is given below:

(i) Rigid bodies
Each rigid body had both translational and rotational inertia and could be orientated in three dimensional space, undergoing arbitrarily large rotations and translations.

(ii) Spring elements
A spring element is a deformable element with only axial stiffness which may interconnect any two nodes of the system.

(iii) Beam element

A beam element has axial stiffness, torsional stiffness and bending stiffness and may interconnect any two nodes.

(iv) Hydrodynamic Element

A hydrodynamic element is a pentahedron, with the two opposing triangular faces considered to be rigid. The element is used for modelling components of the body that exert resistance primarily to compressive deformations.

The model was used primarily to study the effects of the rib cage and viscera on spinal response. However, due to the modular nature of the model it was possible to model the head and neck with the torso, rib cage and spine etc. removed. Figure 2.10 shows the approximate geometry of the model in this format.

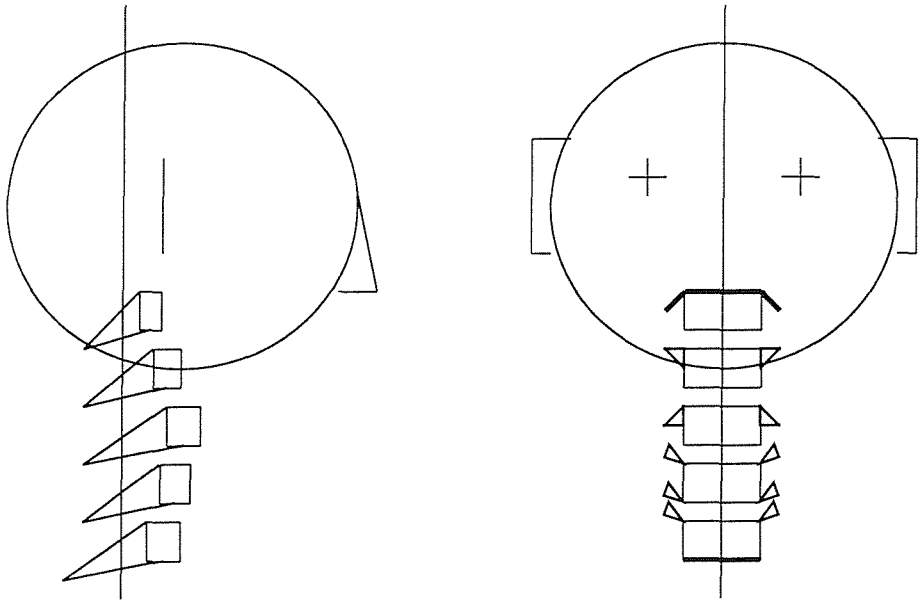

Figure 2.10 Cervical spine/head model (Belytschko *et al.*, 1976)

In the cervical spine-head model (ribs, viscera and thoracic/lumbar vertebrae removed) adjacent vertebrae were connected by elements representing the disk, the interspinous ligaments and the articular facets. The vertebrae were represented by rigid bodies, the

disks by beam elements, the ligaments by spring elements and the articular facets by hydrodynamic elements. Beam elements were also added to represent the cervical musculature. The head was modelled as a single rigid body joined to vertebra C2 by a beam element (C1 was omitted from the model). As this model was intended for pilot ejection simulations a restraint system and seat were also included in the model. These were represented by a series of spring and beam elements.

The geometrical dimensions of the model were scaled to conform to the measured averages of Lanier (1939) by Schultz and Galante (1970). The model also assumed that rotation only took place in the mid-sagittal plane. The material properties used in the model were determined from a wide variety of sources. Some estimations were also made. For example, vertebral disk stiffnesses were determined using experimental data and an approximation based upon the assumption that the stiffness varies in relation to the vertebral level geometry. Inertial properties of the cervical spine were obtained by distributing the mass uniformly at each vertebral level. The mass of the head was chosen to be 4.6 kg and the moment of inertia 400 $kgcm^2$. This was based upon the anthropometric dummy measurements of Bartz (1972).

The model was also used to represent the effect of additional head loading. A helmet in the model was assumed to be rigidly connected to the head. Hence the moment of inertia and mass of the helmet were simply added to that of the head. The helmet mass used was 1.4 kg with a moment of inertia of 100 $kg.cm^2$. The model was also used to illustrate the effect of an eccentric head loading upon the spinal response, representing a helmet-mounted device. This was achieved by including a rigidly connected 0.9 kg mass located 0.102 meters from the mid-sagittal plane.

Solutions to the model were obtained by calculating equations of motion for each element. These were solved using explicit and implicit time integration methods and by using modal techniques.

The model was used to predict the response of the spine, rib cage and complete model under ejection conditions ($10G_z$). The rib cage model was tested under frontal impact

conditions. Modal analyses were conducted on various parts of the model to obtain a better understanding of the dynamic response properties of the body.

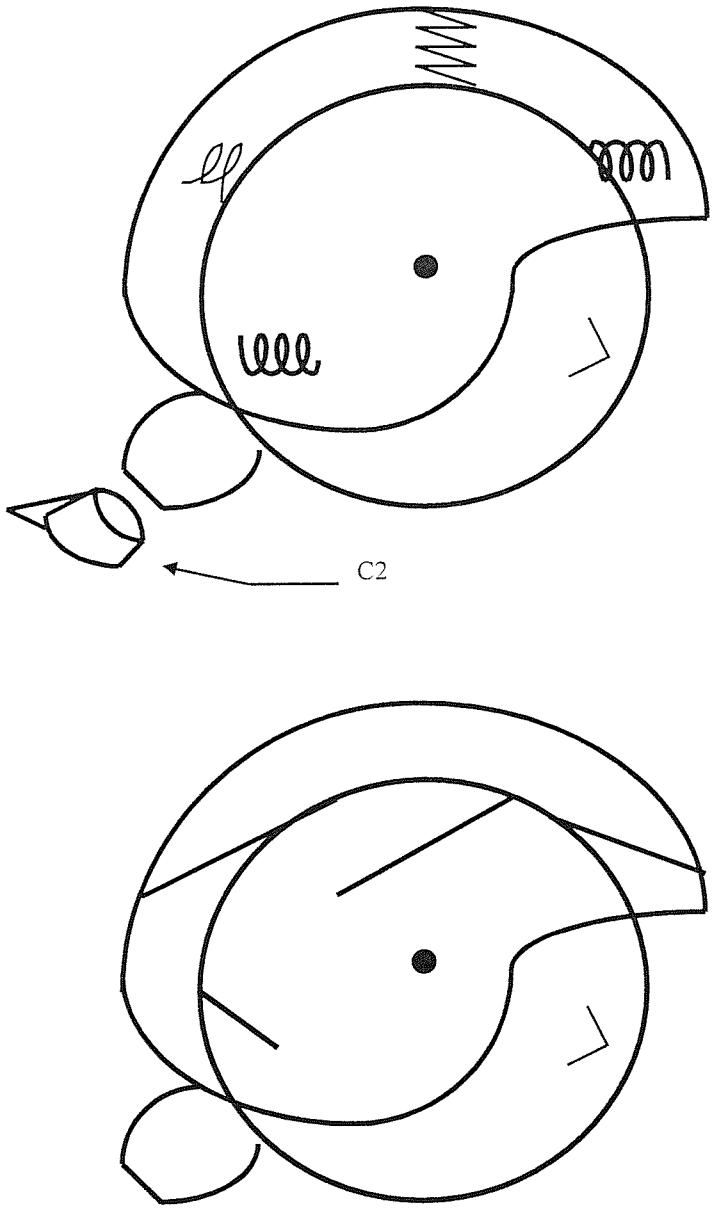

Figure 2.11 Head-helmet representation (Belytschko *et al.* 1976)

The neck-head-helmet model was used to study the effect of increased head loading. It was discovered that the force levels in the cervical spine were significantly greater when a 0.9 kg mass was added to the centre of gravity of the head.

In summary, the model developed by Belytschko *et al.* (1976) is complex. Due to the large number of elements in each section of the body it required a large amount of computational power to solve the equations of motion that were developed. Whilst it has potential for examining a wide variety of dynamic environments it should perhaps be viewed as a qualitative aid to understanding. The model was not verified with experimental data and, due to the wide scatter in the population, it would be deceptive to treat the output from the model in an absolute sense.

The helmet used in the model was assumed to move with the head. However, the authors did suggest an alternative head-helmet model, using springs to model the head-helmet interface at the scalp. Although this model never came to fruition the concept is shown in Figure 2.11.

2.6.3.3 *Privitzer*

Privitzer and Belytschko (1980) further developed the head-spine model of Belytschko *et al.* (1976) by incorporating a more detailed representation of the viscera-abdominal wall system and determining damping parameters with greater accuracy. The model was also compared to experimentally obtained driving force impedance data of human volunteer subjects (a quantity that provides information as to the excitation frequencies at which the maximum mechanical energy is transmitted into the body). The modified model, which included the viscera, was found to be in much better agreement with an experimentally obtained impedance curve produced by Vogt *et al.* (1968) than the earlier model produced by Belytschko *et al.* (1976).

Privitzer and Settecerri (1987) used the head-spine model developed by Belytschko *et al.* (1976) to study the inertial loading effects on the neck and upper spine associated with head or helmet-mounted systems. This was done as a means of estimating risk of injury in pilot ejection scenarios.

The model used a generic helmet, with a mass of 1kg and moment of inertia of 100kg.cm^2. It was assumed that the centre of gravity of the helmet was coincident with the head and that the helmet was rigidly connected to the head, thus the inertial properties were added directly to those of the head. The excitation input to the model was a half-sine acceleration profile, applied in the vertical direction and peaking at 17g after 150ms. The model identified a linear relationship between head encumbrance at a fixed location on the head and the risk of spinal injury. As the additional mass applied to the head (representing a helmet) increased, the risk of spinal injury increased.

Privitzer and Kaleps (1990) in a program investigating the inertial load effect of head-mounted devices used the 3-dimensional mathematical representation of the human head-spine torso structure developed by Belytschko *et al.* (1976). This was used to evaluate the severity of the inertial loading associated with five helmet plus mask configurations and the inertial loading caused by generic head-mounted devices when applied with a simulated aeroplane pilot ejection procedure. It was discovered that the loads developed in the neck and spine increased with increasing head loading and that the inertial loading effects of the head-mounted devices became increasingly more severe as they were located further, particularly anteriorly, from the head centre of gravity.

In each application of the original head-spine model (Belytschko *et al.* 1976) a series of simultaneous equations of motion were derived, using mass, stiffness and damping matrices and by considering the boundary conditions at the edge of each element. Computational finite element packages, such as *Ansys*, are now available to calculate and solve equations of motion, stiffness matrices etc. and produce, if required, modal or harmonic data.

Modelling the human head-neck system using finite element analysis requires an anatomical model of bone, cartilage and soft tissue. Such models can be enormous and sometimes overcomplicated. However, by introducing some lumped parameters, a manageable model can be achieved. Consequently, other authors have simplified the complex model developed by Belytschko *et al.* (1976) into lumped parameter models.

2.6.3.4 *Kitazaki*

Kitazaki (1991) simplified the continuum spine model developed by Belytschko and Privitzer (1978) for pilot ejection problems and adapted it for more comprehensive vibration problems. The simplified model was entirely linear, although the real human structure probably has non-linear characteristics such as stress stiffening of the lumbar disks and hysteretic damping of the viscera. The model used lumped parameters to represent sections of the human body. The spinal column was modelled by a series of beam elements representing the spine S1-L3, L3-T10, T10-T1 and T1-C2, with each element having axial stiffness and bending stiffness but no mass. The motion of the viscera was assumed to occur only in the axial direction and was modelled by three mass elements with translational and rotational inertia at the L5, L3 and L1 level interconnected by rod elements with axial stiffness only. The head and pelvis were modelled by elements with translational and rotational inertia and connected, respectively, to the top of the spine at the C2 level and the bottom of the spine at the S1 level by rigid links.

Modal analysis was conducted to determine the natural frequencies and mode shapes of the system. Eight modes of vibration were extracted at frequencies below 20Hz. They were dominated by a bending mode of the spine, with head fore-aft motion at 0.9Hz, a visceral mode at 3.9Hz and a buttocks mode at 5.39 Hz with vertical motion of the head. This model rigidly connected the cervical spine to the head and consequently was unable to show a pitching motion of the head.

2.6.3.5 *Harvey*

Harvey (1990a) developed a very simple lumped parameter model of the human head-neck system after consideration of the experimental 3-D head transmissibility data gathered by Paddan (1990). Also considered was the range of movement achievable by the human cervical spine from consideration of its anatomy and the frequencies of the spinal axial and flexural mode resonances as reported by Belytschko *et al.* (1976) and Prasad and King (1974). Harvey assumed that translations of the head are caused by flexion-extension of the cervical spine or translation of the whole structure due to flexural

and axial modes of the lower spinal regions. This occurs because the anatomy of the head does not allow much translation of the head relative to the axis or atlas vertebrae.

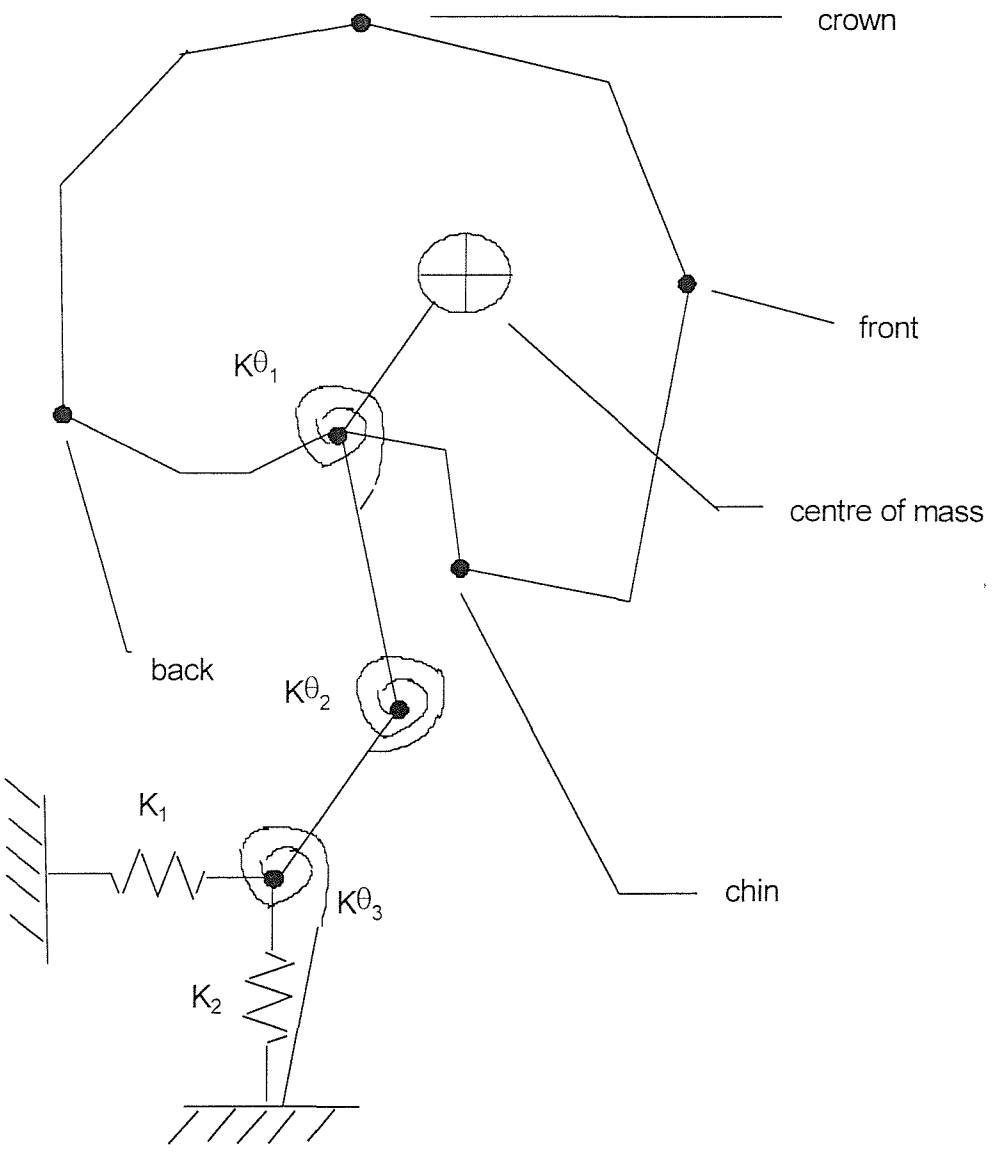

Figure 2.12 Simple model of the human neck-head-helmet system (Harvey, 1990a)

The cervical spine was modelled with two elements only, thus allowing the head to translate in both the *x* and *z*-axes. The influence of the lower spine was included in the model by grounding the base of the model with two longitudinal springs orientated in the x and y direction. The head was modelled as an area with the appropriate centre of mass and mass moment of inertia about the atlanto-occipital joint. This joint was

modelled as a pin-joint of known rotational stiffness. The form of the model can be seen in Figure 2.12.

The model parameters used in Harvey's model were based upon known physiological values where possible, as shown in Table 2.2, but some values were adjusted to make the output of the model more compatible with measured results. The source of the head moment of inertia parameter value is not explained. However, the tabulated value of 393.4kgm^2 is not correct. It is thought that the rotational stiffness of the springs in the spine are incorrect as a result.

A modal and harmonic analysis was conducted upon the model. Two of the resulting modes corresponded with the data measured by Paddan (1990) at frequencies below 10 Hz.

Harmonic analysis of the Harvey model produced transmissibilities at the front and back of the head in the vertical direction, at the chin and crown in the fore-aft direction and at the head centre of mass in the vertical and fore-aft directions. However, the transmissibilities obtained in the measured and predicted cases were not compared due to the different forcing functions. The model assumed the forcing function to be at the neck and to be uni-directional and of constant amplitude. In reality the measured data had a forcing function at the seat. Consequently the forcing function at the neck would depend upon the transmissibility from the seat to the neck and would not be uni-directional or constant at that point.

Table 2.2. Model parameters used in the neck-head model by Harvey (1990)

Head mass	6.35 kg
Body mass	100 kg
Head moment of inertia	393.4 kg.m^2
Longitudinal stiffness	K1 = 6600 N.m^{-1} K2 = 6600 N.m^{-1}
Rotational stiffness	$k\theta_1$ = 252600 N.m.rad^{-1} $k\theta_2$ = 10000 N.m.rad^{-1} $k\theta_3$ = 10000 N.m.rad^{-1}
Mode damping (z base to x head)	x1 = 0.0 % x2 = 0.0 % x3 = 7.0 % x4 = 5.0 %
Mode damping (z base to z head)	z1 = 0.0 % z2 = 10.0 % z3 = 10.0 % z4 = 23.0 %

2.6.3.6 *Woodman*

Woodman (1994) developed two biodynamic models for the neck and head system. These were almost identical to the earlier model by Harvey (1990) with some changes made to the model parameters (using more realistic values of head moment of inertia and torsional spring stiffness). It comprised a combination of point masses, rotational springs, longitudinal springs and quadrilateral areas. The form of the model is shown in Figure 2.11 (as Harvey's model) and a table of the parameters used in the two models can be seen in Table 2.3

Rotational springs were located at the atlanto-occipital joint, C7 and at a point-mid-way between C2 and C7. As in the model developed by Harvey (1990a), the centre of mass of the head was placed 0.0172m forward and 0.0364m above the atlanto-occipital joint.

Table 2.3. Parameters used in the two neck-head biodynamic models by Woodman (1994)

Parameter	Model 1	Model 2
Head mass	6.35 kg	6.35 kg
Head moment of inertia	393.4 kg.m^2	0.02 kg.m^2
Rotational springs	$k\theta_1$ = 252600 N.m.rad-1 $k\theta_2$ = 6600 N.m.rad^{-1} $k\theta_3$ = 1000 N.m.rad^{-1}	$k\theta_1$ = 2500 N.m.rad-^{1} $k\theta_2$ = 10000 N.m.rad^{-1} $k\theta_3$ = 10000 N.m.rad^{-1}

Modal analyses were conducted on both models without the longitudinal springs at the base of the neck (removing the representation of the lower spine). There were three main modes of vibration as a result of this for each model. These are summarised in Tables 2.4 and 2.5.

Table 2.4. Frequencies and mode-shapes extracted from the neck-head biodynamic model by Woodman (1994) - model 1.

Frequency	Description of mode-shape
0.56 Hz	Head pitching about base of neck (C7)
15.7 Hz	Head pitching about base of neck (C7)
57.3 Hz	Head rotating about pivot point midway between C2 and C7

Table 2.5. Frequencies and mode-shapes from the neck-head biodynamic model by Woodman (1994) - model 2.

Frequency	Description of mode-shape
3.9 Hz	Head rotating about base of neck (C7)
8.5 Hz	Head pitching about atlanto-occipital joint
13.3 Hz	Neck bowing about the mid-way point between C2 and C7

The results of the second model were compared with objective data of surface accelerations of the head measured during whole-body vibration (Paddan and Griffin

1992). The model was found to represent the fore-aft motion of the head, although the frequencies of the modes obtained in the model were slightly lower than in the experimental data. The vertical vibration of the head at about 4 Hz appeared to represent pitching of the head in the model at 3.9 Hz; the vertical motion reported at 4Hz by Paddan and Griffin (1992) was not present in the model and was assumed to be due to the motion of the lower spine. However, the model was compared only to power spectral data and not data with specific mode shapes. In addition to this, a harmonic analysis was not conducted upon the model and consequently experimental head-to-helmet transmissibility was not compared with analytical transmissibility data from the model.

Woodman (1994) also proposed a new model which included a helmet. Although this proposal was not developed the form of the proposed model can be seen in Figure 2.13. In a later study Woodman and Griffin (1995) developed a simple biodynamic model of the head and helmet system using the results of experimental studies. The model was comprised of a combination of elements: point masses, beam elements and quadrilateral areas. The scalp coupling between the head and helmet at the front and rear of the head was modelled using beam elements. The stiffnesses of these elements was determined by calculating the value of the shear stiffness of forehead skin Woodman (1995b).

As there appeared to be little slip between the helmet cushion and the scalp, it was assumed that the motion between the head and helmet was due to movement of the scalp at the front and back of the head. The relative motion in the vertical and pitch axes was not considered to be due to movement of the helmet lining. In this model, relative motion between the head and helmet in the fore and aft direction was constrained as the head was assumed to be always in contact with the helmet and there was assumed to be no compression of the scalp or helmet lining.

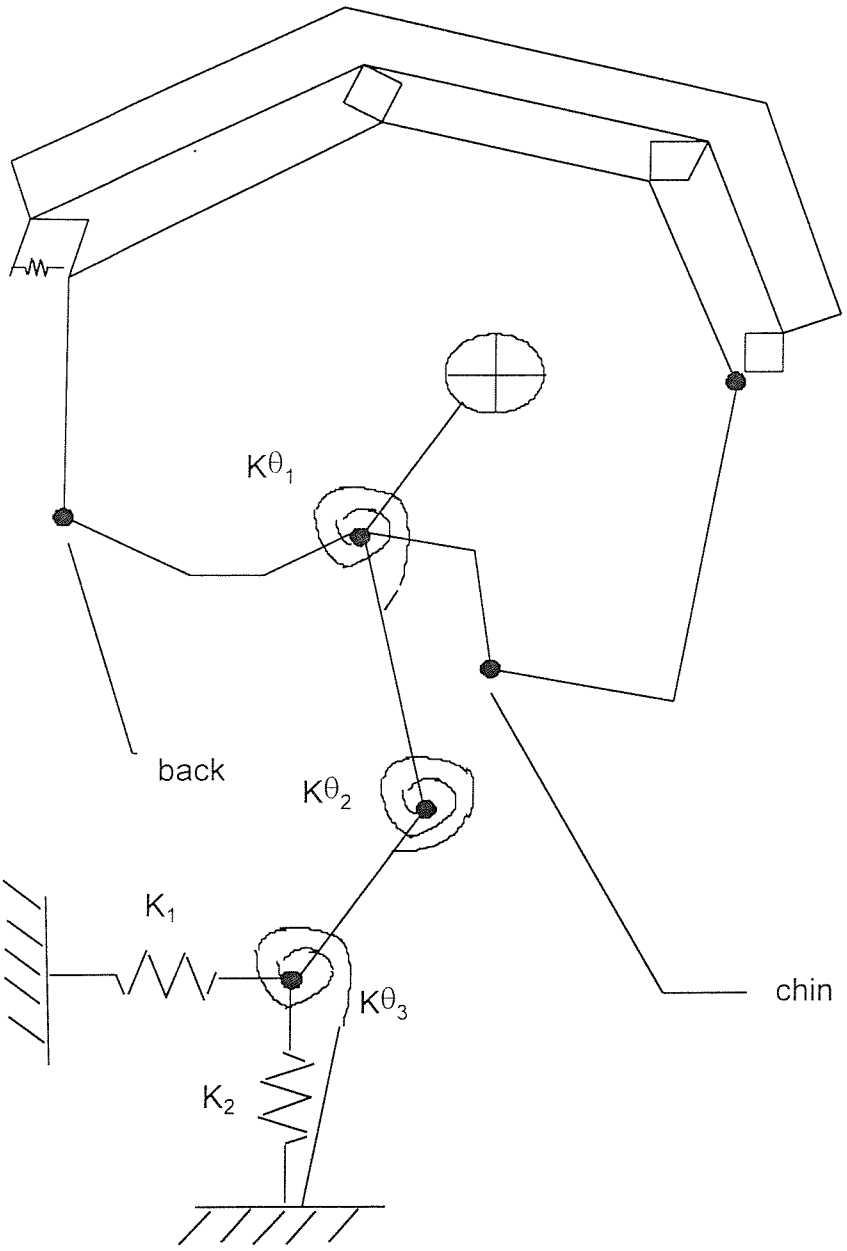

Figure 2.13 Proposed model of human head-neck-helmet system (Woodman, 1994)

Table 2.6. Model parameters for the head-helmet model

Head		Helmet		Scalp beam elements	
Mass (kg)	Moment of inertia ($kg.m^2$)	Mass (kg)	Moment of inertia ($kg.m^2$)	Young's Modulus (N/m)	Length (m)
4.632	0.002	variable	variable	1.1E4	3.0E-3

The results of the model showed that when helmet mass was increased from 1.4 to 4.2 kg the frequency of the peak in the transmissibility between pitch head motion and pitch helmet motion decreased from approximately 10 to 5Hz. Increasing the moment of inertia decreased the frequency of the peak transmission of pitch vibration from the head to the helmet in the frequency range from 2 to 12 Hz. It was also found that as helmet inertia increased it was necessary to consider the effect of the helmet on the head motion.

2.7 CONCLUSIONS

This literature review has concentrated on two main aspects of work: the measurement, quantification and analysis of motion of the human neck, head and the helmet (where appropriate) and biodynamic modelling of the neck-head-helmet system.

Helmets are worn in a number of different dynamic environments and consequently the vibration frequency, magnitude and point of entry to the body can vary. Studies have shown that when running whole-body vibration is self-induced and the vibration magnitude can exceed those recommended from a laboratory shaker platform according to ISO 2631. When jumping, the excitation into the body is impulsive resulting in transient motion of the head and helmet (if worn). In vehicles the vibration input is usually through the buttocks and is often of an approximately steady state nature. In some helicopters, however, the frequency of vibration transmission is dependent upon the main rotor blade passing frequency and motion of the head and helmet dominates at these frequencies. In the laboratory it has been shown that head motion is induced by vertical whole-body vibration and a number of external variables can influence measured motion of the head. These include differences in the subject population (age, weight etc),

posture and the use of a backrest. Therefore, careful observance is required by the experimenter when conducting this type of study maximise repeatability. The use of multiple subjects and statistical analysis of the results is also usually required.

The papers reviewed in the preceding pages have shown that motion of the head occurs in all of the above conditions (i.e. running, jumping, in vehicles and from whole-body vibration). Whilst there were some studies investigating motion of the head in a dynamic environment fewer studies were available which had also investigated helmet motion. However, the few studies that did investigate helmet motion have shown that motion of the helmet on the head does occur with the helmet either moving with or relative to the head depending upon the condition and frequency. It is therefore reasonable to assume that in all dynamic conditions where head motion occurs helmet motion is also likely to occur. There is therefore scope to quantify how the helmet moves on the head in these conditions (i.e. the direction, frequency and magnitude of motion).

When walking, the vertical motion of the head was greater than the fore-aft and lateral components of head motion. Walking speed is approximately proportional to the magnitude and frequency of the dominant vertical and pitch head acceleration. It was found that when wearing a helmet, the head acceleration was reduced in the frequency range between 2 and 5Hz. A linear relationship was established between jumping height and vertical acceleration of the head. No studies were found investigating helmet motion when jumping.

In whole-body vibration experiments most rigid-body motion of the head and helmet was located at frequencies below 10Hz. In this frequency range, helmet pitch acceleration was generally greater than head pitch acceleration. One study investigating the head response to vertical whole-body vibration identified three resonances of the head; at 3, 4.5 and 6.5Hz. Studies investigating the effect of helmet mass on head and helmet motion have shown that the transmissibility of pitch acceleration from head to helmet decreased with increasing helmet mass. One study has also shown that the peak in this frequency is partially controlled by the shear stiffness of the skin at the head/helmet coupling point on the scalp. This would suggest that there is a mode of vibration of the

helmet on the head. It is hypothesised that the frequency of this mode is controlled by helmet mass and scalp stiffness.

Studies investigating the effect of helmet mass and distribution of mass on motion of the neck and head, particularly during pilot ejection scenarios, have shown that as helmet mass increases, the forces and moments in the neck-head system (and consequently risk of injury) can increase. This is particularly associated with forward shifts in the helmet centre of gravity.

There have been a number of mathematical models developed to represent the spine, the spine-neck-head and the head and helmet in a number of simulated dynamic conditions. All head-helmet models, with the exception of the simple model by Woodman and Griffin (1995) have assumed that the helmet is rigidly attached to the head. This is an over-assumption in all instances except at very low frequencies as experimental work has shown that the stiffness of the skin at the forehead can affect head to helmet pitch transmissibility.

The scope of the work in this thesis was therefore to quantify head and helmet motion in running and jumping conditions. The justification for this is that head motion occurs when running and jumping and consequently there must also be motion of the helmet (if worn). The lack of suitable background literature in this area also makes it a suitable target for investigation. There is scope to further investigate the relationship between the scalp-helmet coupling and helmet mass upon the frequency of helmet pitch motion and their relationship with a hypothesised mode of vibration of the helmet on the head. There is also scope to use experimental findings to assist in the development of a new mode of the neck-head-helmet system, representing the helmet as an element independent to the head.

CHAPTER 3. HEAD AND HELMET MOTION WHILST RUNNING

3.1 INTRODUCTION

Compared with whole-body vertical vibration when seated, the motions occurring during running and walking are clearly complex. The pelvis oscillates in the xz and xy planes with alternate steps to a marked degree and the abdominal muscles are probably under greater tension than would be experienced in whole-body vibration (Sandover, 1975).

There have been various studies to investigate the effects of walking on acceleration at different parts of the body and the transmission of vibration between them. Concern was expressed regarding the level of vibration that was produced in walking or running conditions compared with the whole-body vibration levels that were obtained from agricultural and industrial machinery and vehicles (Sandover, 1975).

The literature review in Chapter 2 showed that studies investigating the effect of a helmet on head motion whilst running are scarce. However, movement of the head alone when running is relatively well documented. Many studies show vertical acceleration of the head to be the dominant translational motion which tends to increase in both magnitude and frequency as the running speed increases (Capozzo, 1982).

Previous researchers have made reference to the apparent 'self-induced vibrations' that occur when walking (Simic, 1970, Capozzo, 1982). It has been shown that the levels of whole-body vibration that occur within the body when running are much greater than maximum recommended at a vibrator platform (Sandover, 1975). It would appear that the human body has a unique way of balancing the body when running to conserve energy and to run in a smooth and co-ordinated manner. It is suggested that the head, which moves sinusoidally in the fore-aft direction and increases in magnitude with increasing running speed could act in a similar manner to a dynamic absorber in a mechanical system.

One study investigating the effect of a helmet on head motion showed that wearing a helmet increased the magnitude of the dominant vertical and pitch head acceleration which occurred at the stepping frequency and tended to reduce head accelerations over the frequency range between 2 and 5 Hz (Woodman, 1995a).

The aims of this study were to further investigate head and helmet motion whilst running. In particular a comparison has made between head and helmet motion in each direction of motion in the frequency domain and the relationship between motion of the head and motion of the helmet when running has been studied.

A series of experiments has been conducted with running subjects. The subjects wore a standard British Army Mk VI Combat Helmet and a prototype helmet, both supplied by the Defence Clothing and Textiles Authority. The prototype helmet was designed around a Mk VI helmet but with modifications to allow for the provision of ear defenders and cheek pads. The motions of the head and helmet were measured using a bite- bar and helmet bar and the prototype helmet was used to determine the effect of chin straps, ear defenders and cheekpads on the measured motions of the head and helmet.

3.2 INSTRUMENTATION

Head motion was measured using an instrumented bite-bar. Helmet motion was measured using a similar instrumented bar. The masses of the bite-bar and helmet-bar, including accelerometers, were 180g and 90g respectively.

The instrumented bars housed six translational accelerometers to measure six axes of motion of the head and helmet. Rotational accelerations (roll, pitch and yaw) were determined from signals provided by pairs of translational accelerometers. Miniature Entran EGCS piezo-resistive accelerometers were used in the bite-bar and helmet bar. These were conditioned by a 16 channel *HVLab* Techfilter system and the data was acquired and processed using *HVLab* software.

3.3 EXPERIMENTAL METHOD

Twelve male subjects (median age 24 years 8 months, weight 74.63 kg and height 181.8cm) participated in the experiment. Measurements were made whilst running on the spot[1] at a rate of 120 steps per minute in durations of one minute. The helmet was fitted to the head with the chin strap securely fastened.

---

[1] Running-on-the spot conducted to provide controllable experimental conditions- it is not known how closely this represents 'genuine' running.

A total of five helmet conditions were tested. These were a British Army Mk VI combat helmet and the prototype helmet in four configurations. These were with chinstrap, ear defenders, cheekpads and with all three combined.

Subjects were asked to wear standard issue Army assault combat boots and socks during the running experiment as previous studies have shown that wearing boots reduces the acceleration magnitude at the head and helmet. The subjects were instructed to run on the spot in time to a metronome, lifting their knees and contacting the floor first with their toes.

Data acquisition and analysis were conducted with a *HVLab* Techfilter system. The data acquisition sample rate was 256 samples/s and the data were filtered at 100 Hz. The accelerations at the head and helmet were determined for the full 60 second period of running. Spectra were determined with a resolution of 0.25 Hz, giving 64 degrees of freedom.

3.4 CALIBRATION

The accelerometers were calibrated using three types of test. The first calibration was a static test which involved turning the sensitive axis of the accelerometer through the Earth's gravitational field (±1*g*). The second calibration was a jerk calibration to determine the correct polarity of the system (e.g. accelerometer, cabling, signal conditioning, software package). The third calibration was a dynamic calibration to verify the relative sensitivities of the accelerometers. This was performed by shaking the accelerometers together in their sensitive axes.

3.5 ANALYSIS

The analysis conducted was based upon analysis of the individual time-histories of data measured on a single subject wearing the Mk VI combat helmet and the power spectral densities of the acceleration measurements made on subjects wearing the prototype helmet in its four different configurations.

The power spectral densities were compared statistically at discrete frequencies using the Wilcoxon matched-pairs signed ranks test for statistical differences between individual conditions.

Mean power spectral densities (of twelve subjects) were calculated. This function was used after comparison of individual subject power spectral densities. Inter-

subject variability was found to be good and consequently it was considered acceptable to use the mean function.

3.6 RESULTS

The results of this study are presented in two sections, as acceleration time-histories and as power spectral densities.

3.6.1 Analysis of the acceleration time histories of a single subject

The acceleration time histories, in all directions of motion, at the head and helmet are shown in Figure 3.1.

Comparing head translational acceleration in all three directions, it can be seen that motion occurring at the head was approximately sinusoidal in all cases. Head vertical acceleration was near sinusoidal and was dominant showing motion occurring at 2Hz, the running frequency. Acceleration of the head in the lateral direction had the lowest peak-to-peak amplitude and the greatest range of frequency content. Acceleration in the head fore-aft direction was periodic and repeatable.

Rotational acceleration of the head was dominant in the pitch direction. The waveform shows a repeatable pattern of motion. However, the acceleration was not sinusoidal and a number of frequencies were contained within the waveform. Head roll and yaw motion were not insignificant, although of lower magnitude than head pitch acceleration.

The helmet vertical acceleration was almost identical to the head acceleration in waveform shape and magnitude. This indicates that the head and helmet moved together in the vertical direction when running. The helmet fore-aft time-history showed repeatable but non-sinusoidal acceleration. When compared to the fore-aft head acceleration time history it can be seen that the head moved in opposite phase to the helmet and the helmet had greater acceleration amplitude. Rotational motion of the helmet was not dissimilar to rotational motion of the head. However, it is apparent that the peak-to-peak acceleration in the helmet pitch direction was greater than the peak-to-peak acceleration in the head pitch direction.

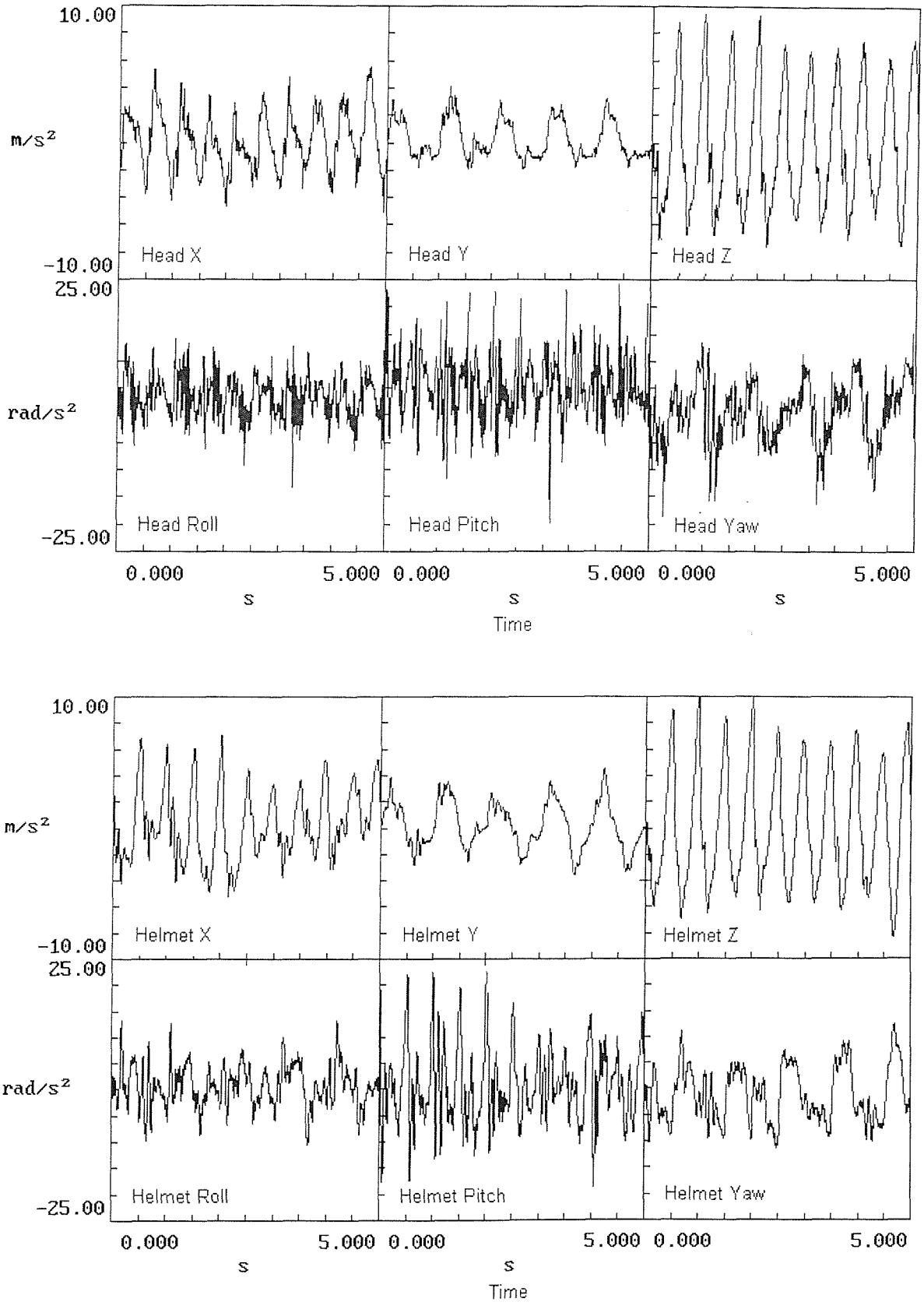

Figure 3.1 Time histories measured at the head and helmet of a single subject in six axes of motion (Mk VI Helmet with chinstrap fastened)

3.6.2 Results from the mean power spectral densities of head and helmet motion

The mean power spectral densities of acceleration measured at the head and helmet of 12 subjects when running is shown in Figure 3.2. Each chart in the figure compares the power spectral density at the head and helmet in each direction of motion.

The Wilcoxon matched-pairs signed ranks test for statistical differences between individual conditions was performed at frequencies identified as being 'of statistical significance' ($p<0.05$) from Figures 3.2 to 3.5. All observations and conclusions made in the remainder of this chapter were statistically significant.

It can be seen in all directions that largest peak in power spectral density occurred at 2Hz. This was the running excitation frequency. The pitch and lateral directions of motion also showed harmonics at 4, 6 and 8 Hz. Comparing charts for head and helmet in each direction of motion in turn shows that there was little difference in motion between head and helmet in the fore-aft direction. In the lateral direction there was more acceleration at the helmet than at the head at 2Hz. The head and helmet had similar levels of vibration at 2Hz in the vertical direction – indicating no attenuation or transmission in acceleration from head to helmet in this direction.

In the rotational directions of motion acceleration was attenuated in the roll direction as it travelled from head to helmet and similar levels of yaw motion were seen at the head and helmet. It was apparent that at 2 and 4 Hz vibrational energy was readily transmitted to the helmet pitch direction.

3.6.3 Comparison between head and helmet power spectral densities with differing helmet attachments

Figures 3.2 to 3.5 show the mean power spectral densities of head and helmet acceleration in each direction of motion for the four configurations of helmet. Comparison of the figures enables the effect of individual helmet attachments (e.g. ear defenders, cheek-pads etc) to be determined.

It can be seen that acceleration in the helmet pitch direction was dominant. Helmet pitch acceleration was invariably greater in amplitude than head pitch motion. This was true for all conditions, with the exception of condition 4 – all helmet fastenings

fitted together. In condition 4 helmet pitch motion was greater than head pitch motion, but to a smaller extent. This indicates that the chin strap, cheek pads and ear defenders all act together to reduce the pitch motion of the helmet.

Motion at the head and helmet in the vertical direction occurred with approximately the same amplitude in all conditions. Translational acceleration was dominant in the vertical direction and it would appear that at the 2Hz driving frequency the helmet moved rigidly with the head. The presence of chinstrap, cheek pads and ear-defenders had little effect upon vertical helmet motion at this frequency.

Extra helmet attachments had little effect in reducing relative fore-aft acceleration between head and helmet. It was not possible to discern a difference in magnitude between power spectral densities of head and helmet in this direction.

Insignificant levels of lateral head acceleration were measured. However, in all conditions a greater magnitude of helmet lateral acceleration was seen (at 2 Hz), although the amplitude of this was insignificant when compared to other motion occurring in the fore-aft and vertical directions. The helmet attachments did not reduce the amplitude of the motion in this direction.

Head roll motion was of greater amplitude than helmet roll motion. However, both ear defenders and cheek pads reduced these relative differences. Ear defenders reduced the level of head yaw motion relative to the helmet. However, roll and yaw motion, in all conditions, were of a much smaller amplitude than pitch motion of the head and helmet.

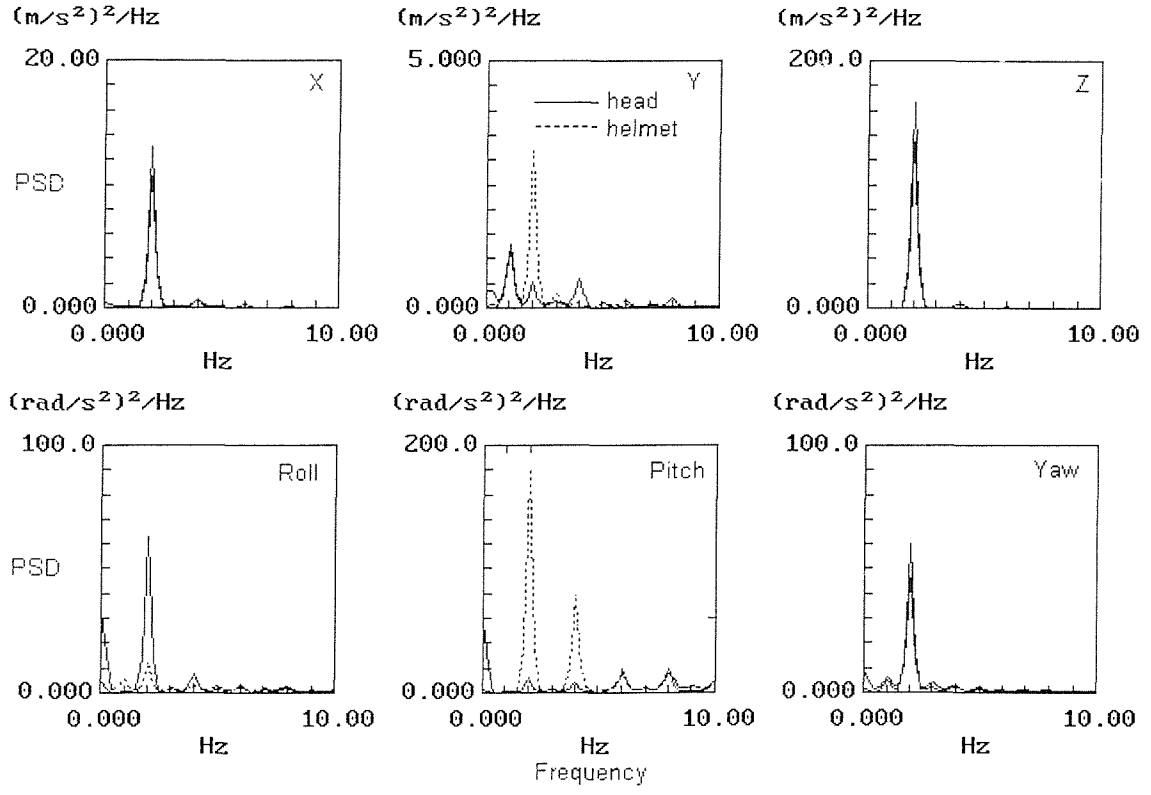

Figure 3.2 Power spectral densities of head and helmet acceleration (Prototype helmet with chin strap)

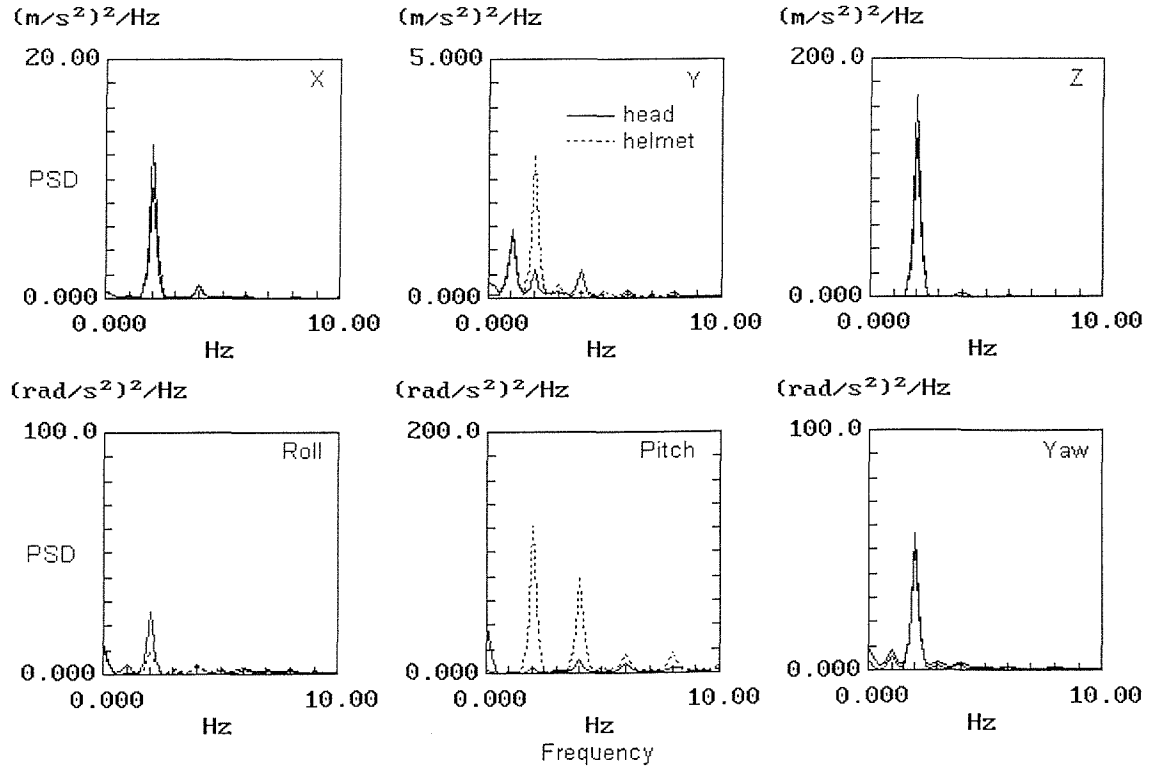

Figure 3.3 Power spectral densities of head and helmet acceleration (Prototype helmet with cheek pads)

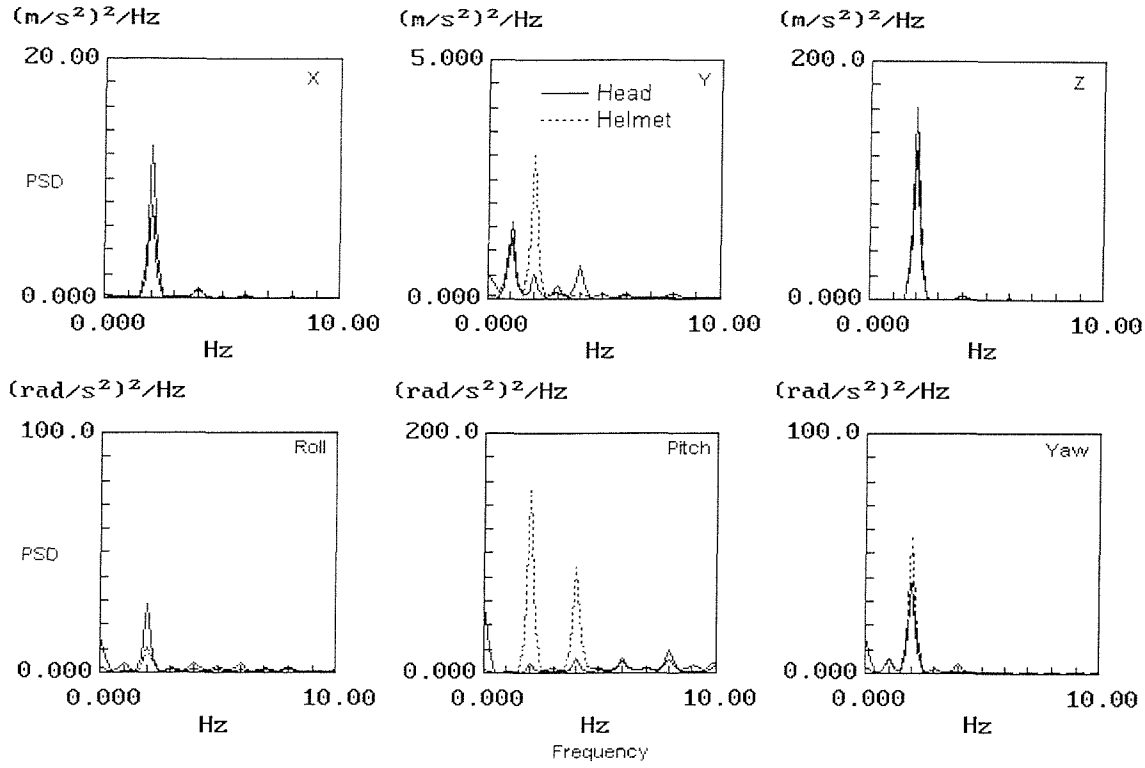

Figure 3.4 Power spectral densities of head and helmet acceleration (Prototype helmet with ear defenders)

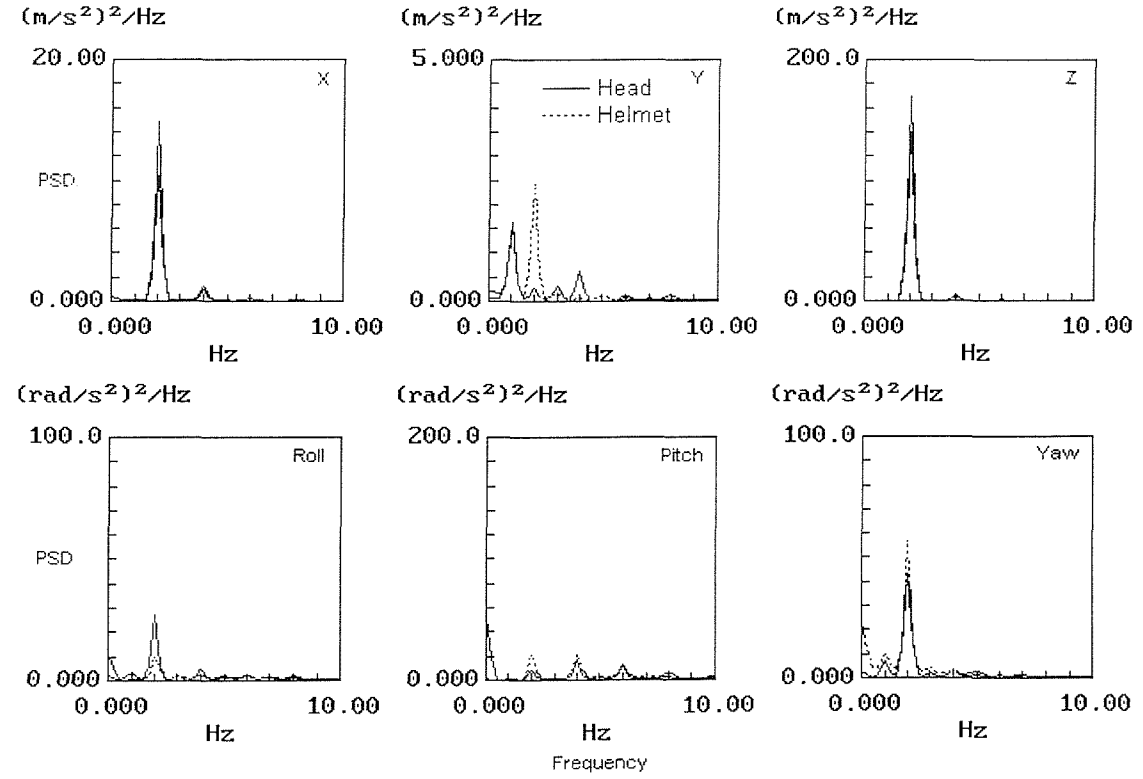

Figure 3.5 Power spectral densities of head and helmet acceleration (Prototype helmet with chin strap, cheek pads and ear defenders)

3.7 DISCUSSION AND CONCLUSIONS

These initial experiments have shown that both translational and rotational motion of the head and helmet occurred when running. The greatest amount of acceleration, in all directions of measurement, occurred at the running speed or excitation frequency. This agrees with the work conducted by Rao and Jones (1974), who identified a peak in head motion at between 1.2 and 2Hz when walking and relates to the conclusions of Capozzo (1982) who noted that vertical acceleration of the head shifted towards higher frequencies as walking speed increased.

Vertical acceleration was found to be the most dominant translational acceleration of the head, followed by fore-aft and lateral acceleration. The power spectral density amplitudes of the motion at 2Hz were in approximate agreement with the z:x:y = 1:0.8:0.5 ratio found by Simic (1970). Consequently, the vertical component of head acceleration was very much greater than the horizontal component, as shown also by Cappozzo (1982). The head vertical acceleration was near sinusoidal, indicating that vibration is transmitted through from the legs through the spine and into the head with little attenuation. All other directions of motion showed time-histories with a regular continuous pattern, but with a greater spectral content.

Rotational acceleration of the head and helmet was most dominant in the pitch direction, showing that the dominant motion of the head and helmet occurred in the mid-sagittal plane (in the pitch, fore-aft and vertical directions). The helmet moved rigidly with the head at 2Hz in the vertical direction. In the fore-aft direction the helmet and head had an approximately equal amplitude, but appeared to move in opposite phase. This would indicate the possibility of a mode of vibration of the helmet on the head. Further investigation is required, however, to confirm this. Pitch motion of the helmet was, in most cases, considerably greater than head pitch motion at 2 and 4 Hz. However, helmet pitch motion was significantly reduced when cheekpads and ear-defenders were fitted to the helmet.

CHAPTER 4 HEAD AND HELMET MOTION WHILST JUMPING

4.1 INTRODUCTION

Jumping introduces shocks and impulses into the body and skeletal system which are unlike the periodic signals seen when walking and running. It could be proposed that the acceleration response at the head and helmet (if worn) would produce a greater acceleration and displacement when jumping than in any of the other ambulation conditions due to the additional shocks introduced into the body that are not present when walking or running.

The previous chapter has shown that movements of the head and helmet are dominated by pitch motion and motion in the mid-sagittal plane at frequencies equivalent to the running excitation frequency.

This chapter has continued the work of the previous chapter by investigating the motion of the head and helmet under jumping conditions. Two experiments were conducted to investigate the motion occurring at the head and helmet when jumping-on-the-spot and transient jumping from height.

4.2 EXPERIMENT 1. HEAD AND HELMET MOTION WHILST JUMPING-ON-THE-SPOT

4.2.1 Introduction

This first experiment was conducted to investigate the effect of jumping rate and helmet type and condition on the motions of the head and helmet. Twelve male subjects were used in the experiment and they were asked to jump-on-the-spot in time to a metronome at rates of 80, 100 and 120 steps per minute. Three experimental conditions were tested: no helmet, Mk VI combat helmet with chin strap fastened and prototype helmet with chin strap fastened. It a suitable hypothesis was; fitting a helmet to the head would result in a reduction in head acceleration and the peak in power spectral density measured at the head and helmet would occur at a frequency equivalent to the initial jumping rate.

4.2.2 Instrumentation

Head motion was measured using an instrumented bite-bar (see Figure 2.2). This was modified to allow for the chin bar on the prototype helmet. Consequently head motion was measured at the chin in these experiments. Motion of the helmet was measured using a similar bar. Figure 4.1 shows the approximate location of the bite-bar on the head.

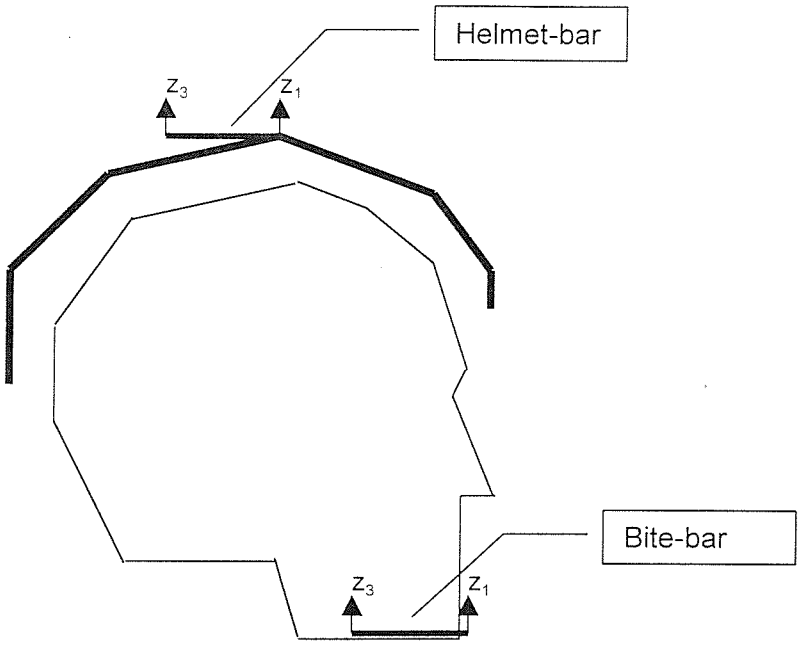

Figure 4.1 Location of helmet and bite-bars.

4.2.3 Experimental method

Twelve subjects participated in the experiment. They were all students or members of staff of Southampton University in the age range between 18 and 25 years with no medical conditions and no history of back or leg injury or pain. Measurements were made in the three following helmet conditions:

1. no helmet
2. standard Mk VI Combat Helmet with chin strap fastened
3. prototype helmet (supplied by the DCTA) with chin strap fastened

The subjects were asked to wear standard-issue Army assault combat boots and were instructed to jump on-the-spot in time to a metronome, at 80, 100 and 120 steps/min for

durations of half a minute with each helmet condition. Subjects were asked to concentrate on their jumping style; keeping both feet together, landing on their toes and keeping their knees as straight as possible.

The order of presentation of the three conditions was balanced across subjects using the Latin squares method.

Data acquisition and analysis were conducted using an *HVLab* Techfilter system. The data acquisition sample rate was 100 samples/sec and the data were filtered at 30Hz. The accelerations at the head and helmet were determined for the full 30 second period of jumping. Spectra were determined with a resolution of 0.25Hz, giving 48 degrees of freedom.

4.2.4 Calibration

Miniature Entran EGCS piezo-resistive accelerometers were used in the experiment as these are capable of accurate low frequency measurements. They were calibrated using two methods. The first calibration was a static test which involved turning the sensitive axis of the accelerometer through the Earth's gravitational field ($\pm$ 1*g*) and adjusting the gain and offset as required. The second calibration was a dynamic calibration to verify the relative sensitivities of the accelerometers. This was performed by shaking the accelerometers together in their sensitive axes.

4.2.5 Analysis

Power spectral densities were calculated for each subject, in each direction of motion. Data were analysed in the mid-sagittal plane directions only (i.e. fore-aft, vertical and pitch) at both the head and helmet.

Each power spectral density was compared statistically for each direction at discrete frequencies across all twelve subjects using the Friedman two-way analysis of variance test for overall statistical differences between all three conditions and the Wilcoxon matched-pairs signed ranks test for statistical differences between individual conditions. A criteria of 5% (i.e. $p<0.05$) was required for statistical significance and differences outside this criteria are not included in the discussion in the results section below.

Mean power spectral densities (of twelve subjects) were calculated. This function was used after comparison of individual power spectral densities. Inter-subject variability was found to be good and consequently it was considered acceptable to use the mean function.

4.2.6 Results

4.2.6.1 Effect of jumping rate

Figures 4.2, 4.3 and 4.4 show the variation in head and helmet motion for each helmet condition (no helmet, Mk VI helmet and prototype helmet, respectively). Each figure shows the mean data from twelve subjects in each direction of motion. The response to each jumping rate in each direction of motion at frequencies between 0 and 10Hz is shown in each graph.

Figure 4.2 shows the effect of jumping rate in each direction when a helmet was not worn. It is apparent, in each direction of motion, that a peak in the power spectral density occurred at each jumping rate. In the head pitch direction significant peaks from harmonics were also seen at higher frequencies.

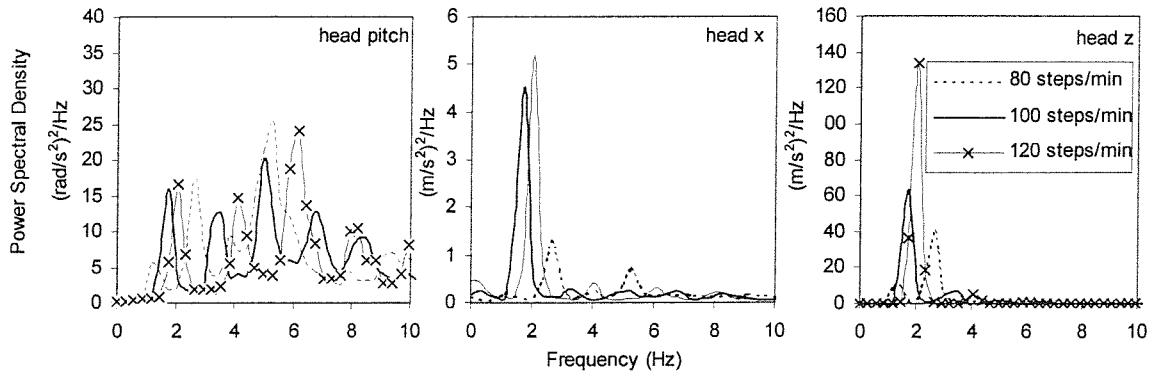

Figure 4.2 Effect of jumping rate on head motion (no helmet, mean of 12 subjects)

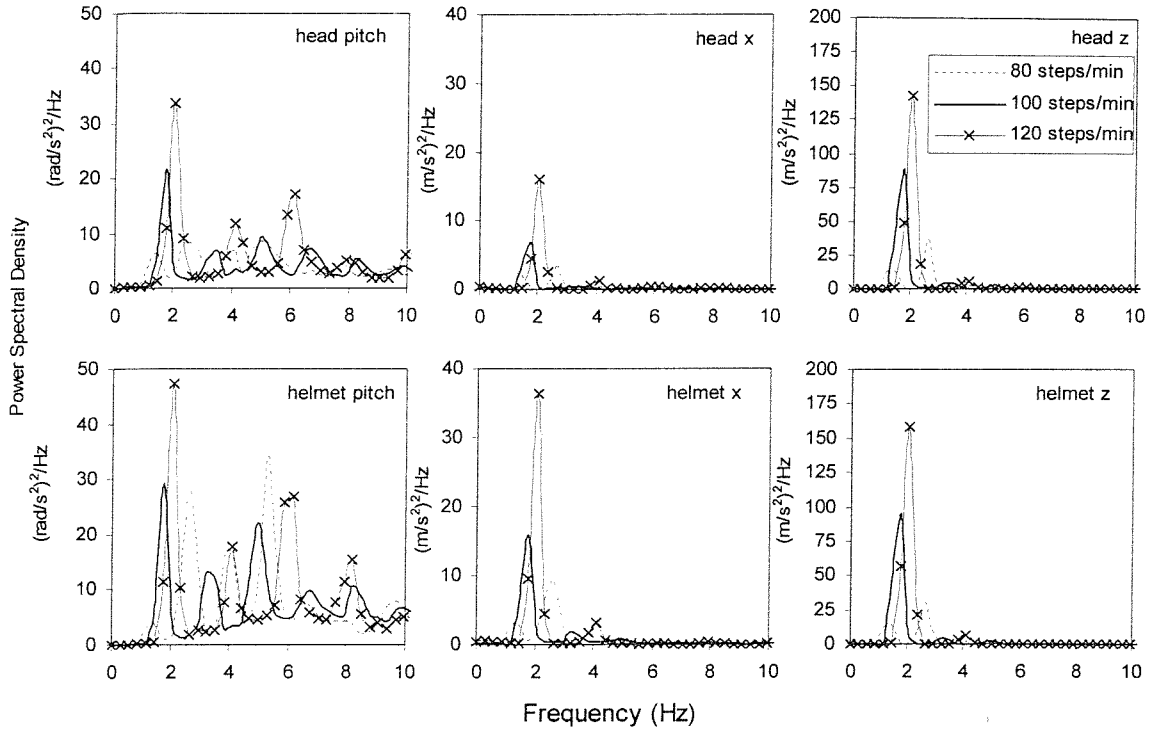

Figure 4.3 Effect of jumping rate on head and helmet motion (Mk VI helmet, mean of 12 subjects)

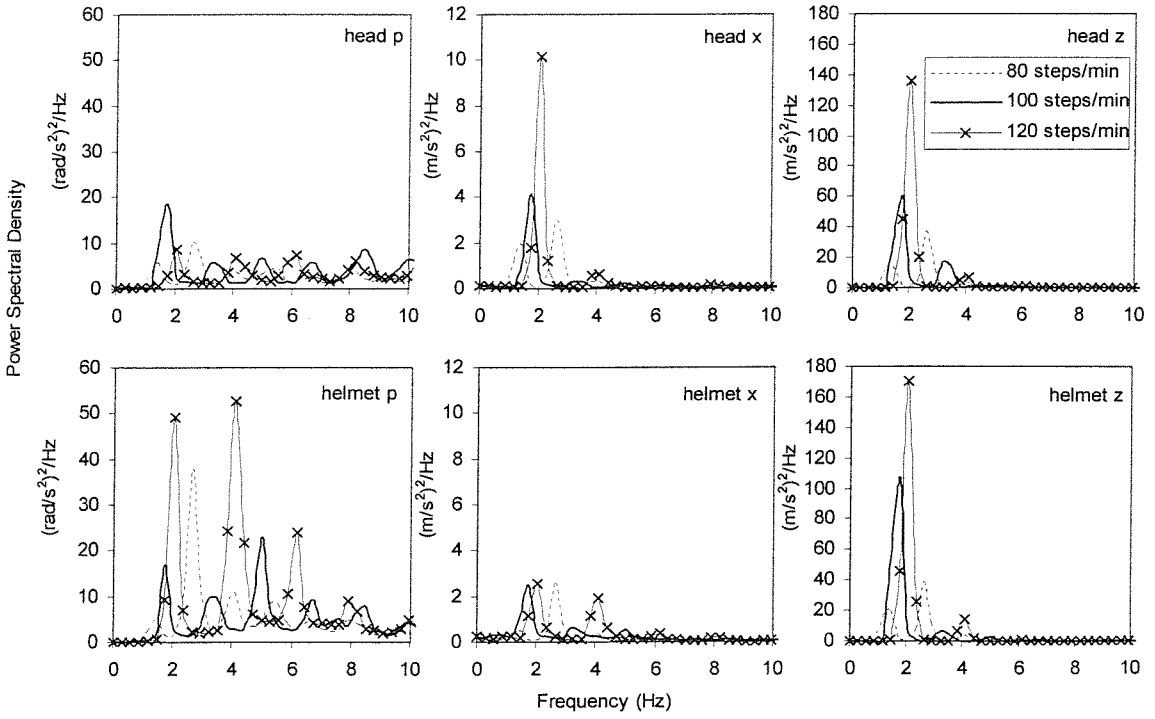

Figure 4.4 Effect of jumping rate on head and helmet motion (prototype helmet, mean of twelve subjects)

The head response when the Mk VI helmet and prototype helmets were worn (Figures 4.3 and 4.4) was consistent with the response obtained when no helmet was worn. A peak in the power spectral density was present at frequencies representative of each jumping rate. The amplitudes of motion in the head and helmet pitch and vertical directions were greater than the amplitudes in the fore-aft axes. The response in the pitch direction at the head and helmet showed some harmonics of the fundamental jumping frequency. In most directions of motion the magnitude of the motion at the jumping frequency increased with jumping rate.

4.2.6.2 Effect of helmet type

Figures 4.5, 4.6 and 4.7 show the changes that occurred to the response of the head when a helmet was worn. Each figure shows the median data from twelve subjects in each direction of motion at discrete frequencies. The difference between helmet conditions in each direction of motion at frequencies between 0 and 10Hz is shown.

At 80 jumps/min (Figure 4.5) placing a helmet on the head did not significantly increase the head vertical acceleration. Head fore-aft acceleration increased substantially when either helmet was placed on the head. Placing a helmet on the head did not change the power spectral density at the head in the pitch direction at the jumping frequency. It did, however, reduce the head pitch acceleration amplitude at frequencies between 2.5 and 10Hz (harmonics of the jumping frequency).

When comparing differences in helmet motion due to the type of helmet, it was apparent that the greatest amount of helmet acceleration at 2.5Hz at the helmet in the vertical direction occurred when the prototype helmet was worn. The greatest amount of acceleration at 1.3, 2.5 and 4.5Hz in the helmet fore-aft and helmet pitch directions occurred when the Mk VI helmet was worn. These differences are probably attributed to differences in the mass and distribution of mass on the two helmets.

At 100 jumps/min (Figure 4.6) adding a helmet to the head reduced the head pitch acceleration at frequencies between 3 and 7Hz.

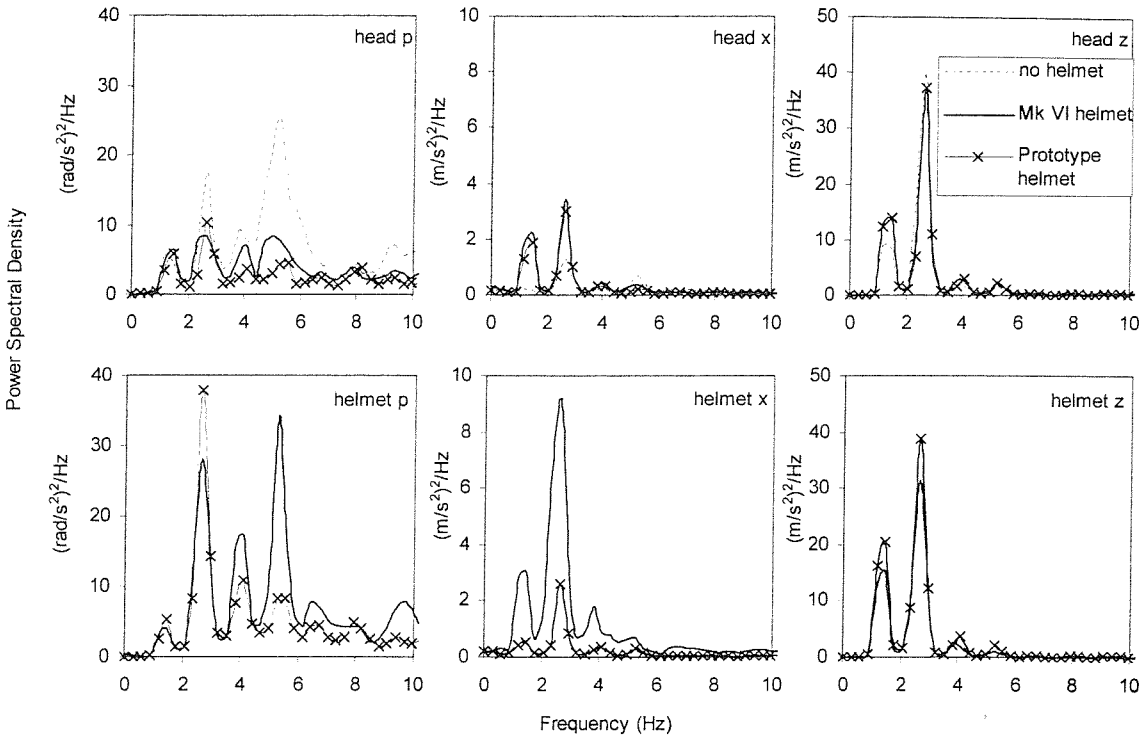

Figure 4.5 Effect of helmet type on head and helmet motion at 80 jumps/min (mean of 12 subjects)

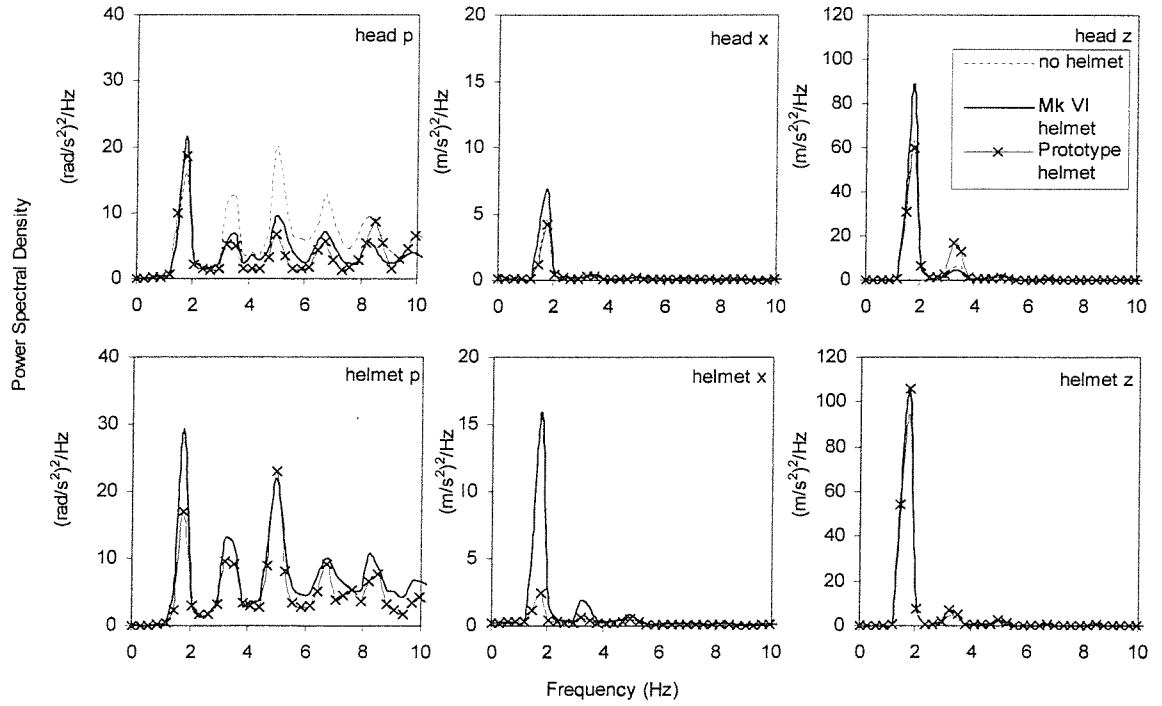

Figure 4.6 Effect of helmet type on head and helmet motion at 100 jumps/min (mean of 12 subjects)

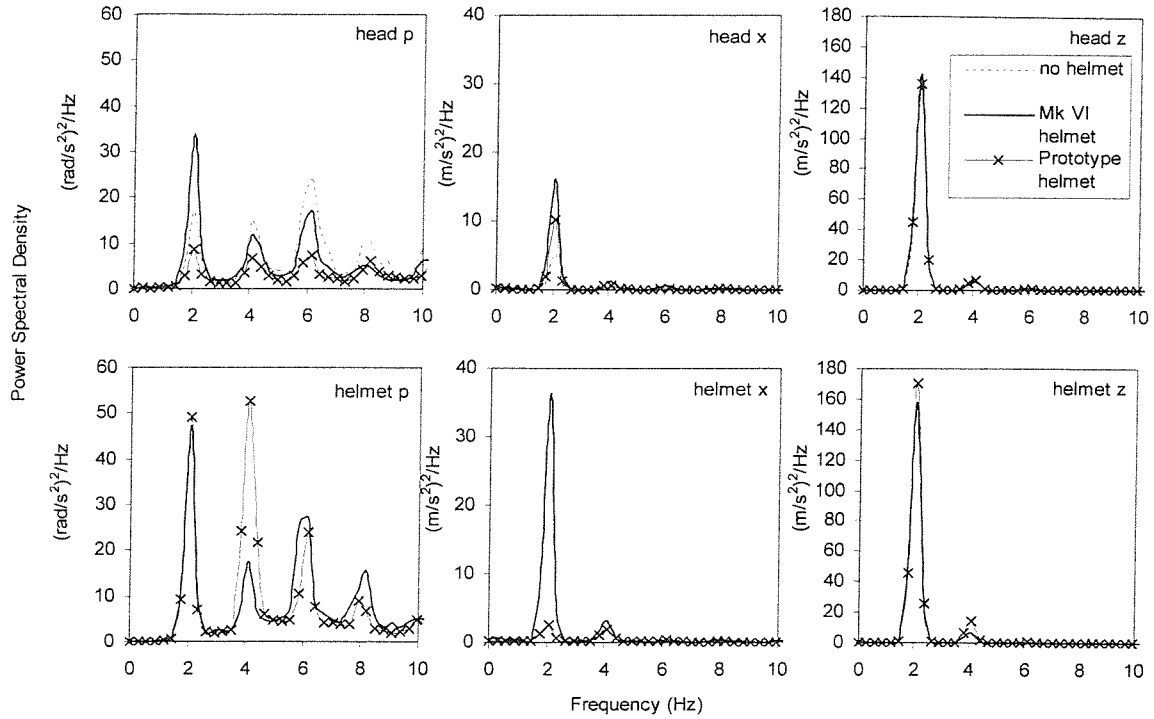

Figure 4.7 Effect of helmet type on head and helmet motion at 120 jumps/min (mean of 12 subjects)

At 120 steps per minute acceleration in the head vertical direction was not affected by helmet condition. In the head fore-aft direction, the Mk VI helmet condition had greater acceleration at 2Hz (the excitation frequency) than the prototype helmet . In the head pitch direction the Mk VI helmet was dominant at 2Hz. The no helmet condition dominated at 4 and 6Hz.

There were peaks in the acceleration of the helmets in the vertical direction at 2 and 4Hz (excitation frequency and 1st harmonic) with the prototype helmet dominant in both. Helmet fore-aft motion showed significant peaks in power spectral density at 2 and 4Hz and showed the Mk VI helmet to be dominant over the prototype helmet. The prototype helmet had dominant acceleration in the pitch direction at 2 and 4Hz.

4.3 *EXPERIMENT 2. THE EFFECT OF TRANSIENT JUMPING FROM DIFFERENT HEIGHTS ON HEAD AND HELMET MOTION*

4.3.1 Introduction

In the second jumping experiment, subjects were asked to jump from three different heights onto a concrete floor in two experimental conditions (no helmet and prototype helmet). The transient response produced at the head and helmet (if worn) was analysed in the mid-sagittal plane directions.

4.3.2 Method

The same subjects were used in the second experiment as in the first jumping experiment. Two experimental conditions were used: subjects wearing no helmet and subjects wearing the prototype helmet. Each subject was asked to jump six times from each of three heights: 20, 40 and 60cm landing onto a concrete floor, for each of the two helmet conditions. Data were measured at the head and helmet in the same way as the first experiment.

4.3.3 Analysis

Each jump produced a transient time-history similar to the one shown in Figure 4.7. The most convenient method of analysing the data was considered to take the peak of the time-history (showing the maximum response at the particular location in the direction of measurement) and calculate the mean value of the six jumps from each height, helmet condition and direction of measurement for each subject. The overall mean of this value was then calculated for all subjects. This method is not ideal as the peak is influenced by the sample rate of the measurement. In the experiment the sample rate was 100Hz and the data was low-pass filtered at 33Hz. This was considered adequate for this initial experiment.

Each peak in acceleration amplitude was compared statistically in each direction across all twelve subjects using the Friedman two-way analysis of variance test for overall statistical differences between all three conditions and the Wilcoxon matched-pairs signed ranks test for statistical differences between individual conditions. All results discussed had a statistical significance of $p<0.05$.

4.3.4 Results

Figure 4.8 shows a typical time-history that was obtained during the jumping from height experiments. The time history shows the different stages throughout the jump. These were the initial launch, the drop and then the impact on the floor and the transient head and helmet motion resulting from the impact.

Figures 4.9a & 4.9b shows the median peak accelerations for each jump. They are broken into groups for each direction of head and helmet motion, each helmet condition and each height jumped.

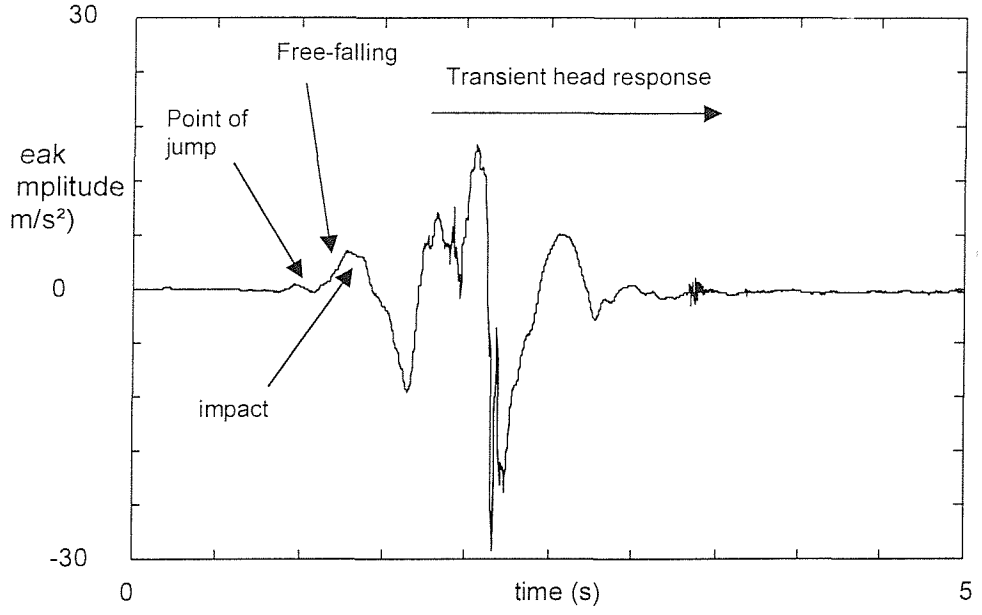

Figure 4.8 Graph of typical time history when jumping from height (vertical head acceleration)

4.3.4.1 Differences between head and helmet

Figures 4.9a and 4.9b show the differences in motion at each direction of the head and prototype helmet. There were no statistical differences between the response at the head and the response at the helmet in the vertical direction, supporting the evidence that the head and helmet move together at low frequencies in the vertical direction. In both the fore-aft and the pitch directions at all three jumping heights there was a lower peak acceleration amplitude at the helmet than at the head.

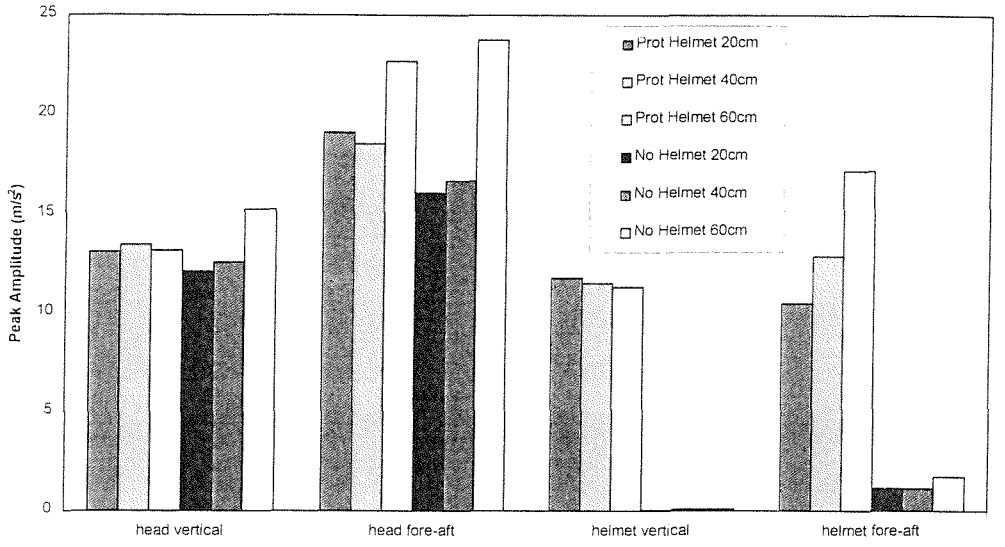

Figure 4.9a Peak translational acceleration magnitudes when jumping from 20, 40 and 60cm (Median of 12 subjects)

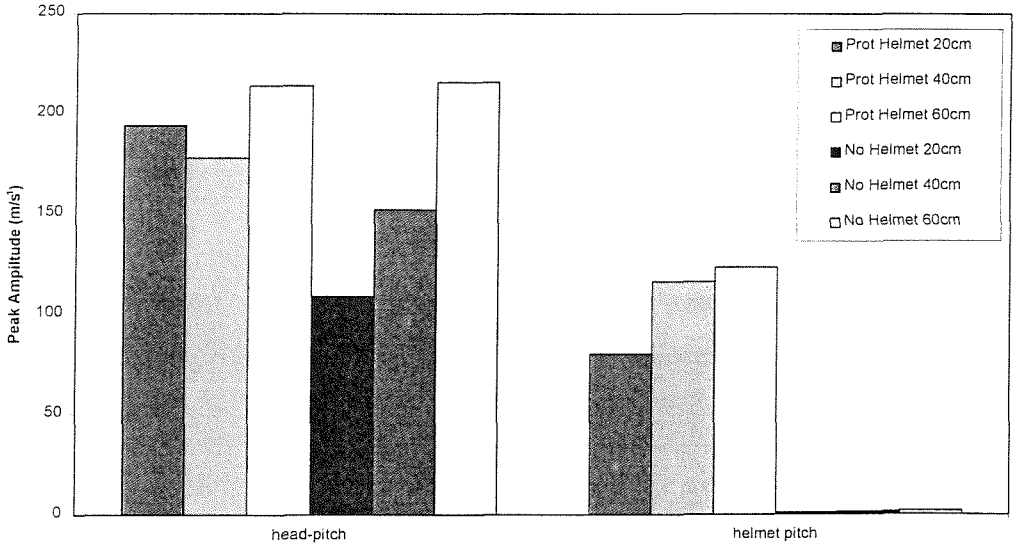

Figure 4.9b Peak pitch acceleration magnitudes when jumping from 20, 40 and 60cm (Median of 12 subjects)

4.3.4.2 The effect of a helmet on head motion

Figures 4.9 and 4.9b also show the effect of the helmet on head motion when jumping from height. The presence of a helmet did not change the peak head vertical or fore-aft acceleration when jumping from any height. In the pitch direction, removing the helmet reduced the amplitude of pitch head motion when jumping from heights of 20 and 40cm. However, this change was not seen when jumping from a height of 60cm.

4.3.4.3 The effect of jumping height

Head vertical acceleration was not affected by jumping height. When wearing the prototype helmet the head fore-aft peak acceleration increased as the jumping height increased from 20 to 60cm. The peak acceleration in the head fore-aft direction increased as the jumping height increased from 20 to 60 and 40 to 60cm. In the head-pitch direction the peak acceleration amplitude increased as the jumping height increased when the helmet was not worn.

Comparisons of the peak helmet vertical acceleration with height were statistically insignificant. In both helmet fore-aft and helmet pitch directions as the jumping height increased so did the acceleration amplitude measured on the helmet.

4.4 CONCLUSIONS

When jumping on the spot three main peaks in acceleration were observed. These occurred at 2, 4 and 5Hz and were dependent upon the jumping rate. As with the running experiment the main power spectral density of each head-helmet system occurred at a frequency determined by the jumping rate of the subject. This indicates a strong transmission path through the body to the head and helmet.

Vertical acceleration of the head, when jumping, was not affected by the presence of a helmet. When a helmet was present on the head the vertical helmet acceleration amplitude was the same as the vertical head acceleration amplitude at the jumping frequency. This indicates that there was no relative motion between head and helmet in the vertical direction at the excitation frequency.

Fore-aft acceleration of the Mk VI helmet when jumping on the spot was considerably greater than fore-aft motion of the head at the excitation frequency and 1st harmonic. This would indicate relative movement of the helmet on the head and supports the hypothesis in Chapter 3 that there could be a mode of vibration of the helmet on the head moving in the fore-aft and pitch directions. However, when jumping from height the fore-aft and pitch peak acceleration amplitude of the head was greater than that of the helmet. Further investigation is therefore required to confirm this finding.

When jumping on the spot, differences in the peak acceleration response in all directions were observed between the Mk VI and prototype helmets. This is thought to be due to the differing mass and distributions of mass on the helmet.

When jumping from height there was an approximately linear relationship between the peak acceleration of the head and helmet in the pitch and fore-aft directions and the jumping height.

CHAPTER 5 HEAD AND HELMET MOTION DURING EXPOSURE TO WHOLE-BODY VERTICAL VIBRATION

5.1 INTRODUCTION

Chapters 3 and 4 investigated motion of the head and helmet while running and jumping. These experiments concluded that the head-helmet system is driven at a single frequency whilst running or jumping and peaks in the spectrum of the head and helmet acceleration response were dominant at the running or jumping rate. The previous experiments also concluded that there could be a mode of vibration of the helmet on the head due to relative motion of the head and helmet in the fore-aft axis.

This chapter continues the work of the two previous chapters, investigating the motion of the head and helmet under whole-body random broadband vibration. It also investigates the effect of helmet mass and distribution of mass on motion of the head and helmet.

There have been some studies investigating the effect of helmet mass and/or moment of inertia on the loading of the spine, the risk of injury, the wearer's comfort and performance etc. Helmet design emphasis is usually based upon the prevention of cranial injury. As a result of this there may be deficiencies in the helmet performance in other areas. It has been shown that the helmet mass, placement of the mass and the shape of a helmet are important factors in reducing the probability and severity of neck injuries (Frievalds and McCauley, 1990).

Particular practical applications in which helmets are worn and could cause injury are in ejections from fighter aircraft. Anton (1987) reported that the risk of sustaining a neck fracture on ejection is between 1 and 2%. Increasing the mass on the head, particularly in association with forward shifts of the centre of gravity may increase the incidence of fracture. Dijke *et al.* (1993) investigated the effect of helmet-mounted devices on neck loading. They found that the neck loading within high-G environments was significantly reduced by reducing the mass of the helmet or by shifting the centre of gravity backwards.

In addition to affecting comfort, concentration, and causing the risk of physical injury, the helmet mass, and the distribution of mass, will influence the relative motion

between head and helmet. Woodman and Griffin (1993) investigated the relationship between helmet mass and the transmission of fore-aft seat vibration to the head and helmet. It was concluded that placing a helmet on the head reduced the fore-and-aft frequencies measured at the head. Placing a helmet on the head also reduced the pitch movement that occurred on the head at 5Hz. A mode of vibration, containing both pitch head and pitch helmet motion decreased from 10Hz to 5Hz as the helmet mass increased from 1.4 to 4.2kg.

Parameters such as muscle stiffness and head mass also determine the natural frequencies and mode shapes of the head and upper neck. Some modes of vibration at the head arise from or are part of modal frequencies at locations lower on the spine. Kitazaki and Griffin (1998) used experimental modal analysis to extract the natural frequencies and vibration mode shapes of the human body. Eight modes were found.

5.2 EXPERIMENTAL METHOD

5.2.1 Introduction

An experiment was conducted to investigate the effect of helmet mass and distribution of mass on the motions of the neck, head and helmet. Twelve male subjects were used in the experiment (all with no history of back or neck injury). They were subjected to broad-band random whole-body vertical vibration for 1 minute in each of the eight experimental conditions. A Mk VI Combat Helmet (modified to allow extra mass to be applied to the helmet) was used in the experiment. Masses were added to the helmet at differing locations to change its mass and moment of inertia. The experimental conditions are listed in Table 5.1.

5.2.2 Instrumentation

A 1m vertical stroke electro-hydraulic vibrator supplied the vibration stimulus which was applied to each subject. Subjects sat in a normal upright posture on a rigid seat, without a backrest, which was mounted to the vibrator. They were exposed to a broadband random stimulus at frequencies between 0.25 and 30Hz with a magnitude of 1 m/s^2 r.m.s. for a 1 minute duration for each of the eight experimental conditions. The vertical vibration of the shaker was measured using an Entran EGCS piezo-resistive accelerometer mounted on the vibrator platform.

Table 5.1 Experimental Conditions

		Total helmet mass (kg)	Details of location of extra mass
Condition 1	Mk VI helmet	2.95	mass located 'low and central
Condition 2	Mk VI helmet	2.95	mass located 'low and forward'
Condition 3	Mk VI helmet	1.9	mass located 'low and central'
Condition 4	No helmet	n/a	n/a
Condition 5	Mk VI helmet	1.3	no extra mass
Condition 6	Mk VI helmet	1.9	mass located 'high and central'
Condition 7	Mk VI helmet	2.95	mass located 'high and central
Condition 8	Mk VI helmet	2.95	mass located 'high and forward'

Acceleration of the head and helmet was measured using a bite-bar and a helmet bar. Each bar housed six miniature Entran piezo-resistive accelerometers to measure translational acceleration. The masses of the bite-bar and helmet bar, including accelerometers were 180 and 90g respectively.

The motion at the base of the neck (T1) was measured using a polystyrene mount. Three miniature Entran EGCS piezo-resistive accelerometers were attached to the mount to measure the motion in two vertical axes and one fore-aft axis. The total mass of the instrumentation used to measure neck motion was 10g. The mount was attached to the skin at TI using strong adhesive surgical tape as shown in Figure 5.1

Surface acceleration measurements were made at TI on the spine. When accelerometers are attached on the body surface, local tissue-accelerometer vibration may result in a difference between the accelerometer measurement and the acceleration of the spine or neck. There are direct methods of measuring the acceleration at the vertebrae, but these involve invasive procedures and were not practical for use in this experiment. Therefore, a mathematical method was used to correct errors incurred by relative motion between the accelerometer and the TI vertebra. This method is detailed in Appendix 2. In brief, the method comprises of measuring the transient response of the polystyrene measuring block when mounted on the skin in each of the three measurement locations. From this measurement the natural frequencies and damping of the local system (i.e. the accelerometer and skin system) are estimated. These two values are then used to calculate a weighting function that is then used to correct the data measured in each direction on the neck.

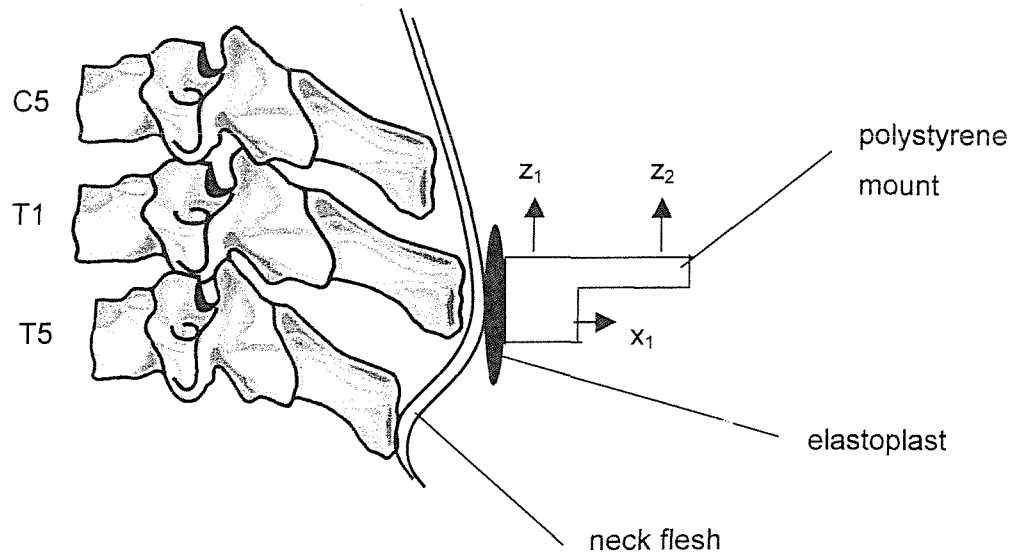

Figure 5.1. Mounting of accelerometers on the neck

5.2.3 Analysis

Data acquisition and analysis were conducted using an *HVLab* Techfilter system. The data acquisition sample rate was 100 samples/sec and the data were filtered at 30Hz. The accelerations at the head, helmet and neck (T1) were determined for the full sixty second vibration exposure. Spectra were determined with a resolution of 0.10Hz, giving 24 degrees of freedom.

Data were analysed in the mid-sagittal plane directions only (i.e. fore-aft, vertical and pitch) at all measurement locations. Transfer functions and coherencies were calculated between the measurements made at locations on the neck, head and helmet and the vertical input at the seat. Transmissibilities from the seat to each measurement location were also calculated.

Each transmissibility was compared statistically in each direction at discrete frequencies across all twelve subjects using the Friedman two-way analysis of variance test for overall statistical differences between all conditions and the Wilcoxon matched-pairs signed ranks test for statistical differences between individual conditions.

Mean transfer functions (of twelve subjects) were calculated. This was considered to be an appropriate function to use because of the good intersubject variability achieved. Appendix 5 contains graphs showing this variability. Coherency values were used to check that the transfer functions were viable before conclusions were drawn. Examples of some coherency graphs are shown in Appendix 5.

The transfer functions were used to conduct a modal analysis upon the experimental results. Experimental modal analysis relies upon the theory that the dynamic behaviour of a structure can be defined in terms of its modal properties of the natural frequencies, the mode shapes and the damping. The technique seeks to extract the modal properties from measured data, generally from transfer functions, and uses these data to produce animated mode shapes of the resonances that occur in the system.

5.3 RESULTS

5.3.1 Transmissibilities of seat to head and helmet motion

5.3.1.1 Introduction

The transfer functions obtained in each of the eight conditions were analysed in three categories.

5.3.1.2 Effect of a helmet on head and neck motion

Conditions 4 (no helmet) and 5 (standard Mk VI helmet) were compared to determine the effect of a helmet upon head and neck motion. Figure 5.2 shows a graph comparing the mean transmissibilities of twelve subjects in each direction of measurement obtained in condition 4 with those obtained in condition 5. The transmissibilities are calculated between vertical acceleration of the vibrator table and the acceleration of the head or helmet. A criteria of 5% (i.e. $p<0.05$) was required for statistical significance and differences below this criteria are not discussed.

Head fore-aft acceleration at frequencies between 3 and 6.5Hz and between 6.5 and 16 Hz was reduced when the helmet was present (i.e. $p< 0.05$, see Figure 5.2). At frequencies between 2 and 3 Hz the helmet reduced the level of vibration transmitted to the head vertical direction. However, at frequencies between 3.7 and 6.6 Hz the Mk VI helmet produced levels of vibration at the head in the vertical direction which were greater than the no-helmet condition. When the Mk VI helmet was worn the levels of head pitch vibration at 3.12 and 5.08 Hz were reduced.

Neck fore-aft vibration significantly increased when a helmet was worn at 1.07, 1.17, 2.64, 3.03, between 3.12 and 3.71 Hz and at frequencies between 10.55 and 15.5 Hz. A frequency shift of the main peak from 4.5Hz with no helmet to 3 Hz when the

Mk VI helmet was worn was also apparent. The acceleration in the neck vertical direction increased when the helmet was worn at frequencies between 3.78 and 5.7 Hz and reduced at frequencies between 8.2 and 17.3 Hz.

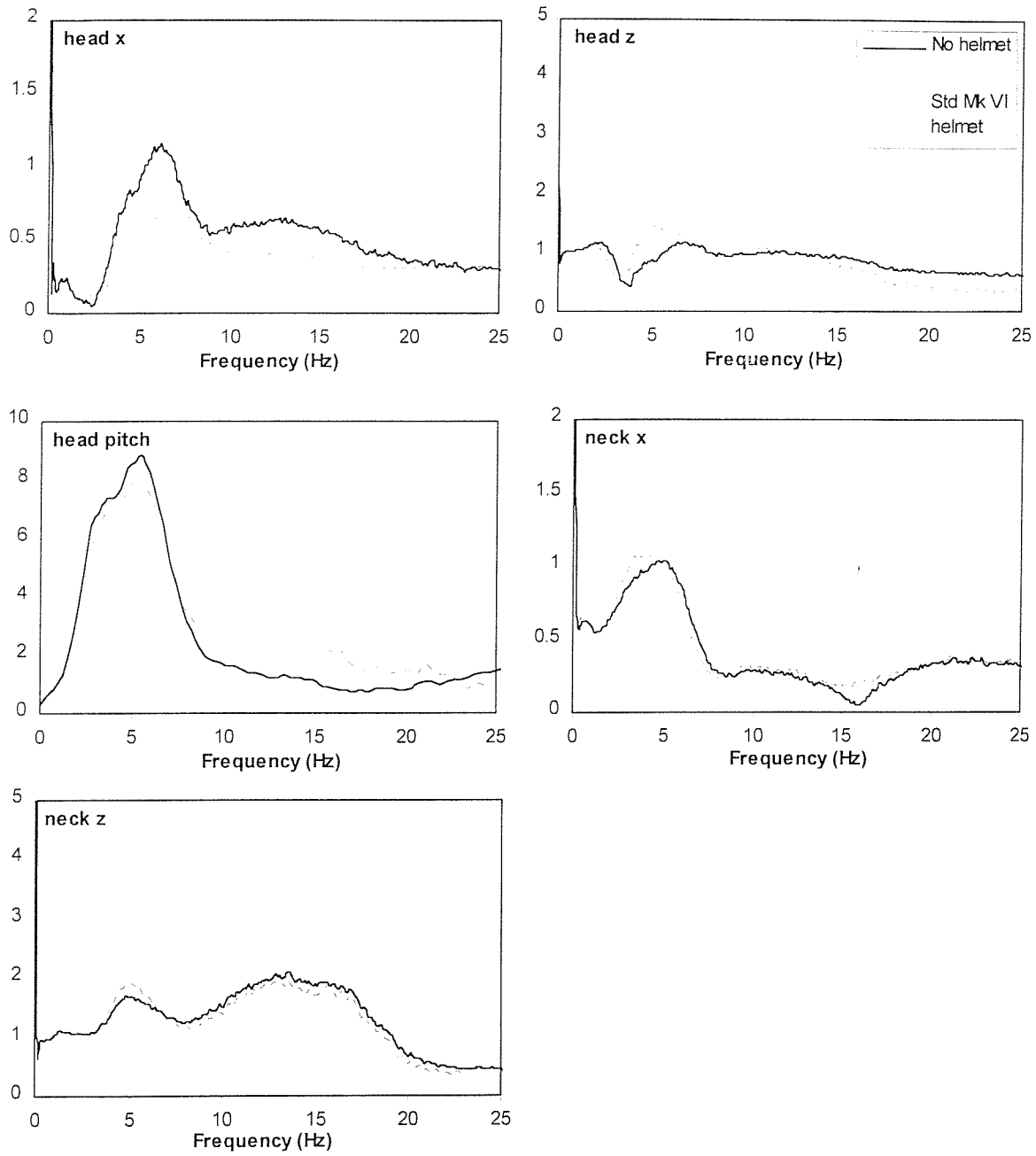

Figure 5.2 Mean transmissibilities from seat to head and helmet showing the effect of a helmet on head and neck motion

5.3.1.3 Effect of location of helmet mass on neck, head and helmet motion

Conditions one, seven and eight (see Table 5.1 for condition definitions) were compared to determine the effect of the location of additional helmet mass on helmet,

head and neck motion. Figure 5.3 shows a comparison of the mean transmissibilities of these three conditions in each direction of measurement.

The head fore-aft and vertical transmissibility showed a defined trend at all frequencies between 4 and 16Hz, with the greatest transmissibility occuring in condition 7 (2.95kg helmet, mass high, centre). Moving the extra mass forward in condition 8 (2.95kg helmet, mass high forward) reduced the transmissibility. The head fore-aft transmissibility was reduced further in condition 1 (mass placed low and central).

The head pitch transmissibility was also affected by the location of the helmet mass. At frequencies between 2.3 and 4Hz the pitch transmissibility was found to be greater with the mass located at a low and central location. At frequencies between 5.5 and 7.4Hz the transmissibility was greater with the mass located high and in the centre of the helmet than in the conditions when the mass was located high and forward or low and central.

Lowering the helmet mass greatly increased the transmissibility of vertical seat acceleration to helmet fore-aft acceleration at frequencies between 2.25 and 5.66Hz. The location of the mass on the helmet appeared not to influence the helmet vertical acceleration at most frequencies. The helmet pitch motion was influenced by the mass location only at frequencies between 16 and 25Hz. At these frequencies it was observed that locating the additional mass high and central on the helmet produced the greatest amount of helmet pitch motion. Moving the mass forward reduced the helmet pitch motion and moving the mass to a lower location significantly reduced the helmet pitch transmissibility at frequencies between 16 and 25Hz.

The neck vertical transmissibility only produced significantly different results at frequencies between 4.5 and 7.5Hz. At these frequencies it was shown that smaller transmissibilities resulted when the mass was located lower on the helmet.

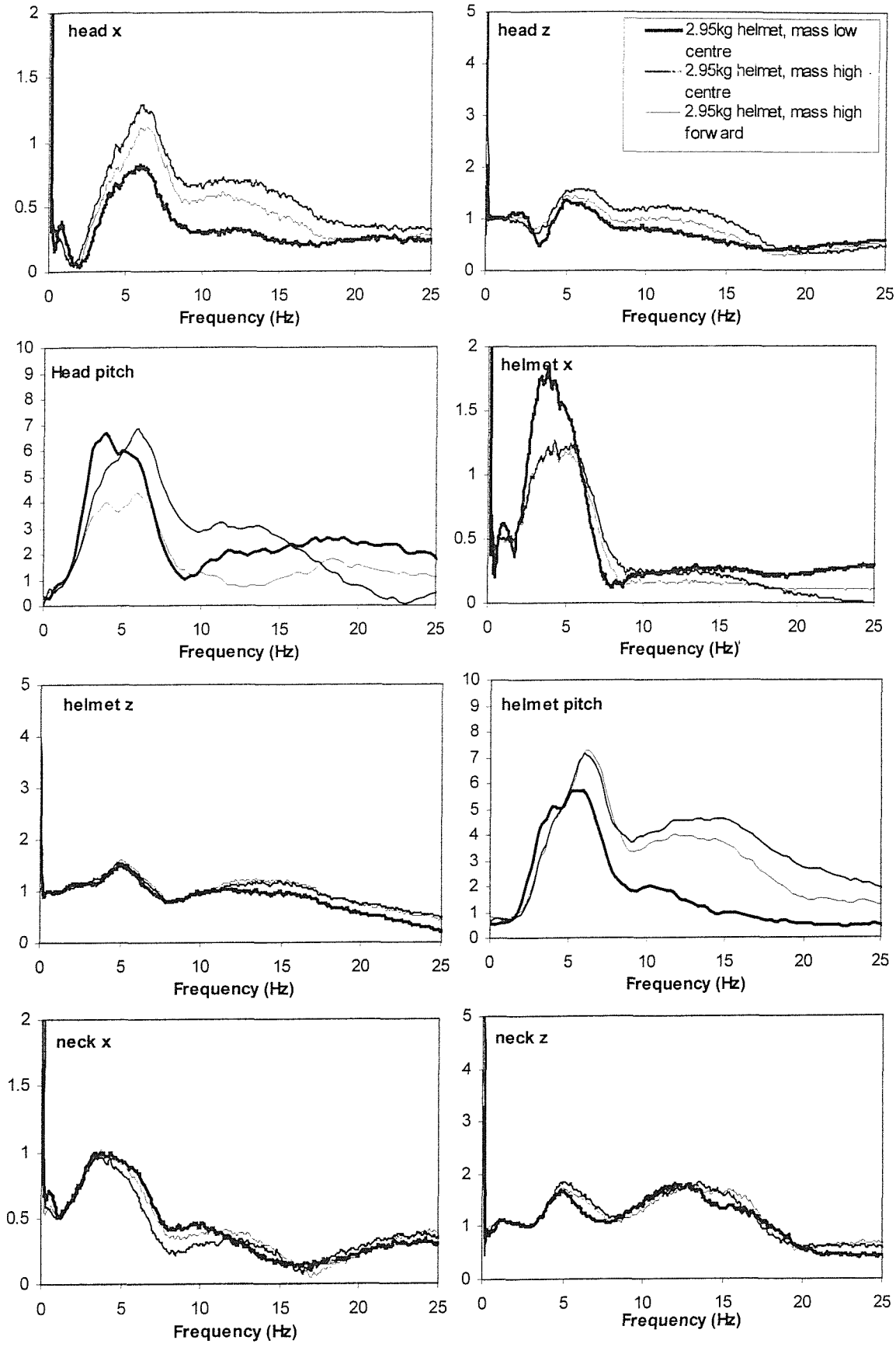

Figure 5.3. Effect of location of helmet mass on neck, head and helmet motion

5.3.1.4 Effect of helmet mass on neck, head and helmet motion

Conditions one (2.95kg helmet), three (1.9kg helmet) and five (1.3kg helmet) were compared to determine the effect of helmet mass on helmet, head and neck motion. Figure 5.4 shows a comparison of the mean transmissibilities of these three conditions in each direction of measurement.

It can be seen from Figure 5.4 that increasing the mass of the helmet reduced the transmissibility to the head fore-aft direction at frequencies between 3.5 and 9Hz. At frequencies between 9 and 18Hz the transmissibility reduced as the helmet mass increased.

The motion in the head vertical direction was not affected by helmet mass to the same extent as the motion in the head fore-aft direction. However, at frequencies between 3.6 and 5.96Hz the 1.3kg helmet produced a marginally greater transmissibility than the 1.9kg helmet. At frequencies between 9 and 16 Hz the 2.95kg helmet produced a significantly lower transmissibility to the head vertical direction than the helmets weighing 1.9 and 1.3kg. The helmet mass did not affect head pitch transmissibility at frequencies upto 4.9Hz. At frequencies between 4.9 and 8.2Hz, the helmet with the greatest mass produced the lowest level of head pitch transmissibility. Between 11 and 12 Hz the 1.9kg helmet possessed a lower transmissibility than the 1.3kg helmet. However, at frequencies between 14.6 and 20Hz, the 2.95kg helmet produced a greater transmissibility than the 1.3kg helmet.

At frequencies between 3.1 and 3.3Hz the 2.95kg helmet produced a greater level of helmet fore-aft transmissibility than the 1.9kg helmet. However, at frequencies between 4.59 and 8.2Hz the 2.95kg helmet produced less motion in the fore-aft direction than the 1.9kg helmet. In the helmet vertical direction there were less differences between conditions. However, at frequencies between 10.2 and 12Hz it can be seen that as the helmet mass decreased the transmissibility in the helmet vertical direction decreased. At frequencies between 4.69 and 5.86Hz the 1.9kg helmet produced a higher transmissibility in the helmet pitch direction than the 1.3kg helmet. It can also be seen that the helmet pitch transmissibility at frequencies between 16 and 25Hz decreased with increasing helmet mass.

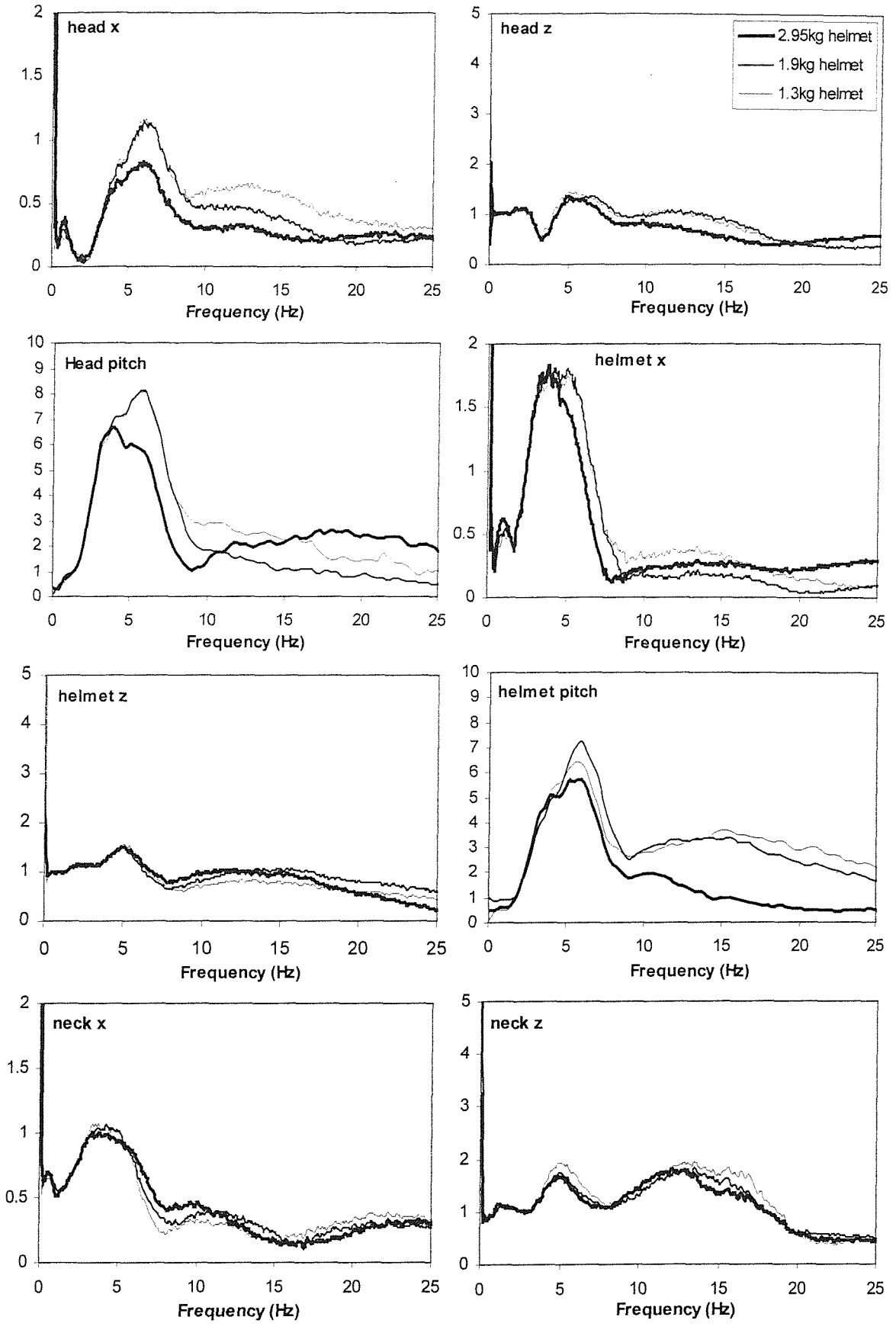

Figure 5.4 Effect of mass on neck, head and helmet motion

The 2.95kg helmet produced a lower level of neck fore-aft transmissibility than the 1.9kg helmet at some frequencies between 2.54 and 5.2Hz. At frequencies between 6.9 and 11Hz, however, the 2.95 kg helmet produced higher transmissibilities than the other two helmets. Neck vertical motion was influenced at frequencies between 3 and 8Hz where it was observed that the 1.3kg helmet resulted in greater transmissibility to the neck than the two heavier helmets. At frequencies between 13 and 17Hz the transmissibility was found to increase with decreasing helmet mass.

5.3.2 Modal Analysis

5.3.2.1 Introduction

Experimental modal analysis was conducted on six of the experimental conditions. Animated mode shapes and natural frequencies were obtained in each condition.

5.3.2.2 Procedure

Experimental modal analysis relies on the assumption that the dynamic behaviour of a structure can be described in terms of the modal properties of the natural frequencies, the mode shapes and the damping. The technique seeks to extract the modal properties from measured data, generally from transfer functions. Two assumptions are made when applying the experimental modal analysis technique to the human body. These are that the body behaves in a linear manner and that the damping of the human body is hysteretic. A theoretical explanation of experimental modal analysis is described in Appendix 3.

The modal analysis was conducted using ICATS (Imperial College Analysis, Testing and Software). A multi degree of freedom method was employed, using the Global-M method of curve fitting. This method is based upon a singular value decomposition of a system matrix expressed in terms of measured FRF properties and then on a complex eigensolution which extracts the required modal properties. The modal properties were then used to produce animated mode shapes of each natural frequency.

5.3.2.3 Results

Four modes of vibration occurred in each condition when a helmet was present. The mode shapes obtained in each condition were sufficiently similar to be able to assume that they were the same modes. Consequently, observations have been

made regarding the differences in modal frequency occurring due to changes in helmet condition.

Figure 5.7 shows the mode shapes and frequencies that occurred in the modal analysis of the standard Mk VI helmet. However, the general mode shapes of the neck-head-helmet system can be summarised as follows:

Mode1: Vertical and fore-aft motion at the neck, head pitch and fore-aft motion and helmet pitch, fore-aft and vertical motion.

Mode 2: Vertical, pitch and fore-aft motion at the neck, predominantly pitch motion at the head and pitch, fore-aft and vertical motion at the helmet.

Mode 3: Vertical and pitch motion at the neck, head and helmet. Fore-aft motion was also seen at the helmet.

Mode 4: Pitch, fore-aft and vertical motion of the neck, very little motion was seen at the head and helmet.

Figure 5.5 indicates the variation of modal frequency with helmet condition at each mode. From the graph it can be seen that helmet condition had very little effect on the frequency in mode 1, which was always approximately 3.6Hz, regardless of helmet mass or location of the mass. Adding a helmet to the head (when the additional helmet mass was located below the helmet centre of mass) produced a reduction in the frequency of mode 2. As the helmet mass increased from 1.9 to 2.5kg there was a small reduction in the frequencies of modes 2 and 3. However, as the helmet mass increased from the standard helmet mass of approximately 1.4kg to 1.9kg the frequencies of modes 2 and 3 both increased. This is not what would be expected, but could be attributed to the change in moment of inertia and/or centre of rotation of the helmet due to its additional mass. The location of the mass of the 2.95kg helmet made a small difference to the frequencies of modes 2 and 3. Placing the mass higher on the head resulted in modes 2 and 3 having higher natural frequencies. The frequency of mode 4 generally decreased in frequency as helmet mass increased and as additional mass was located higher and further forward on the helmet.

Mode 4 showed motion of the neck dominating motion of the head or helmet. This motion could be attributed to one of the following: (i) a flexural mode of the spine or

(ii) relative motion between the accelerometers and the bone at the measurement point on the neck.

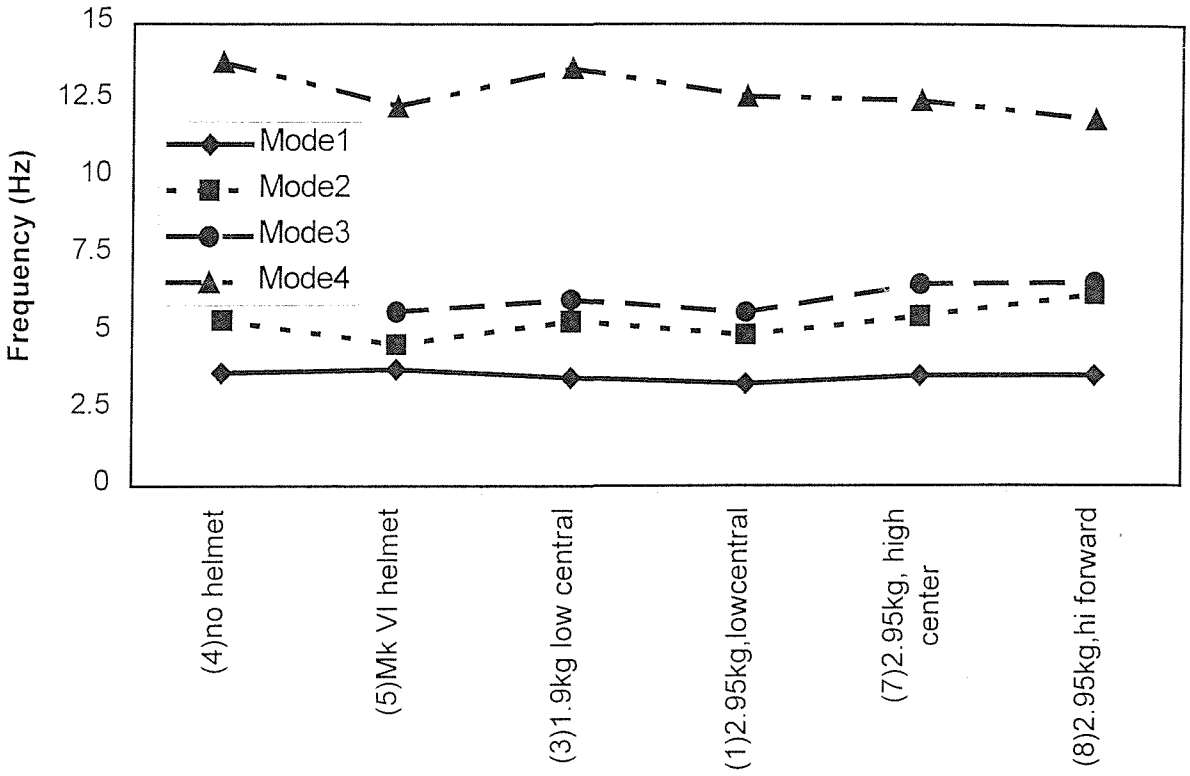

Figure 5.5 Effect of helmet condition on modal frequency

5.3.2.4 Comparison between 'no helmet' and 'Mk VI helmet' conditions

Figures 5.6 and 5.7 show the frequencies and mode shapes that were obtained in conditions 4 and 5 (without and with standard Mk VI helmet respectively).

The head and neck alone produced three mode shapes. The first, at 3.68Hz, showed fore-aft and pitch motion of the neck and predominantly pitch and fore-aft motion of the head. The second mode of the head and neck occurred at 5.37Hz. This produced vertical motion of the neck, with some fore-aft and pitch motion, causing head pitch and vertical motion. There was little head fore-aft motion in this mode. The third mode occurred at 13.76Hz and showed predominantly neck vertical motion, with some pitch motion of the neck. There was little motion of the head, in all directions, at this frequency.

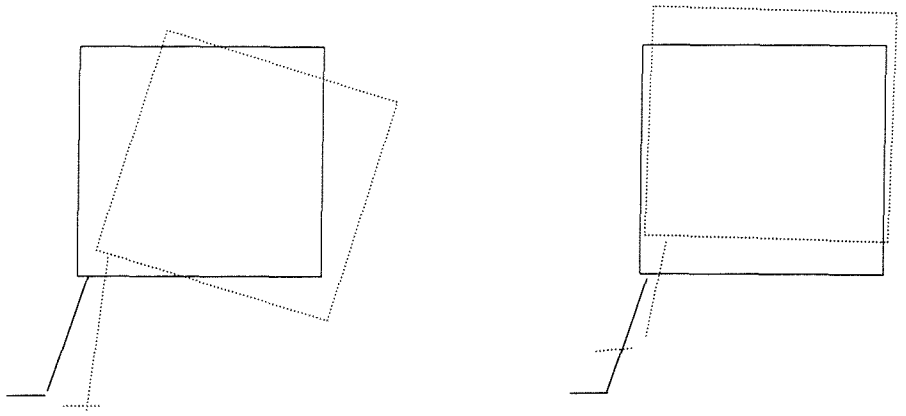

Mode 1: 3.68Hz

Mode 2: 5.37Hz

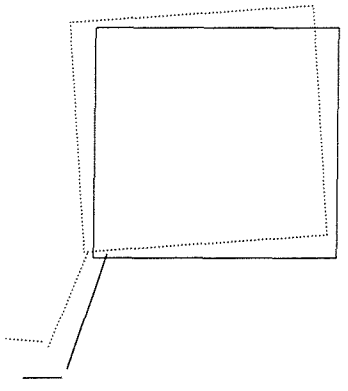

Mode 3: 13.78Hz

Figure 5.6 Mode shapes and frequencies extracted in condition 4 - (no helmet)

Four modes were extracted in the standard Mk VI helmet condition (see Figure 5.7). The first occurred at 3.8Hz and showed vertical and fore-aft motion at the neck, head pitch and fore-aft motion and helmet pitch, fore-aft and vertical motion.

Mode 2 occurred at 4.6Hz and produced vertical, pitch and fore-aft motion at the neck, predominantly pitch motion at the head and pitch, fore-aft and vertical motion at the helmet.

The third mode, at 5.07Hz produced vertical and pitch motion at the neck, head and helmet. Fore-aft motion was also present at the helmet. Mode 4 occurred at 12.31Hz with pitch, fore-aft and vertical motion of the neck. Little motion of the head and helmet was observed in this mode.

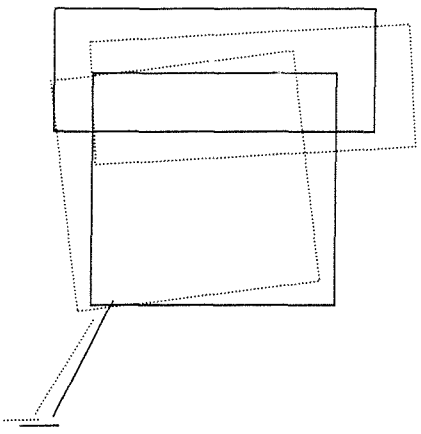

Mode 1: 3.8Hz

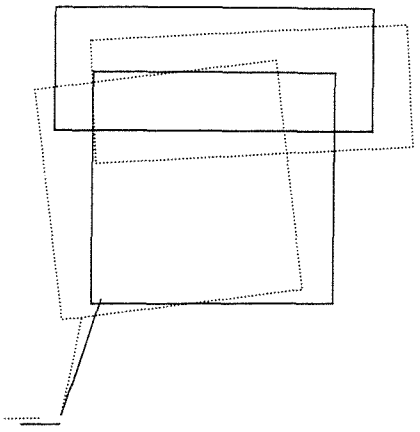

Mode 2: 4.6Hz

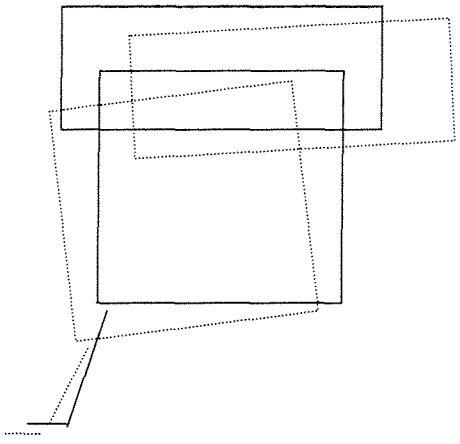

Mode 3: 5.07Hz

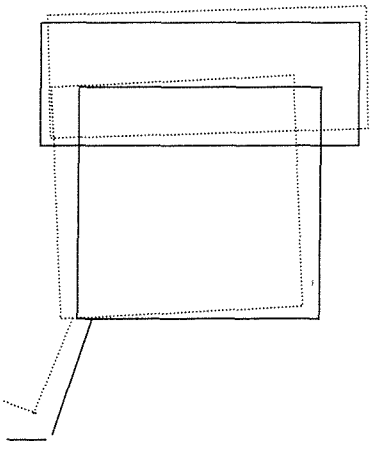

Mode 4: 12.31Hz

Figure 5.7 Mode shapes and frequencies extracted in condition 5 (i.e. standard Mk VI helmet)

From the above data it can be observed that adding the helmet to the neck-head system produced an extra mode of vibration (i.e. mode 3 at 5.07Hz). This extra mode is attributed to the additional degrees of freedom introduced into the system when a helmet is added and it is thought that this mode is consequently a mode of vibration of the helmet on the head.

5.4 CONCLUSIONS

The study described in this chapter has quantified acceleration of the head and helmet during whole-body vertical vibration. The study has shown that head motion at frequencies between 3 and 5Hz was reduced in the fore-aft and pitch directions by placing a helmet on the head. Head motion was reduced at all frequencies between 3 and 16Hz in the fore-aft direction by placing a helmet on the head. Head vertical

motion at frequencies between 3 and 6Hz increased when a helmet was placed on the head.

Head motion was found to be affected by the distribution of mass on a helmet. At frequencies between 4 and 16Hz the greatest transmissibility to the head fore-aft and vertical directions occurred when additional helmet mass was located high and central on the helmet. These transmissibilities reduced as the mass was moved lower and further forward on the helmet.

At frequencies between 3.5 and 6Hz the seat-to-head transmissibility, in all three mid-sagital plane head directions, decreased with increasing helmet mass. This could indicate a mode of vibration of the helmet on the head with frequency related to helmet mass. At frequencies between 9 and 16Hz head fore-aft and vertical transmissibility decreased with decreasing helmet mass.

It is believed that the variability in the transmissibility is attributable to resonance behaviour of the neck-head-helmet system. Although the neck-head-helmet system is highly damped, adding mass and relocating mass on the helmet affected the natural frequencies and mode shapes of the system.

Three modes of vibration were extracted from the experimental modal analysis of the human neck-head system. Four modes were extracted from the neck-head-helmet system. Placing a helmet on the head caused the second mode of the neck-head system to decrease in frequency and an extra mode (mode 3), showing the helmet pitching on the head, was introduced. The frequency of this mode was influenced by helmet mass.

The other modes of vibration, variants of which were also present in the neck-head system, are described as follows. Mode 1: pitch and fore-aft head motion, with the helmet (if present) moving in all directions of motion. The frequency of this mode was unaffected by helmet mass or location of mass on the helmet. The second mode was a pitching mode of the head with the helmet (if present) moving in all directions in the mid-sagital plane. The frequency of this mode tended to decrease with increasing helmet mass. The fourth mode was a bending mode of the upper thoracic and cervical spine, with no head or helmet motion. The frequency of this mode was largely unaffected by helmet mass or location of mass.

CHAPTER 6 MODELLING THE NECK-HEAD-HELMET SYSTEM

6.1 INTRODUCTION

The literature review in Chapter 2 of this thesis has shown that, despite the limitations caused by non-linearity and the assumption of viscous damping, attempts in biodynamic modelling of the head and helmet have been made. In some cases models have been written with a degree of success, whilst others have been written as building blocks to more complete and more accurate models.

The literature review highlighted several models of the neck-head-helmet system. Most of these models were written primarily to determine the effect of large forces on spinal vertebrae. Some authors added a helmet to their models simply by rigidly attaching mass to the top of the head.

Experimental evidence presented in the previous three chapters suggests that a helmet can move independently of the head in the fore-aft and pitch directions of motion. This would imply a loose coupling of the scalp at the fore-head. However, with the exception of the head-helmet model by Woodman and Griffin (1995) no models have been written to allow the helmet to move independently of the head.

The evidence suggesting that the helmet moves independently to the head implies that there is a mode of vibration of the helmet on the head. A modal analysis conducted upon experimental data in Chapter 5 showed that adding a helmet to the head produced an additional mode of vibration.

This chapter introduces and explains new finite element models of the neck-head system and the neck-head-helmet system. The results of the experimental modal analysis described in Chapter 5 were used to optimise the models. These models are regarded as 'experimental' in nature. However, they are also regarded as building blocks towards a model which could prove a useful tool in predicting the risk of injury when wearing a helmet in different conditions.

6.2 NECK-HEAD MODEL

The neck-head model was originally developed by Harvey (1990a). Harvey's model has been improved by redefining the model's geometry, the head mass and the moment of inertia. In addition, mass, with moment of inertia about T1 has been added to the neck (at the mid point between T1 and the atlanto-axial joint). The value of the head moment of inertia was changed significantly due to the apparent unreliability of the source of the value used in Harvey's model. This resulted in changes to the neck stiffness values which were adjusted by tuning the model response to match the response obtained in the experimental modal analysis. This approach is deemed acceptable in a simple model in that it is not possible to obtain these values independently from anthropodynamic data. Table 6.1 below shows the parameters used in the revised neck-head model and Figure 6.1 shows the form of the revised model.

The new geometry values were taken from the NASA Anthropometric Source Book (1973) and were based upon measurements taken on a sample of 2420 male US Airforce personnel in 1967, aged between 18 and 45 years. The head and neck masses were taken from Walker *et al.* (1973) and were based upon a male weighing 75kg.

Table 6.1 Modal parameters used in the revised neck-head model

Parameter		Value	Source
Head mass		4.75kg	Walker et al (1973)
Head I		0.02kg.m^2	Chandler et al (1975)
Neck mass		1.165kg	Walker et al (1973)
Neck I		0.02kg.m^2	Chandler et al (1975)
Neck stiffnesses	k_1	6000N/m	Peckham
	k_2	7370N/m	Peckham
	$k\theta_1$	100N.m.rad^{-1}	Harvey (1990)
	$k\theta_2$	100N.m.rad^{-1}	Harvey (1990)
	$k\theta_3$	250N.m.rad^{-1}	Harvey (1990)

A modal analysis was conducted upon the final neck-head model and three main modes of vibration occurred. The mode shapes and frequencies of the first two modes matched those obtained in the experimental analysis, however, the third mode

was 0.4Hz away from the measured experimental frequency. Despite this the mode shape was observed to be the same.

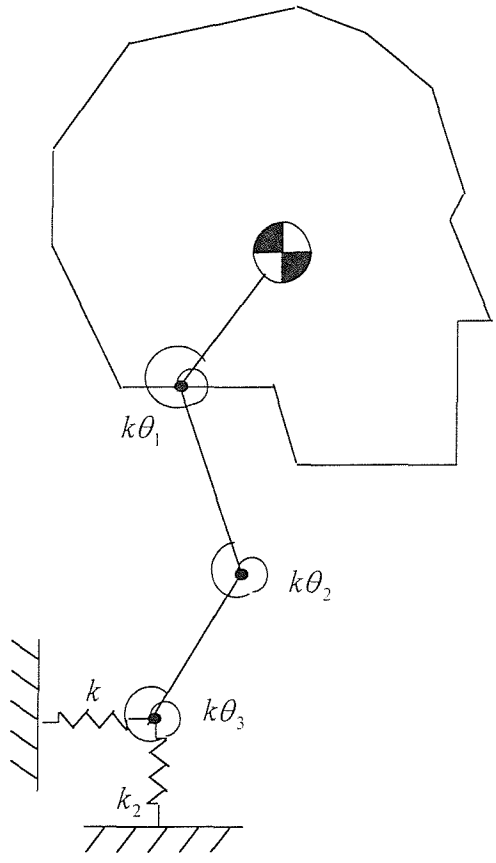

Figure 6.1 Neck-head model

Figures 6.2 to 6.4 show the mode shapes and frequencies of the three modes of vibration that occurred in the neck-head system. The first mode at 3.6Hz showed fore-aft motion of the neck and pitch and fore-aft motion of the head. Mode 2 occurred at 5.3Hz and showed vertical and fore-aft motion of the neck and vertical and pitch motion of the head. The third mode occurred at 13.3Hz. This mode shape showed vertical and pitch motion of the neck at T1 and very little motion of the head in any direction.

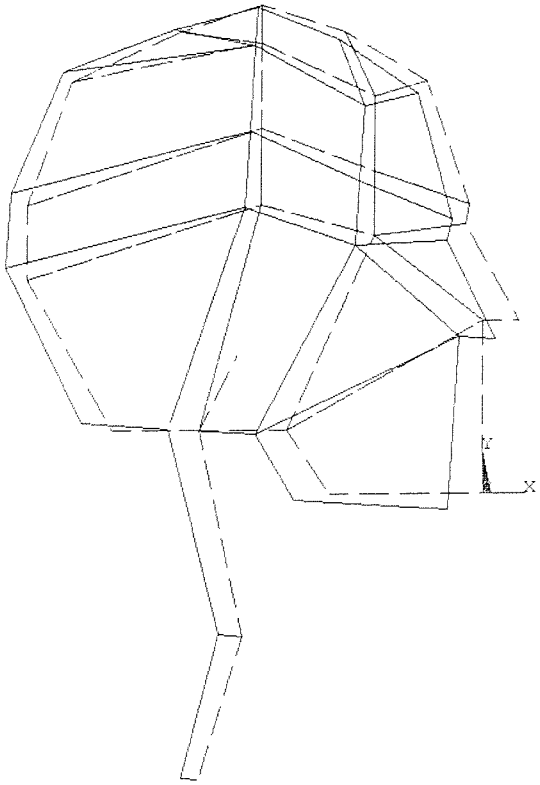

Figure 6.2 Neck-head model, mode 1, 3.65Hz

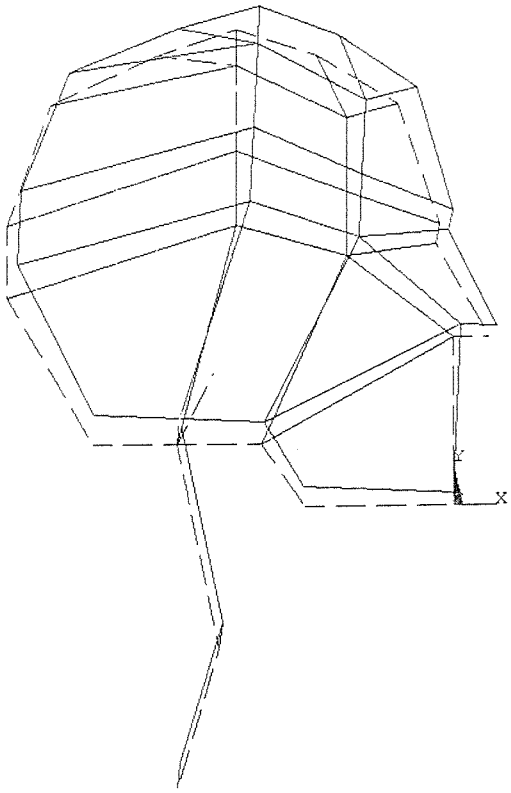

Figure 6.3 Neck-head model, mode 2, 5.35Hz

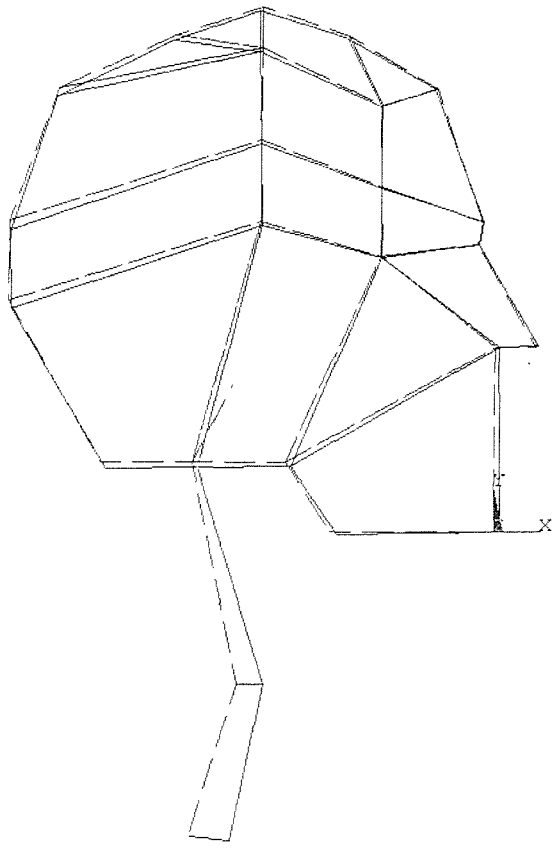

Figure 6.4 Neck-head model, mode 3, 13.3Hz

6.3 NECK-HEAD-HELMET MODEL

A new model of the neck-head-helmet system has been developed. This is based upon the neck-head model described in Section 6.2 with additional elements to represent the helmet and the scalp coupling between head and helmet.

The head was made up of five quadrilateral areas, with a centre of mass located 1.72cm forward and 3.64cm above the atlanto-occipital joint. The centre of mass was fixed to the atlanto-occipital joint using a rigid link. The helmet was also constructed from five quadrilateral areas with a centre of mass fixed to the helmet using a rigid link. The connection between the helmet and the head was at the skin contact points at the front and rear of the head. For simplicity the chinstrap and other forms of attachment were omitted. The neck was modelled using two beam elements. These were connected to each other and the head using torsional springs. The base of the neck was connected to ground using a torsional spring and two linear springs, giving an approximate representation of the lower spine.

Table 6.2. shows the values of the additional parameters used in the neck-head-helmet model. Appendix 4 gives a complete listing of the model code.

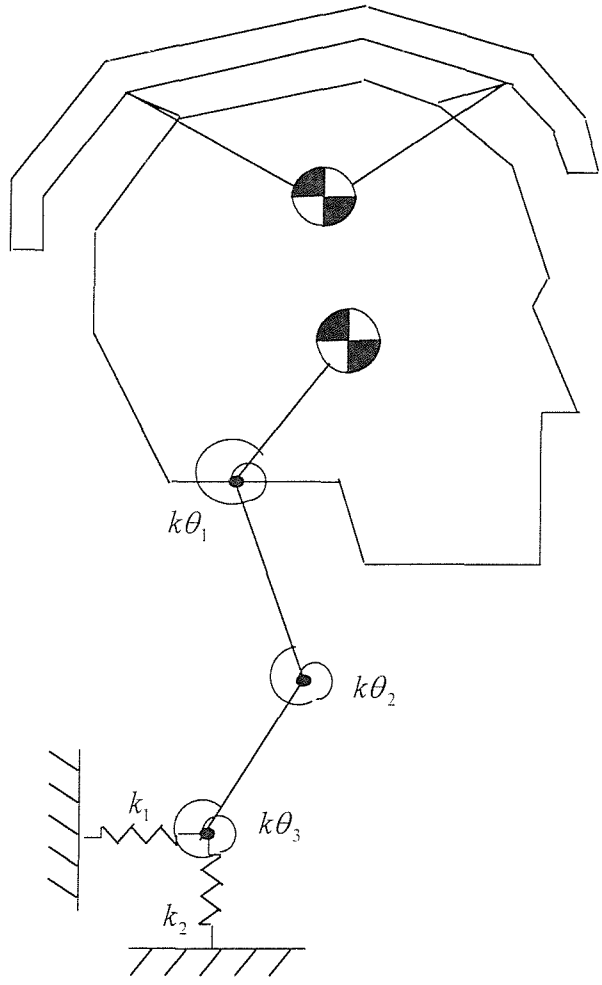

Figure 6.5 Neck-head-helmet model

Table 6.2 Parameters used in neck-head-helmet model

Parameter	Value
Helmet mass	1.3kg
Helmet I	0.02kg.m^2
Head-helmet coupling Young's modulus	265N.m^{-1}
Head-helmet coupling cross-sectional area	0.01m^2

When a modal analysis was conducted upon the model four mode shapes were produced. The value of the head-helmet coupling Young's modulus was adjusted so that the frequency of the extra mode obtained matched the frequency of the equivalent mode in the experimental modal analysis. Figures 6.4-6.7 show the mode shapes that occurred.

The first mode occurred at a frequency of 3.1 Hz and showed fore-aft motion of the neck, pitch and fore-aft motion of the head and pitch motion of the helmet. The second mode had a natural frequency of 4.8Hz and showed vertical and fore-aft motion of the neck, vertical and pitch motion of the head and vertical, pitch and fore-aft motion of the helmet. Mode 3 occurred at 5.1Hz with fore-aft motion of the neck and pitch motion of the head and helmet. The forth mode occurred at 13.3Hz and showed vertical and pitch motion of the neck at T1 and very little motion in any direction at the head.

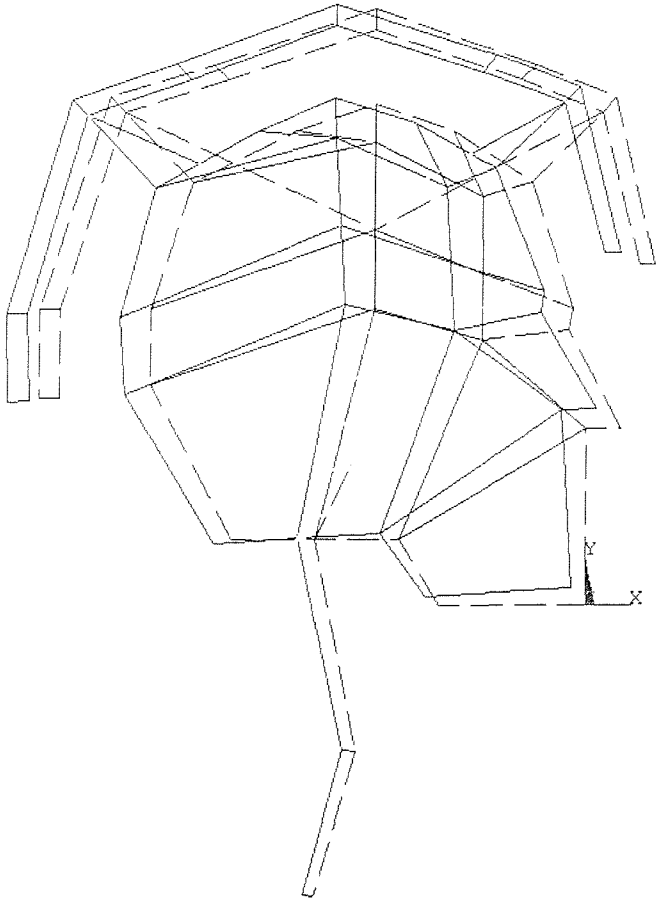

Figure 6.4 Neck-head helmet model, mode 1, 3.1Hz

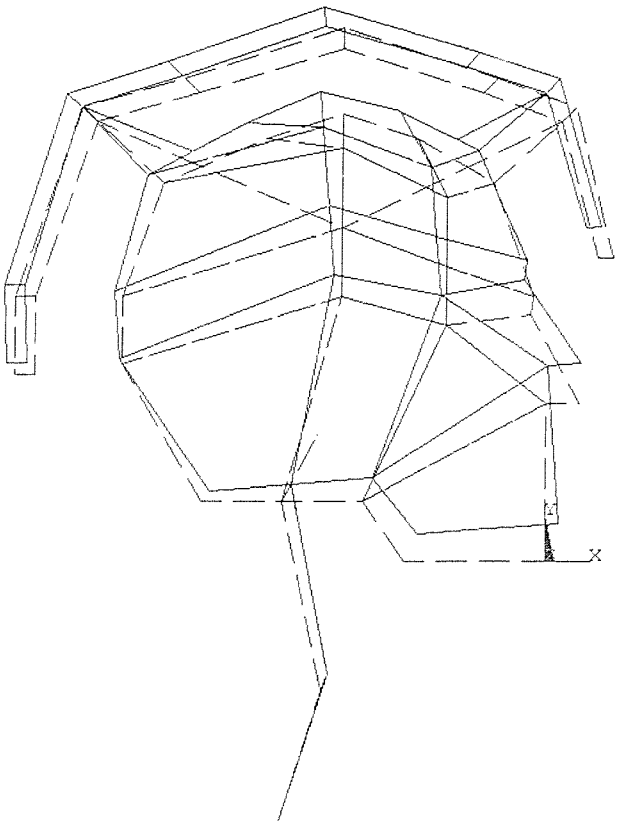

Figure 6.5 Neck-head helmet model, mode 2, 4.8Hz

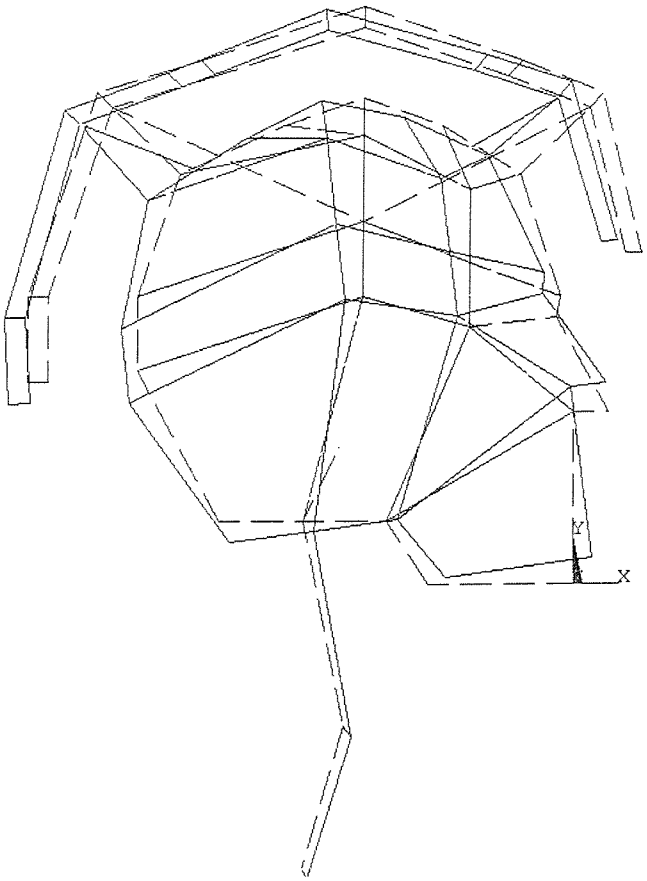

Figure 6.6 Neck-head-helmet model, mode 3, 5.1Hz

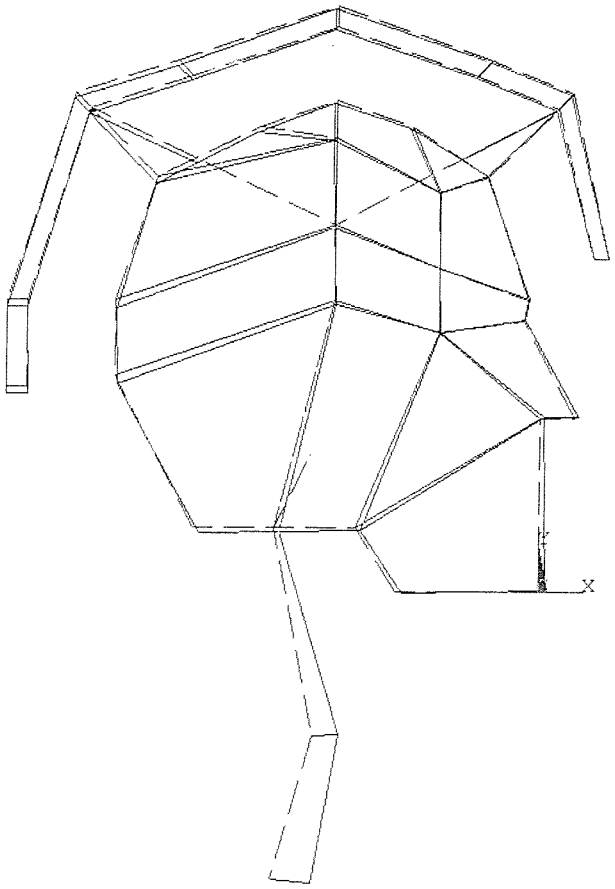

Figure 6.7 Neck-head helmet model, mode 4, 13.269Hz

6.4 DISCUSSION

6.4.1 Dynamics of the neck-head system

Chapter 5 established that the neck-head system had three principal modes of vibration, occuring at approximately 3.7, 5.4 and 13.8Hz. The mode shape of the first mode at 3.7Hz is described as vertical and fore-aft motion of the neck and pitch and fore-aft motion of the head. This corresponds well with the first mode of vibration obtained from the neck-head-helmet model. From the transmissibility graphs (Figure 5.2) it can be seen that at this frequency the neck fore-aft motion is a maximum and there is a similar level of neck vertical motion. This, as suggested by Kitazaki (1994) could be a bending mode of the spine (with the ends free) which produced a reduction in vertical motion of the head and caused the head to move in predominantly the pitch and fore-aft directions.

Figure 5.2 shows a peak in the transmissibility of seat vertical acceleration to the head pitch direction at the second mode of vibration (5.4Hz). The graphs also show a

greater level of neck vertical motion than neck fore-aft motion at this frequency. Modal analysis at this frequency showed the head to have motion in the pitch, fore-aft and vertical directions. The second analytical mode occurred at 5.4Hz and the mode shape was similar to the experimental mode shape. Kitazaki (1994) identified the principal whole-body vibration resonance at 4.9Hz as an entire body mode. A head pitching mode was also identified at 5.6Hz and was attributed to a bending mode of the lumbar and lower thoracic spine. This is consistent with the work of Paddan and Griffin (1993) who showed a resonance in the transmissibility from vertical seat motion to pitching motion of the head at frequencies between 5 and 6Hz. There is insufficient evidence available from this experiment to directly link this mode to either of the two modes discovered by Kitazaki (1994). However, from the experimental and analytical work contained in this thesis the second mode of vibration can be classified as a pitch mode of the head.

The third mode of vibration occurred at 13.8Hz. The mode shapes showed vertical and pitch motion of the neck at T1 and very little motion of the head in any direction. Figure 5.2 shows a peak in neck vertical motion at this frequency. Kitazaki (1994) discovered a similar mode-shape at 14Hz showing bending of the upper lumbar and cervical spine (unconfirmed due to differences between subjects). Although confirmation is not possible due to lack of experimental data further down the spine, it is thought that this mode could be the same as Kitazaki's mode at 14Hz.

In summary, the neck-head model has identified three modes of the neck and head system. Tuning of the model resulted in a reasonable degree of correlation between analytical and experimental modal analysis results. The three experimentally obtained modes were predicted by the neck-head model and it is reasonable to state that these are the main modes of the neck-head system. The extra modes that were discovered by Kitazaki (1994) may be attributed to motion occuring at other parts of the anatomy.

6.4.2 Dynamics of the neck-head-helmet system

Placing a helmet upon the neck-head system increased the number of degrees of freedom in the system. Four experimental mode shapes were extracted in modal analyses of the neck, head and helmet system. It is thought that three of those modes were attributed to the neck-head system. Data from the experimental modal analyses (shown in Chapter 6) support this theory, although the modal frequencies varied due to the additional mass in the system from the helmet. The extra mode of

vibration, in the standard helmet condition, occurred at 5.1Hz. This was thought to be a mode of the helmet on the head and is related to the pitch mode of the head. Adding a helmet to the system caused the frequency of the head pitch mode to decrease and a new mode was observed at a higher frequency (5.1Hz). This mode shows the helmet pitching on the head and is partially controlled by the helmet mass and the stiffness of the head-helmet coupling.

6.4.3 Application of the neck-head-helmet model

Minor alterations were made to the neck-head-helmet model to represent helmets with different mass and moment of inertia. In particular, the model was used to represent other helmet conditions in which experimental modal analysis data were available (as illustrated in Chapter 5). The modal output from the neck-head-helmet model was compared with the results of the experimental modal analyses.

The mode shapes obtained from the model were observed to be the same as the mode-shapes obtained in the experimental modal analysis. However, there was some variation between modal frequencies. Table 6.3 shows a comparison between the modal frequencies obtained in the model and in the experimental modal analysis.

It can be seen that the model predicted the frequency of modes of vibration of the neck-head-helmet system with a maximum error of 18.4% in the conditions when an additional helmet mass was either located uniformly around the helmet centre of mass or at a location below the helmet centre of gravity. The model was less reliable when additional helmet mass was located over or above the helmet centre of gravity.

Table 6.3 Comparison between predicted and measured modal analysis results

Helmet Condition	Mode no	Experimental modal frequency (Hz)	Model modal frequency (Hz)	% difference
Condition 5 Standard Mk VI helmet	1	3.8	3.1	-18.4
	2	4.6	4.8	4.3
	3	5.07	5.1	0.05
	4	12.31	13.17	7.1
Condition 1 2.95kg helmet, mass low central	1	3.34	2.96	-11.3
	2	4.9	4.29	-12.4
	3	5.63	5.29	-6.0
	4	12.63	13.17	4.3
Condition 3 1.9kg helmet, mass low and central	1	3.52	3.11	-13.1
	2	5.35	4.64	-13.2
	3	6.0	5.36	-10.6
	4	12.56	13.232	5.3
Condition 7, 2.95 kg helmet mass high and central	1	3.58	2.8096	-21.8
	2	5.5	4.35	-20.1
	3	6.53	4.87	-25.4
	4	12.49	13.27	6.2
Condition 8, 2.95kg helmet, mass high and forward.	1	3.6	2.23	-38.1
	2	6.2	3.95	-36.3
	3	6.6	4.63	-29.8
	4	11.9	13.26	11.4

CHAPTER 7 SUMMARY AND CONCLUSIONS

The literature review revealed a general lack in knowledge of the dynamics of the head and helmet system. No literature was found to quantify how the head and helmet interact when running and jumping. It was shown that helmet movement is independent of head motion at some frequencies, leading to the hypothesis that there is an independent mode of vibration of the helmet on the head. It was also established that the coupling of the scalp tissue between head and helmet and the mass of the helmet may both play a role in determining the frequency of the mode.

The investigation into head and helmet motion when running and jumping showed that most motion occurred in the mid-sagittal plane. When running and jumping it was observed that the greatest amount of motion occurred at the running or jumping excitation frequency. At the excitation frequency the head and helmet moved together in the vertical direction. In the fore-aft direction the head and helmet moved relative to each other. It was thought that this relative motion could be attributed to a mode of vibration of the helmet on the head. In transient jumping, an approximately linear relationship was observed between jumping height and acceleration of the head and helmet in the fore-aft and pitch directions.

To further investigate the frequency response of the head-helmet system an experiment was carried out to measure head and helmet motion during exposure to broadband whole-body vertical vibration. The results were presented as transmissibilities from the seat to the measurement location and in an experimental modal analysis. The experiment showed that head motion at frequencies between 3 and 5Hz was reduced in all directions of motion by placing a helmet on the head. Head motion in the fore-aft direction was reduced at frequencies between 3 and 16Hz by placing a helmet on the head. Head pitch motion was affected by the location of additional helmet mass. At frequencies between 3.5 and 6Hz the seat-to-head transmissibility in all three head directions decreased with increasing helmet mass; at frequencies between 9 and 16Hz head fore-aft and vertical transmissibility decreased with decreasing helmet mass. These changes in transmissibility are thought to be linked to resonant behaviour of the head-helmet system.

Three modes of vibration were extracted from an experimental modal analysis of the human neck-head system. Four modes were extracted from the neck-head-helmet system. Placing a helmet on the head caused the second mode of the neck-head system to decrease in frequency and an extra mode, showing the helmet pitching on the head, was introduced. This mode is thought to be a mode of vibration of the helmet on the head.

A finite element model of the neck-head-helmet system was developed. The natural frequencies and vibration mode shapes of the model were compared with the experimental data. Three modes were calculated for the neck-head system and four modes were calculated for the neck-head-helmet system.

The calculated response of the finite element models, together with the output from the experimental modal analysis, has provided evidence to suggest that there is a mode of vibration of the helmet on the head, the frequency of which is influenced by the scalp stiffness and helmet mass.

It is anticipated that this work could be continued in a number of ways. In particular, further areas of study could involve investigation and research in detail into the head-helmet skin interaction, which is clearly complex. The model could be further improved by re-modelling the skin scalp and other areas (after suitable experimental research) in which the helmet and body come into contact. The model could be also expanded to include the spine and lower back. It is also recommended that a harmonic analysis is conducted upon the model. This would, for example, enable head-to-helmet transmissibilities to be calculated and it would also be possible to predict the variation in neck loading due to a particular helmet type. Given time the model has the potential to be able to predict the response of the neck, head or helmet to a helmet of defined mass and moment of inertia under any particular operational condition.

APPENDIX 1. EXPLANATION OF MULTIPLE-IN MULITPLE-OUT TRANSFER FUNCTION SYSTEM

A1.1 One-in, one-out

Transfer function and coherency data is sometimes calculated by assuming a one-in, one-out model as shown in Figure A1.1 below.

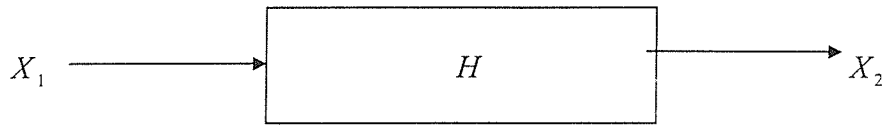

Figure A31.1: A one-in one-out system

Using this method, the transfer function between output X_2 and input X_1 is calculated assuming that the other inputs and outputs have no influence on X_2 and X_1.[1]

The transfer function is then calculated using the cross spectral density method, as follows

$$H = \frac{G_{12}}{G_{11}} \qquad \textbf{(A1.1)}$$

where G_{12} is the cross spectral density of input X_1 to output X_2, and

G_{11} is the power spectral density of input X_1.

By definition, the coherency function states how much of an output is linearly dependent on the input. In a one-in one-out system this does not take into account the influences of other directions of input motion on the output direction of motion.

Coherency γ^2 between X_2 and X_1 is calculated as follows

$$\gamma^2 = \frac{|G_{12}|^2}{G_{11}G_{12}} \qquad \textbf{(A1.2)}$$

[1] In reality in the head-helmet system motion of the head and helmet will have small influences on other directions. For example, motion at the helmet will be caused by elements of fore-aft, vertical and pitch motion of the head (with smaller influences from the other directions).

where G_{22} is the power spectral density of X_2.

A1.2 Three in, one out

Analyses for the calculation of the partial coherence function for a two-in one-out system have been discussed by Bendat and Piersol (1966). The analysis for a three-in one-out system as shown in Figure A1.2 is an extension of the two-in one-out system involving the repetitive use of some basic equations.

By introducing a three-in one-out analysis to the head-to-helmet system it is possible to produce transfer functions which are more representative of the system. It is subsequently possible to eliminate the effect of two of the inputs (head motion) on the third input and the output (helmet motion).

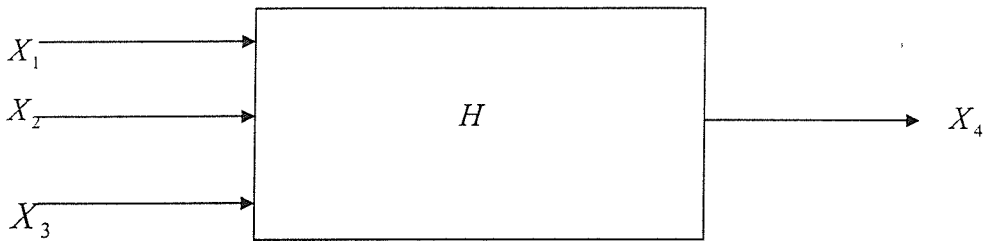

Figure A1.2 A three-in one-out system

This system can be simplified using a decomposition technique as shown in Figure A1.3

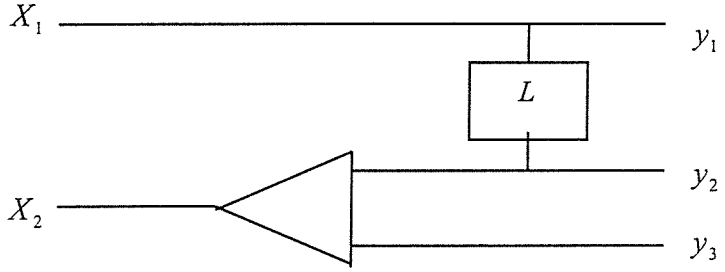

Figure A1.3 Decomposition of two signals

The input X_2 is decomposed into two parts: y_2 which are linearly correlated with input X_1 via a linear filter L and y_3 which is not correlated with X_1.

If all inputs and outputs are decomposed as described above, then the effect of X_1 will be removed from X_2 - X_4 as shown below in Figure A1.4.

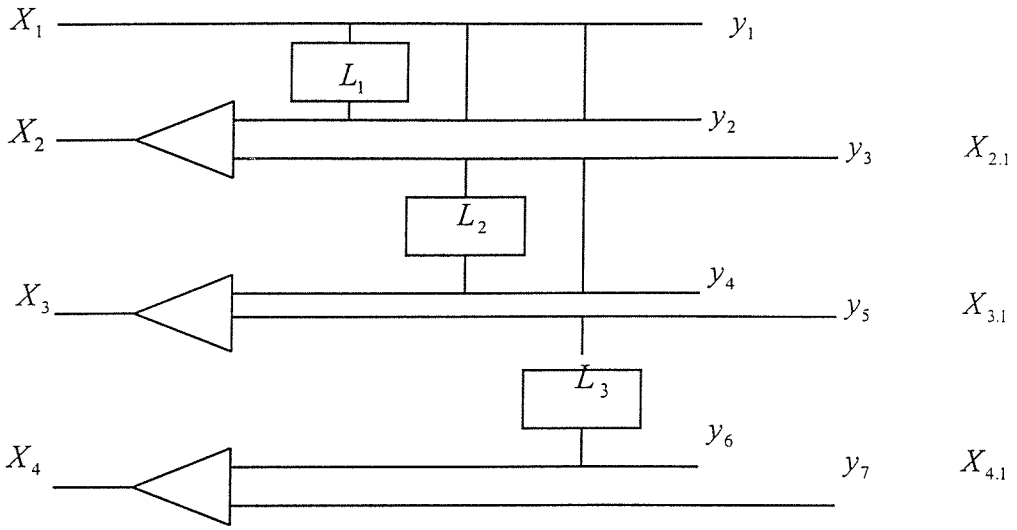

Figure A1.4 Decomposition of four signals

Now, as y_2 and X_2 are coherent

$$G_{y2y2} = G_{22}\gamma_{12}^{\ 2} \qquad \textbf{(A1.3)}$$

where G_{y2y2} is the mean power spectral density of y_2

G_{22} is the mean power spectral of X_2

$\gamma_{12}^{\ 2}$ is the ordinary coherence between X_2 and X_1

However,

$$G_{22} = G_{y2y2} + G_{y3y3} \qquad \textbf{(A1.4)}$$

$$= G_{22}\gamma_{12}^{\ 2} + G_{22.1} \qquad \textbf{(A1.5)}$$

and therefore the power spectral density of X_2 conditioned by X_1 is given by

$$G_{22.1} = G_{22} - G_{22}\gamma_{12}^{\ 2} \qquad \textbf{(A1.6)}$$

The same method can be applied to y_4 and y_6 to give the following relationships for power spectral densities conditioned by X_1.

$$G_{33.1} = \left(1 - \gamma_{13}{}^2\right) G_{33} \qquad \textbf{(A1.7)}$$

$$G_{44.1} = \left(1 - \gamma_{14}{}^2\right) G_{44} \qquad \textbf{(A1.8)}$$

Having established these values the system can subsequently be simplified to a two-in one-out system (having eliminated the effect of X_1).

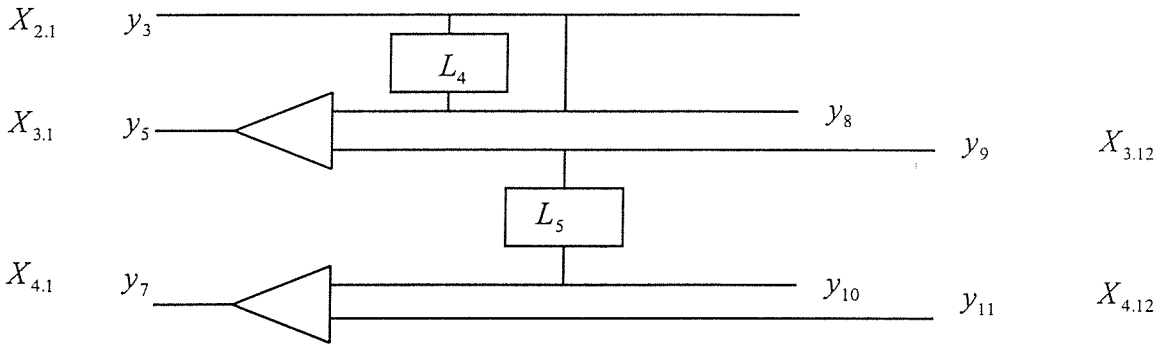

Figure A1.5 Decomposition of three signals

Using the same method employed in equations A3.4 and A3.5 the power spectral densities $G_{33.12}$ and $G_{44.12}$. (i.e. the effects of X_1 and now X_2 removed from X_3 and X_4) are represented by the following relationships

$$G_{33.12} = \left(1 - \gamma_{23.1}{}^2\right) G_{33.1} \qquad \textbf{(A1.9)}$$

$$G_{44.12} = (1 - \gamma_{24.1}{}^2) G_{44.1} \qquad \textbf{(A1.10)}$$

$\gamma_{23.1}{}^2$ is the coherence function between $X_{2.1}$ and $X_{3.1}$, given by

$$\gamma_{23.1}{}^2 = \frac{|G_{23.1}|^2}{G_{22.1} G_{33.1}} \qquad \textbf{(A1.11)}$$

This can now be simplified into a one-in one-out system as shown in Figure A1.6.

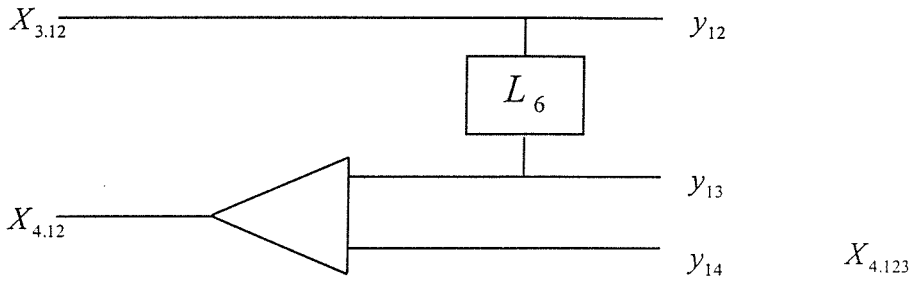

Fig A1.6 Decomposition of two signals

$X_{4.123}$ is the output X_4 conditioned by X_1, X_2. and X_3 consequently it is the noise in the system. The power spectral density of this term (using the same method as above) is given by

$$G_{44.123} = \left(1 - \gamma_{34.12}{}^2\right) G_{44.12} \qquad \textbf{(A1.12)}$$

where $\gamma_{34.12}{}^2$ is the coherence between $G_{33.12}$ and $G_{44.12}$.

The transfer function between $X_{3.12}$ and $X_{4.12}$ using the cross spectral density method is given by

$$TF_{43.12} = \frac{G_{34.12}}{G_{44.12}} \qquad \textbf{(A1.13)}$$

where $G_{34.12}$ is the cross-spectral density between $X_{3.12}$ and $X_{4.12}$. It can be shown that this is expressed as

$$G_{34.12} = G_{34.1} - \frac{G_{24.1}}{G_{22.1}} G_{32.1} \qquad \textbf{(A1.14)}$$

The partial coherence function between $X_{3.12}$ and $X_{4.12}$ is defined as follows

$$\gamma_{34.12}{}^2 = \frac{|G_{34.12}|^2}{G_{33.12} G_{44.12}} \qquad \textbf{(A1.15)}$$

APPENDIX 2- A DATA CORRECTION METHOD FOR SURFACE MEASUREMENT OF VIBRATION ON THE HUMAN BODY

(Extracted from Kitazaki, 1994)

The following describes a data correction method for the surface measurement of vibration on the human body.

The method assumes a single degree of freedom linear model for the local tissue-accelerometer system, within the frequency range of interest, on the spine in the vertical axis (shear direction of tissue) and in the fore-and-aft axis (normal direction of tissue) respectively. The local system can be described by the mass of an accelerometer and tissue involved in the local vibration, *m*, the stiffness of tissue, *k* and the viscous damping coefficient of tissue, *c*, which is all attached to the body system which may have multiple degrees of freedom as shown in figure A2.1.

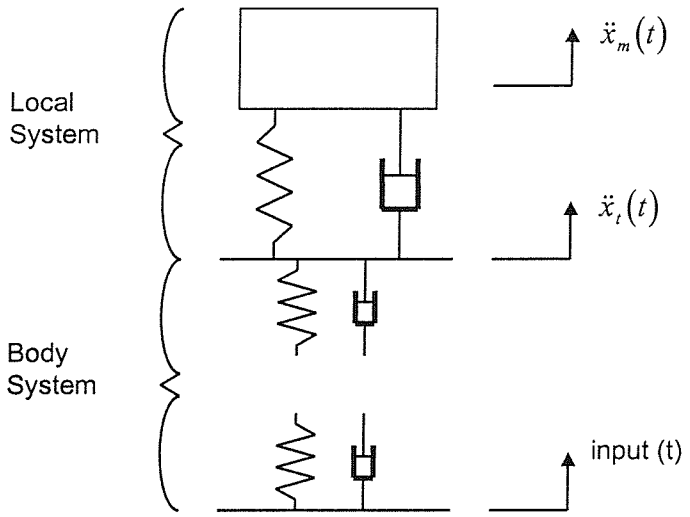

Figure A2.1 Equivalent model for the local system of an accelerometer mounted on the body surface

The input point of the body system occurs at the buttocks and the input is acceleration or force. Let the true acceleration of the spine be $\ddot{x}_t(t)$ and the measured acceleration be $\ddot{x}_m(t)$ which is the response of the system to he input, $\ddot{x}_t(t)$.

The acceleration transfer function of the local system, $T_l(f)$, is the same as the displacement transfer function, which is given by:

$$T_l(f) = \frac{\mathrm{F}\{\ddot{x}_m(t)\}}{\mathrm{F}\{\ddot{x}_t(t)\}} = \frac{\mathrm{X}_m(f)}{\mathrm{X}_t(f)} \qquad \textbf{(A2.1)}$$

where: $\omega = 2\pi f$; $\mathrm{F}\{\ddot{x}_m(t)\} = \mathrm{X}(f)$ means a Fourier transform from the time domain to the frequency domain. If the transfer function of the local system, $T_1(f)$, is determined, the Fourier transform of the true acceleration of the spine, $\mathrm{F}\{\ddot{x}_t(t)\}$, can be obtained from the Fourier transform of the measured acceleration $\mathrm{F}\{\ddot{x}_m(t)\}$:

$$F\{\ddot{x}(t)\} = F\{\ddot{x}(t)\}C(f) \qquad \textbf{(A2.2)}$$

where

$$C(f) = \frac{1}{T_1(f)} \qquad \textbf{(A2.3)}$$

Therefore, $C(f)$ is the correction frequency to eliminate the effect of the local tissue-accelerometer vibration from the measurement acceleration. The time-history of the true spinal acceleration, $\ddot{x}_t(t)$, is obtained by carrying out an inverse Fourier transform of equation A2.2.

The true transfer function of the body system, $T_t(f)$ can be calculated from the measured function, $T_m(f)$, and the correction frequency function, $C(f)$:

$$T_t(f) = T_m(f)C(f) \qquad \textbf{(A2.4)}$$

where

$$T_t(f) = \frac{F\{\ddot{x}_t(t)\}}{F\{input(t)\}} \qquad \textbf{(A2.5)}$$

$$T_m(f) = \frac{F\{\ddot{x}_m(t)\}}{F\{input(t)\}} \qquad \textbf{(A2.6)}$$

The input can be force or acceleration. When the input is force, the transfer functions, $T_m(f)$, are termed accelerances. When the input is acceleration, they are termed acceleration transfer functions.

The equation of motion about the mass of the local system in Figure A2.1 is given by:

$$m\ddot{x}_m(t) + c(\dot{x}_m(t) - \dot{x}(t)) + k(x_m(t) - x_t(t)) = 0 \qquad \textbf{(A2.7)}$$

Solving equation (A2.7) by substituting $x_t(t) = X_t e^{j\omega t}, x_m(t) = X_m e^{j\omega t}$, the theoretical acceleration, or displacement, transfer function of the local system, $T_l(f)$, is obtained:

$$T_l(f) = \frac{j\omega c + k}{-m\omega^2 + j\omega c + k} \qquad \textbf{(A2.8)}$$

Using the natural frequency, ω_0, damping ratio, ξ, and frequency ratio, β, equation (A2.8) is simplified into equation (A2.9):

$$T_l(\beta) = \frac{1 + 2j\xi\beta}{1 - \beta^2 + 2j\xi\beta} \qquad \textbf{(A2.9)}$$

where:

$$\omega_0 = 2\pi f_0 = \sqrt{\frac{k}{m}} \qquad \textbf{(A2.10)}$$

$$\xi = \frac{c}{2\sqrt{mk}}$$

$$\beta = \frac{\omega}{\omega_0} = \frac{f}{f_0}$$

Therefore, the correction frequency function is:

$$C(\beta) = \frac{1-\beta^2+2j\xi\beta}{1+2j\xi\beta} \qquad \textbf{(A2.11)}$$

If the natural frequency, f_0, and the damping ratio, ξ, of the local system are found, the correction frequency function, $C(\beta)$, is determined.

The natural frequency and the damping ratio of the local system are estimated so as to determine the correction frequency function, using the spectral analysis of the free vibration of the local system. Displacing the accelerometer on the body surface and releasing it while a subject is sitting or standing still causes free vibration. The equivalent model for the free vibration test is shown in Figure A2.2.

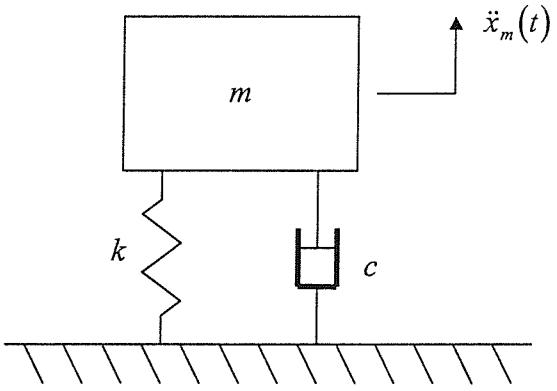

Figure A2.2 Equivalent model of the local system in free vibration

The equation of motion about the mass of the local system is:

$$m\ddot{x}_m(t) + c\dot{x}_m(t) + kx_m(t) = 0 \qquad \textbf{(A2.12)}$$

The initial conditions for the free vibration test are given by:

$$x_m(0) = x_0, \dot{x}_0 = 0 \qquad \textbf{(A2.13)}$$

To solve equations A2.12 and A2.13, a Laplace transform is more useful than a Fourier transform. In fact, a Laplace transform is the same as a Fourier transform, when s is made equal to $j\omega$. By carrying out the Laplace transform of equation A2.12, with the initial conditions A2.13, a Laplace transform of the displacement response, $X_m(s)$, is obtained:

$$X_m(s) = \frac{(ms + c)x_0}{ms^2 + cs + k} \qquad \textbf{(A2.14)}$$

where: s is a Laplace operator. A Laplace transform of the acceleration response, $A_m(s)$, is calculated from equation A2.14, with the initial condition in A2.13:

$$A_m(s) = \frac{ksx_0}{ms^2 + cs + k} \qquad \textbf{(A2.15)}$$

Substituting $s = j\omega$ and using the relationship (A2.10), equation A2.16 is obtained:

$$A_m(\beta) = -\frac{j\omega_0 x_0 \beta}{1 - \beta^2 + 2j\xi\beta} \qquad \textbf{(A2.16)}$$

where: $A_m(\beta)$ is the Fourier transform of the acceleration response to free vibration of the local system. The modulus of the free vibration response is:

$$\left|A_m(\beta)\right|_{\max} = \frac{\omega_0 x_0}{2\xi} \text{ at } \beta = 1 \qquad \textbf{(A2.17)}$$

Therefore, the modulus of the free vibration response reaches a peak at the natural frequency.

Damping can be estimated from the width of the modulus curve around the peak. Letting equation (A2.17) equal to half the power of the peak given by equation (A2.18), equation A2.19 is obtained:

$$\xi = \pm\frac{1-\beta^2}{2\beta} \qquad \textbf{(A2.18)}$$

Using the width of the curve, with Δf_- and Δf_+ in the lower and upper sides as shown in figure A2.3, the frequency ratio corresponding to the half-power points is obtained:

$$\beta = 1 \pm \frac{\Delta f_\pm}{f_0} \qquad \textbf{(A2.19)}$$

Substituting equation A2.20 into equation A2.19, the damping ratio is obtained:

$$\xi_\pm = \mp\frac{1-\left(1 \pm \frac{\Delta f_\pm}{f_0}\right)^2}{2\left(1 \pm \frac{\Delta f_\pm}{f_0}\right)} \qquad \textbf{(A2.20)}$$

When damping is quite small, equations (A2.21) can be approximated to $\xi_\pm = \frac{\Delta f_\pm}{f_0}$.

However, the approximation is not quite appropriate for the heavy damping of the human body.

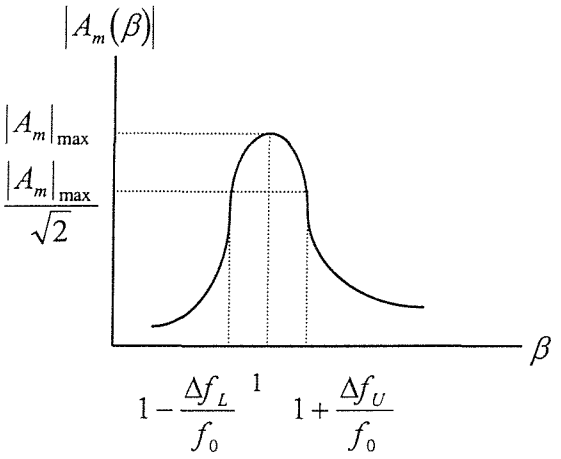

Figure A2.3 Half Power Point of a Single Degree of Freedom System

By the above means, a correction function is obtained by substituting the natural frequency and damping ratio into equation (A2.11). The advantage of this method is that correction works not only for the additional mass of the accelerometers but also for the mass of skin and shallow tissue around the contact area involved in the local vibration, because the method does not use the mass and stiffness of the local system directly.

APPENDIX 3 FUNDAMENTALS OF EXPERIMENTAL MODAL ANALYSIS

(Extracted from Kitazaki, 1994)

Experimental modal analysis replies upon the theory that the dynamic behaviour of a structure can be described in terms of its modal properties of the natural frequencies, the mode shapes and the damping. The technique seeks to extract the modal properties from measured data, generally from transfer functions. Two assumptions are made when applying the experimental modal analysis technique to the human body. These are that the body behaves in a linear manner and that the damping of the human body is hysteretic.

The equation of motion for a linear structure with N degrees of freedom and viscous damping can be described by equation A3.1

$$[M]\{x(t)\}+i[H]\{x(t)\}+[K]\{x(t)\}=\{f(t)\} \qquad \textbf{(A3.1)}$$

where: $[M]$ is the $N\times N$ viscous damping matrix; $[K]$ is the $N\times N$ stiffness matrix; $\{\ddot{x}(t)\}$ and $\{x(t)\}$ are the $N\times 1$ acceleration and displacement response vectors; $\{f(t)\}$ is the $N\times 1$ applied force vector. The free response (i.e. $\{f(t)\}=0$ solution of equation A2.1 provides N eigenvalues; ${\lambda_1}^2$, ${\lambda_2}^2,\ldots,{\lambda_N}^2$ and associated eigenvectors; $\{\phi_1\}$, $\{\phi_2\},\ldots,\{\phi_N\}$. For this general case, both the eigenvalues and the eigenvectors are mathematically complex. The eigenvalues are of the form:

$${\lambda_r}^2={\omega_r}^2(1+i\eta_r) \qquad \textbf{(A3.2)}$$

where: ω_r is the undamped natural angular frequency for the rth mode. In the special case of proportional damping where the damping matrix is described by equation A3.3, both the eigenvalues and the eigenvectors take real values.

$$[H]=\beta[M]+\gamma[K] \qquad \textbf{(A3.3)}$$

The complex eigenvectors, which correspond to the complex mode shape vectors, can be scaled in such a way that the orthogonality properties may be expressed by the relationships:

$$[\phi]^T[M][\phi]=[I] \qquad \textbf{(A3.4a)}$$

$$[\phi]^T[K][\phi]=\left[\omega_r{}^2\right] \qquad \textbf{(A3.4b)}$$

$$[\phi]^T[H][\phi]=\left[\eta_r\omega_r{}^2\right] \qquad \textbf{(A3.4c)}$$

where: $[\phi]$ is the modal matrix whose columns are mode shape vectors (i.e. $[\phi]=[\{\phi_1\},\{\phi_2\},\ldots\{\phi_N\}]$; $[I]$ is the identity matrix; $\left[\omega_r{}^2\right]$ is the diagonal matrix of $\omega_r{}^2$; $\left[\eta_r\omega_r{}^2\right]$.

Transforming equation A3.1 using the modal coordinates and letting $\{x(t)\}=\{X\}e^{j\omega t}$, $\{f(t)\}=\{F\}e^{j\omega t}$, the displacement response is obtained:

$$\{X\}=\sum_{r=1}^{N}\frac{A_{jkr}+iB_{jkr}}{\omega^2-\omega^2+i\eta_r\omega_r{}^2} \qquad \textbf{(A3.5)}$$

The receptance (displacement/force) between the sites j and k, α_{jk}, can be written by a decoupled equation (A3.6):

$$\frac{X_j}{F_k}=\alpha_{jk}=\sum_{r=1}^{N}\frac{A_{jkr}+iB_{jkr}}{\omega_r{}^2-\omega^2+i\eta_r\omega^2{}_r} \qquad \textbf{(A3.6)}$$

with:

$$A_{jkr}+iB_{jkr}=\phi_{jr}\phi_{kr} \qquad \textbf{(A3.7)}$$

where: X_j is the displacement response at the site j; F_k is applied at the site k; $\phi_{j\eta}\ \phi_{kr}$ are the mode shapes for the rth mode at the sites j and k which correspond to deformation ratios for the rth mode; ω is the angular excitation frequency; A_{jkr} and B_{jkr} are termed the modal constants. Equation A3.6 indicated that the response is expressed by a summation of all the modes. It can be approximated to a single term corresponding to the dominant rth mode with a constant and complex residual term representing the contributions of the remaining modes:

$$\alpha_{jk} \cong \frac{A_{jkr} + iB_{jkr}}{{\omega_r}^2 - \omega^2 + i\eta_r {\omega_r}^2} + residual \qquad \textbf{(A3.8)}$$

Experimental modal analysis extracts the modal properties of the natural frequencies, ω_r, the damping, η_r, and the modal constants, A_{jkr} and B_{jkr} for each mode, generally based on equation A3.6. Finally, the modal matrix, $[\phi]$, is determined using the relationship A3.7 and the deformation of the structure can be plotted at each mode.

There are various methods for extracting the modal properties. A widely used single degree of freedom method is based on the fact that the frequency response around the resonance (equation A3.8) may be displayed as a circular locus when plotted on an Argand diagram (complex plane). The modal properties are extracted from the best fit circle based on equation A3.8. The method used in this study has been based upon a single-degree-of-freedom model classified as the dynamic stiffness (1/receptance) method. Reversing equation A3.8, equation A3.9 is obtained:

$$\frac{1}{\alpha_{jk}} = \frac{{\omega_r}^2 - \omega^2 + i\eta_r {\omega^2}_r}{A_{jkr} + iB_{jkr}} \qquad \textbf{(A3.9)}$$

with:

$$\alpha_{jk}^{\cdot} = \alpha_{jk} - residual \qquad \textbf{(A3.10)}$$

If the real and imaginary components of equation A3.9 are plotted against ω^2 with an assumption of the proportional damping for the structure (i.e. B_{jkr} =0), it is possible to extract the modal properties directly from slopes and intercepts of the straight lines.

APPENDIX 4- ANSYS TEXT FILE OF NECK-HEAD-HELMET MODEL

```
/COM ********* MODEL 4 IS ALL NEW HEAD-NECK HELMET MODEL ***************
/COM
/COM ****REWRITTEN WITH UPDATED GEOMETRY AND OTHER PROPERTIES ****
/COM *******VERIFIED USING EXPERIMENTAL MODAL ANALYSIS RESULTS ********
/COM
/COM ******************PROGRAM FOR ANSYS PREP7 (WITH PREPROCESSING) ****
/COM *******************FOR MODAL AND HARMONIC ANALYSIS**********************
/COM
/COM ************************* LAYING THE FOUNDATION *******************************
/COM
/FILENAME, H2
/TITLE, Reuben Peckham, Neck-head Model Mk 2, October 1998
/UNITS, SI
/PREP7
/COM
/COM ==================THE HEAD ================================
/COM
ET,1,42                         *PLANE 42 ELEMENT FOR THE HEAD
MP,EX,1,10.E9           *       HEAD'S YOUNG'S MODULULS
ET,2,21,,,3                     MASS 21 ELEMENT FOR HEAD C OF MASS
/COM                            WITH 2-D ROTARY INERTIA
R,1,4.75,0.0211                 MASS AND MOMENT OF INERTIA OF HEAD
ET,3,3                          BEAM 3 ELEMENT FOR RIGID LINK JOINING
/COM                            HEAD TO C OF MASS
ET,4,14,,6              *       COMBINI14 TORSIONAL SPRING-DAMPER,
/COM                            ROTATING ABOUT Z AXIS
ET,5,14,,1              *       COMBINI14 TORSIONAL SPRING DAMPER, UX
/COM                            D OF F
ET,6,14,,2              *       COMBINI14 TORSIONAL SPRING DAMPER, UY
/COM                            D OF F
/COM
/COM ******************************* NODES FOR THE HEAD ****************************
/COM
N,1,0,0                 *       DEFINING HEAD NODES
```

```
N,2,0,0.0803
N,3,0.0169,0.0803
N,4,-0.0082,0.125
N,5,-0.0064, 0.1346
N,6,-0.10175,0.2277
N,7,-0.2099,0.1
N,8,-0.13,0.03
N,11,-0.2099,0.1346
N,12,-0.1899,0.192
N,13,-0.0264,0.192
N,14,-0.064075,0.215
N,15,-0.139425,0.215
N,16,-0.17,0.03
N,17,-0.09,0.03
N,18,-0.07,0
N,19,-0.10175,0.1346
N,20,-0.10175,0.17
N,21,-0.10175,0.21
N,22,-0.05,0.185
N,23,-0.05,0.15
N,24,-0.05,0.12
TYPE,1                  *       DEFINING ELEMENT TYPE 1- PLANE42
/COM                            STRUCTURE FOR HEAD
MAT,1           *               DEFINING MATERIAL TYPE 1- SPECIFYING YM
/COM                            OF HEAD
E,1,2,17,18     *               DEFINING QUAD ELEMENTS FOR HEAD
E,2,3,4,24
E,2,24,17
E,4,5,23,24
E,5,13,22,23
E,13,14,22
E,22,14,6,21
E,23,22,21,20
E,23,20,19,24
```

```
E,19,8,17,24
E,8,19,7,16
E,19,20,11,7
E,12,11,20,21
E,12,21,15
E,15,21,6
/COM
/COM ****************************** HEAD CENTER OF MASS ****************************
/COM
N,25,-0.1128,0.064          *       LOCATION OF HEAD CENTER OF MASS
TYPE,2                              *REFERS TP MASS 21 ELEMENT FOR HEAD
/COM                                C OF MASS
REAL,1                              *REFERS TO MATERIAL CONSTANT 1 FOR
/COM                                HEAD
E,25                        *       SPECIFIES NODE 25 AS AN ELEMENT
/COM
/COM ******************************************** RIGID LINKS ***************************
/COM
MP,DENS,2,1.E-3                     * DEFINING DENSITY OF RIGID LINK AS
/COM                                NOMINAL
MP,EX,2,1.E10                       * DEFINING YM OF RIGID LINK AS V. STIFF
/COM                                * IE RIGID LINK IS V.LIGHT BUT VERY STIFF
R,2,1.E-4,1.4E-4,0.05               * REAL CONSTANT 2- CSA, INITIAL STRAIN,
/COM                                HEIGHT
TYPE,3                              * USE ELEMENT TYPE 3 DEFINED AS BEAM 3
MAT,2                               * DEFINING MAT PROPERTIES 2 FOR RIGID
/COM                                LINK
REAL,2                              * DEFINING REAL CONSTANTS 2 FOR RIGID
/COM                                LINK
E,8,25                              * DEFING LINK BETWEEN NODES 8 AND 25
/COM
/COM ************************************* RIGID LINKS IN NECK ************************
/COM
N,10,-0.13,-0.1325                  * LOCATION OF NECK LINKS
```

```
N,9,-0.11,-0.06625
TYPE,3                          * DEFNING ELEMENT TYPE 3- BEAM 3
ELEMENT
MAT,2                           * DEFINING MATERIAL PROPERTIES 2
REAL,2                          * DEFINING REAL PROPERTIES 2
/COM
/COM
/COM                            * SO THE PROPERTIES OF THE NECK BEAM
/COM                             ARE THE SAME AS
/COM                            * THE LINK IN THE HEAD
N,26,-0.13,0.03                  *EXTRA NODE, IN SAME POINT AS NODE 8- TO
/COM                            JOIN SPRING TO
N,27,-0.11,-0.06625              *EXTRA NODE, IN SAME POINT AS NODE 9- TO
/COM                            JOIN SPRING TO
N,28,-0.13,-0.1325               *EXTRA NODE, IN SAME POINT AS NODE 10-
/COM                            TO JOIN SPRING TO
/COM
E,8,9                           * DEFINING NECK LINKS AS ELEMENTS
E,9,10                          *
R,20,1.695,0.02                 * DEFINING NECK MASS AND MOMENT
/COM                            OF INERTIA
TYPE,2                          * ELEMENT TYPE 2- SIMPLE MASS
REAL,20                         * USING NECK MASS OF 1.695KG
E,9                             * DEFINING ELEMENT 9 AS HAVING MASS
/COM
/COM ****************************** NECK SPRINGS ****************************************
/COM
R,3,100                          * DEFINING TORSIONAL SPRING STIFFNESS
/COM                            AS 100 KO1
R,4,100                          * DEFINING TORSIONAL SPRING STIFFNESS
/COM                            AS 100 KO2
R,5,250                          * DEFINING TORSIONAL SPRING STIFFNESS
/COM                            AS 250 KO3
/COM
```

```
TYPE,4                          *USE ET4- COMBINI14 SPRING DAMPER-AS
/COM                            TORSIONAL SPRING
/COM                            * ABOUT Z
REAL,3                          *REAL CONSTANT 3- KO1
E,8,26                          *MAKE SPRING BETWEEN NODES 8 AND 26-
/COM                            (AT SAME LOCATION)-K01
REAL,4                          *REAL CONSTANT 4- WITH STIFFNESS FOR
/COM                            KO2
E,9,27                          *MAKE SPRING BETWEEN NODES 9 AND 27 (AT
/COM                            SAME
/COM                            LOCATION)-KO2
REAL,5                          *REAL CONSTANT 5- WITH STIFFNESS FOR
/COM                            KO3
E,10,28                         *MAKE SPRING BETWEEN NODES 10 AND 28
/COM                            (AT SAME LOCATION)-KO3
/COM
/COM        STATUS- NOW TORSIONAL SPRINGS IN THE NECK ARE
/COM                    ALSO COMPLETE.
/COM
/COM ********************** SPINAL TRANSLATIONAL SPRINGS **********************
/COM
R,6,6000                        *STIFFNESS OF LINEAR SPRING K1
R,7,7370                        *STIFFNESS OF LINEAR SPRING K2
TYPE,5                          *ET 5- LINEAR SPRING WITH UX DEGREE OF
/COM                            FREEDOM
REAL,6                          *REAL CONSTANT 6 K1 HAS STIFFNESS 6000
E,10,28                         MAKE LINEAR SPRING K1 BETWEEN NODES 15
/COM                            AND 18 (AT SAME LOCATION)
TYPE,6                          *ET6- LINEAR SPRING WITH UY DEGREE OF
/COM                            FREEDOM
REAL,7                          REAL CONSTANT 7 K2 HAS STIFFNESS 6600
E,10,28                         MAKE LINEAR SPRING K2 BETWEEN NODES 15
/COM                            AND 18
D,28,ALL                        CONSTRAINS BASE OF SPRINGS FROM
```

```
/COM                    MOVING
/COM
/COM ************************************** HELMET GEOMETRY ************************
/COM
N,29,0.025,0.1546
N,30,0.0325,0.1546
N,31,0.00685,0.22345
N,32,-0.0325,0.23825
N,33,-0.10175,0.26095
N,34,-0.172675,0.23825
N,35,-0.22315,0.22345
N,36,-0.25315,0.1346
N,37,-0.25315,0.0946
N,38,-0.26313,0.0946
N,39,-0.26315,0.1346
N,40,-0.23022,0.23052
N,41,-0.179745,0.24532
N,42,-0.10175,0.27095
N,43,-0.02543,0.24532
N,44,0.01392,0.23052
TYPE,1
MP,EX,5,1.E9                    * DEFINING ET1-PLANE 42 QUAD FOR
ELEMENT
MAT,5
E,29,30,44,31                   * CREATING HELMET ELEMENTS
E,31,44,43,32
E,32,43,42,33
E,33,42,41,34
E,35,34,41,40
E,35,40,39,36
E,36,39,38,37
/COM
/COM            HELMET CENTER OF MASS AND RIGID LINKS
/COM
```

```
R,8,1.3,0.02                    * HELMET MASS IS 1.3KG, MOI IS 0.02
REAL,8
TYPE,2                          * HELMET C OF MASS IS A POINT MASS
E,20                            * DEFNING NODE 20 AS LOCATION FOR
HELMET C OF MASS
TYPE,3                          * RIGID LINK
REAL,2                          * MAT CONST 2
E,31,20                         * RIGID LINK JOINING HELMET TO ITS CENTER
OF MASS
E,35,20
/COM
/COM ******************SCALP BEAM ELEMENTS BETWEEN HEAD AND HELMET*****
/COM
R,9,1.8.E-32,1.E-4,0.03         * REAL CONSTANTS 9, CSA=1E-2M2,
/COM                            IZZ=1E-4, HEIGHT=0.005
MP,EX,6,265                     * YM OF 265 OF SCALP
MP,NUXY,6,0.3                   * POISSON RATIO
MP,DENS,6,1.E-3                 * NOMINAL DENSITY OF SCALP
MAT,6                           * MATERIAL CONSTANT 6
REAL,9                          * USE REAL CONSTANT 9
TYPE,3                          * USE BEAM3 ELEMENT
E,13,31                         * MAKING SCALP ELEMENTS BETWEEN
 /COM                           HEAD AND HELMET
E,12,35
FINISH
/COM============================THE SOLUTION=====================
/SOLU
ANTYPE,MODAL
MODOPT,SUBSP,4
SOLVE
FINISH
/SOLU
EXPASS,ON
MXPAND,6
```

```
SOLVE
FINISH
/POST1
```

APPENDIX 5- SUPPLEMENTARY GRAPHS TO DEMONSTRATE INTERSUBJECT VARIABILITY AND COHERENCY

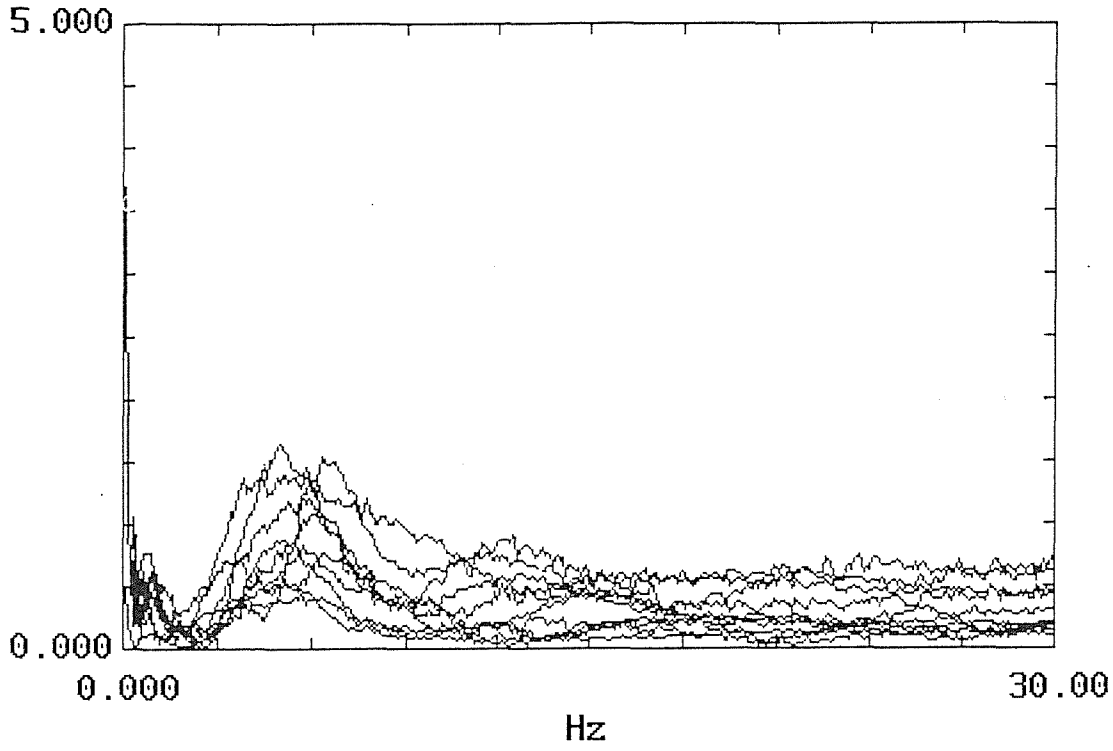

Figure A5.1 Transmissibility (Seat z to Head x) Intersubject Variability, Std Mk VI Helmet

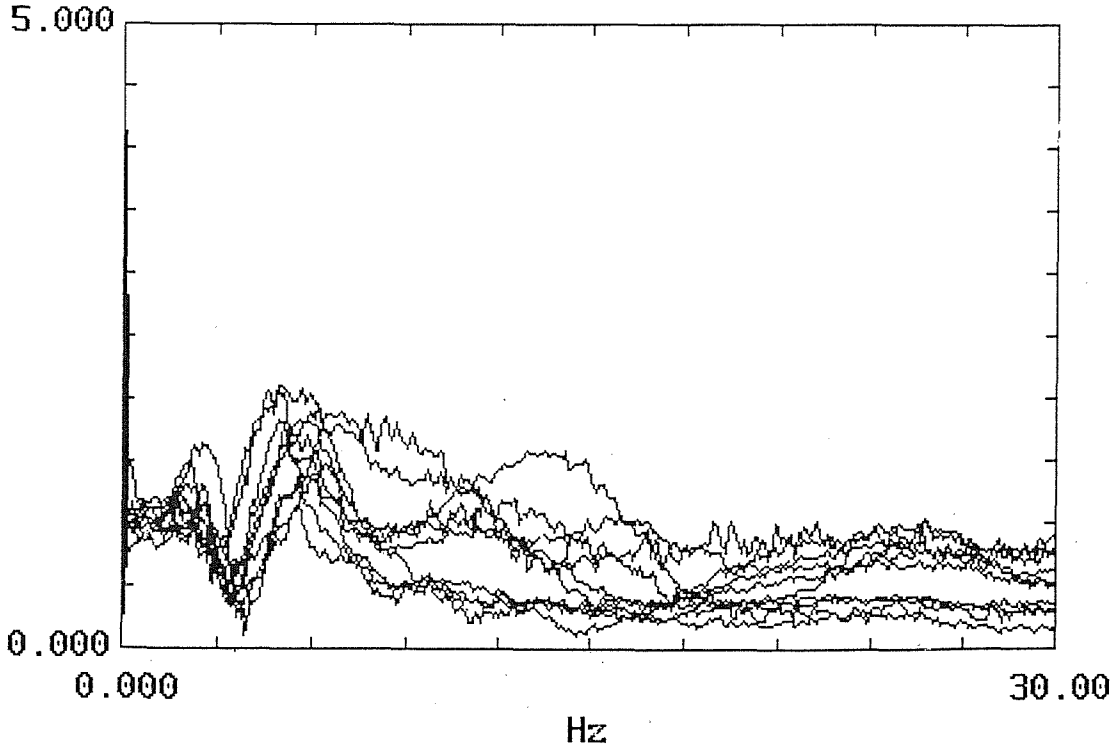

Figure A5.2 Transmissibility (Seat z to Head z) Intersubject Variability, Std Mk VI Helmet

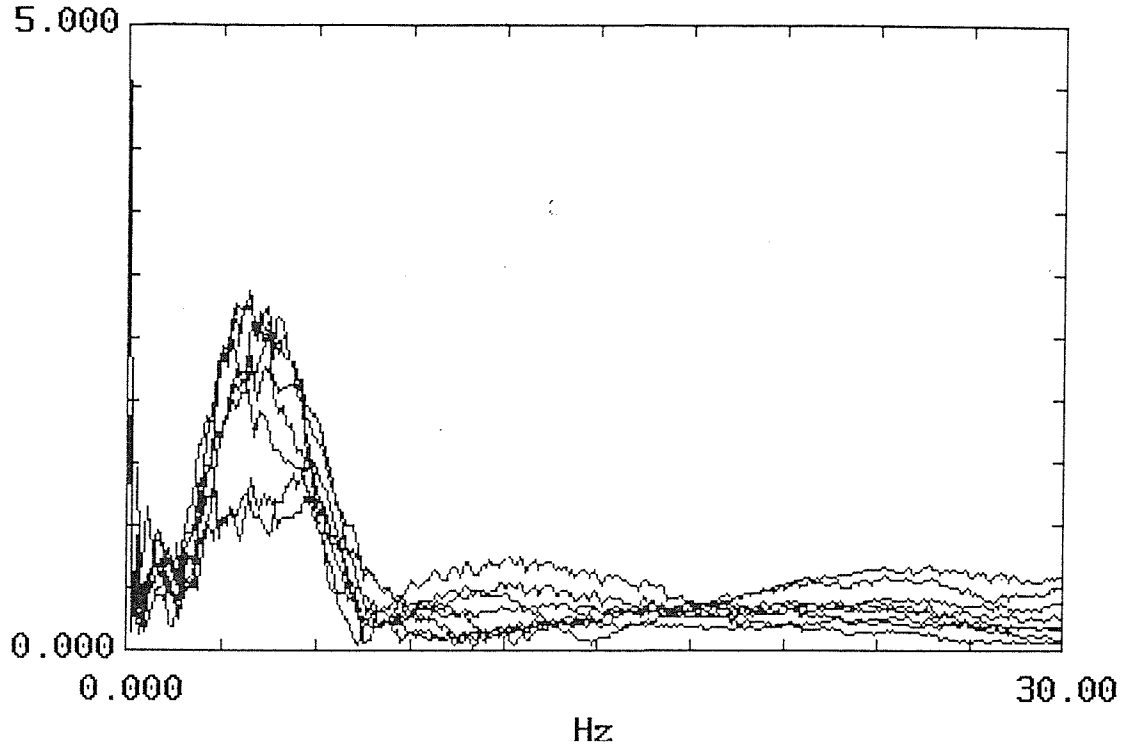

Figure A5.3 Transmissibility (Seat z to Helmet x) Intersubject Variability, Std Mk.VI Helmet

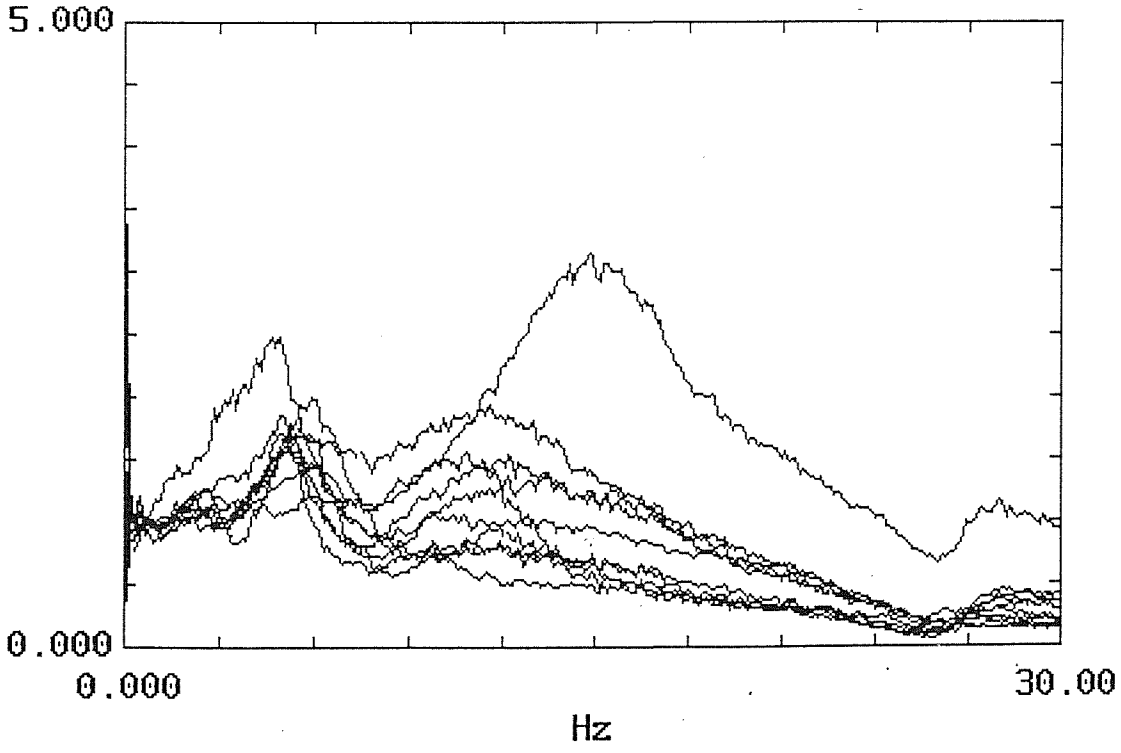

Figure A5.4 Transmissibility (Seat z to Helmet z) Intersubject Variability, Std Mk VI Helmet

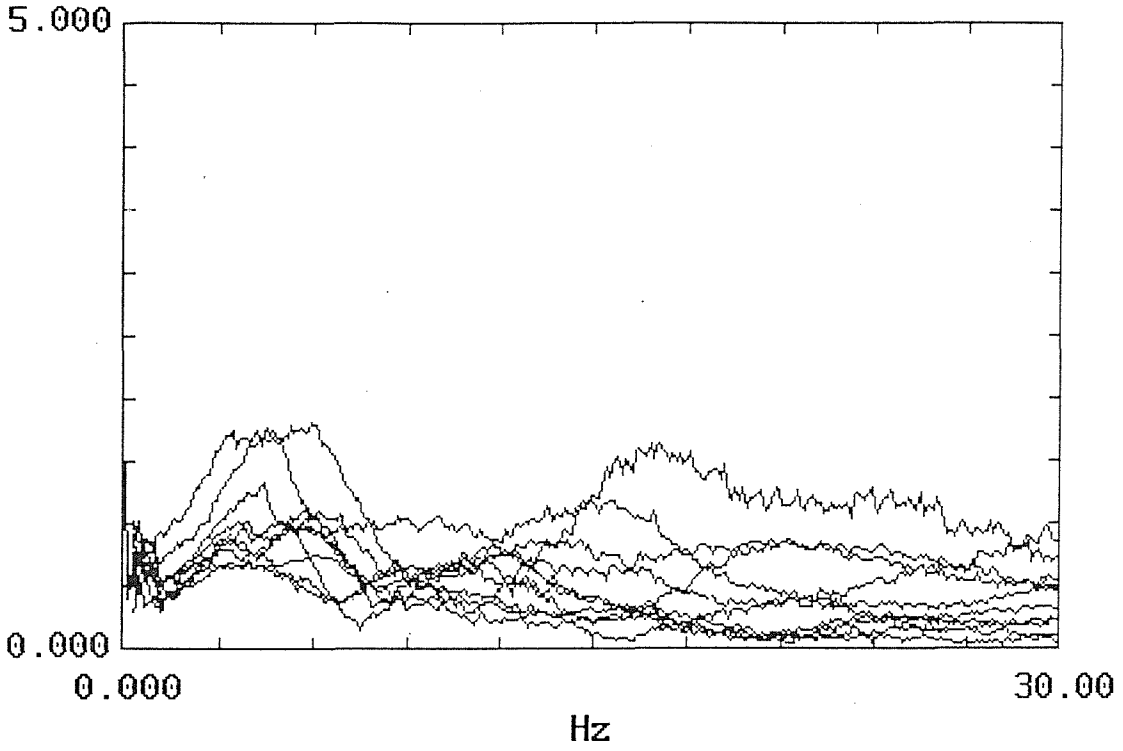

Figure A5.5 Transmissibility (Seat z to Neck x) Intersubject Variability, Std Mk VI Helmet

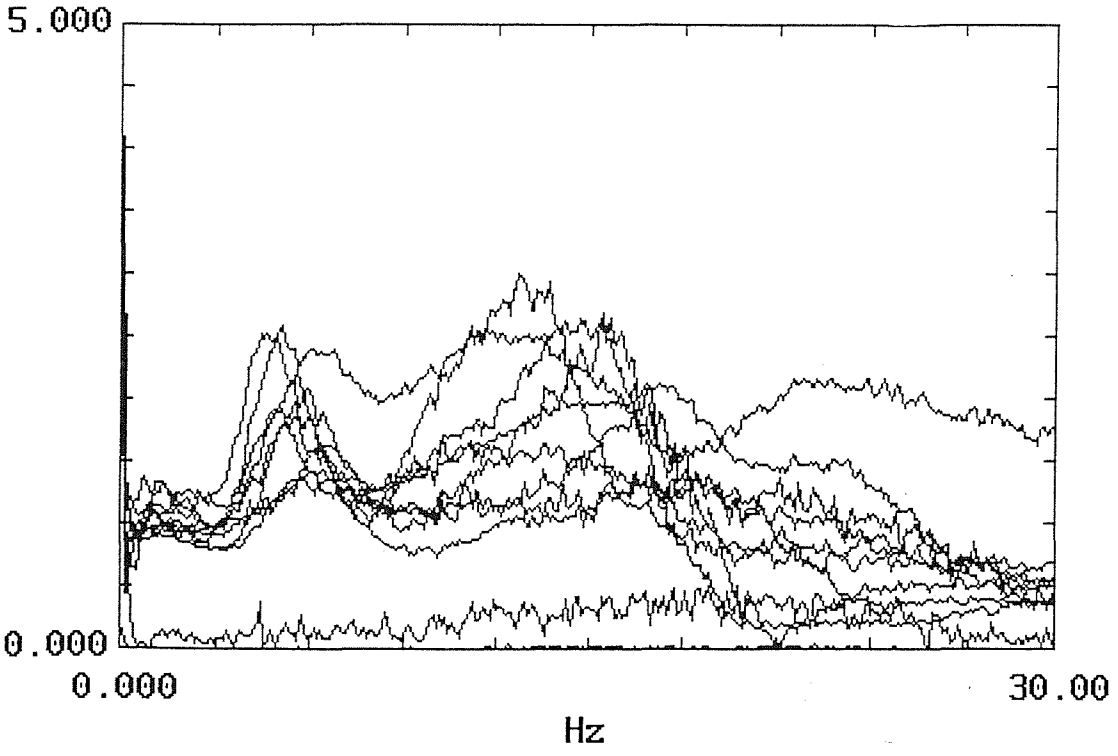

Figure A5.6 Transmissibility (Seat z to Neck z) Intersubject Variability, Std Mk VI Helmet

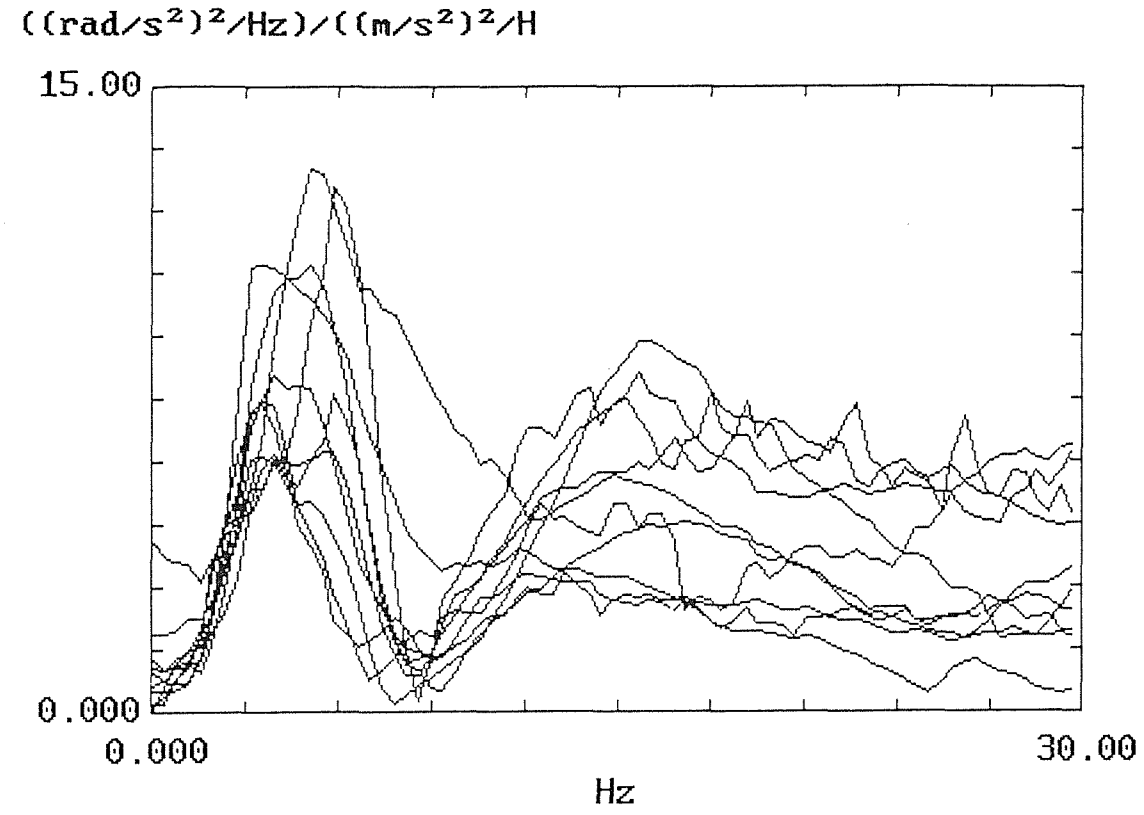

Figure A5.7 Transmissibility (Seat z to Head pitch) Intersubject Variability, Std Mk VI Helmet

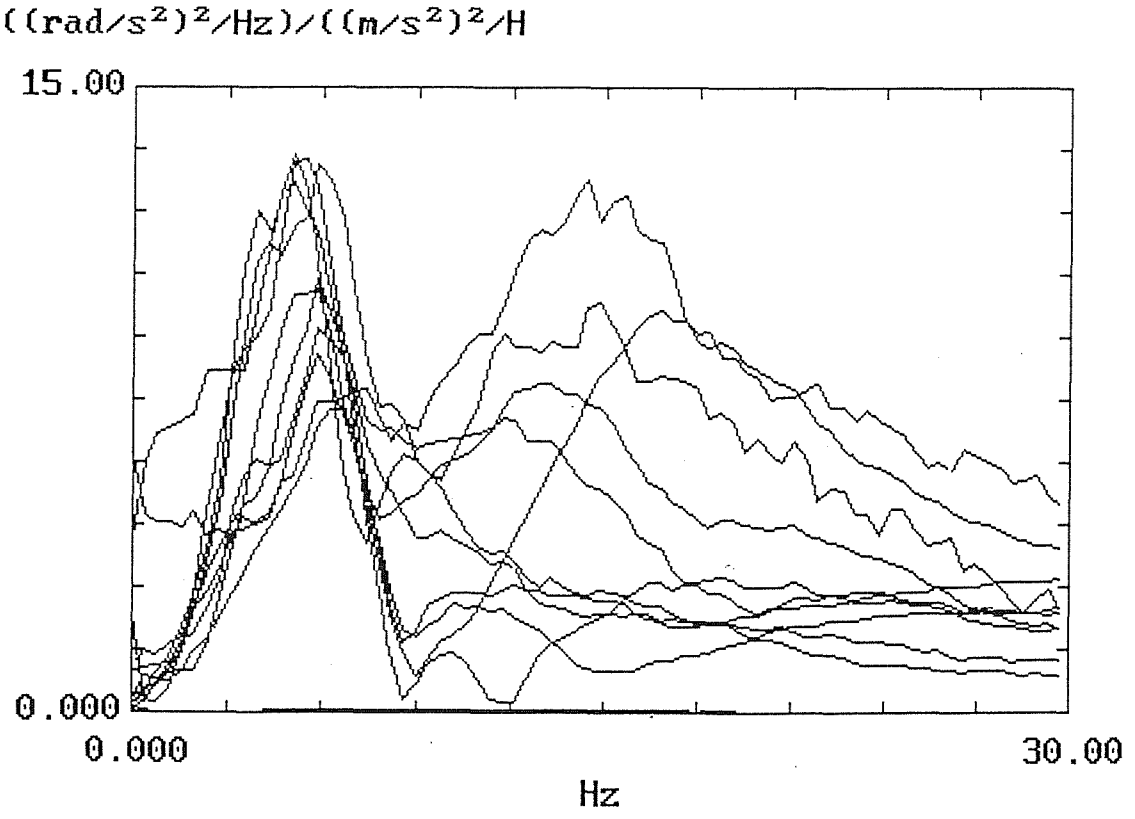

Figure A5.8 Transmissibility (Seat z to Helmet pitch) Intersubject Variability, Std Mk VI Helmet

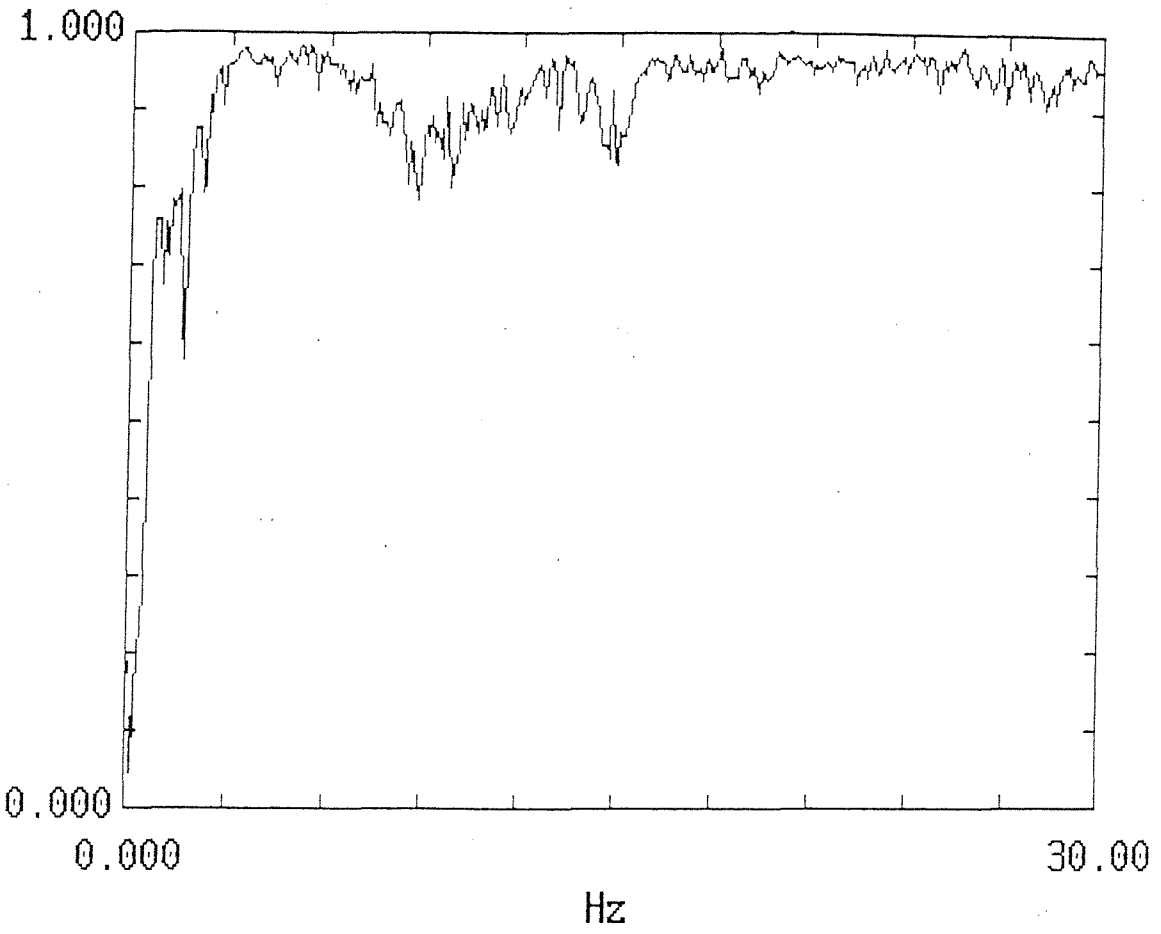

Figure A5.9 Coherency (Seat z to Head x), Std Mk VI Helmet

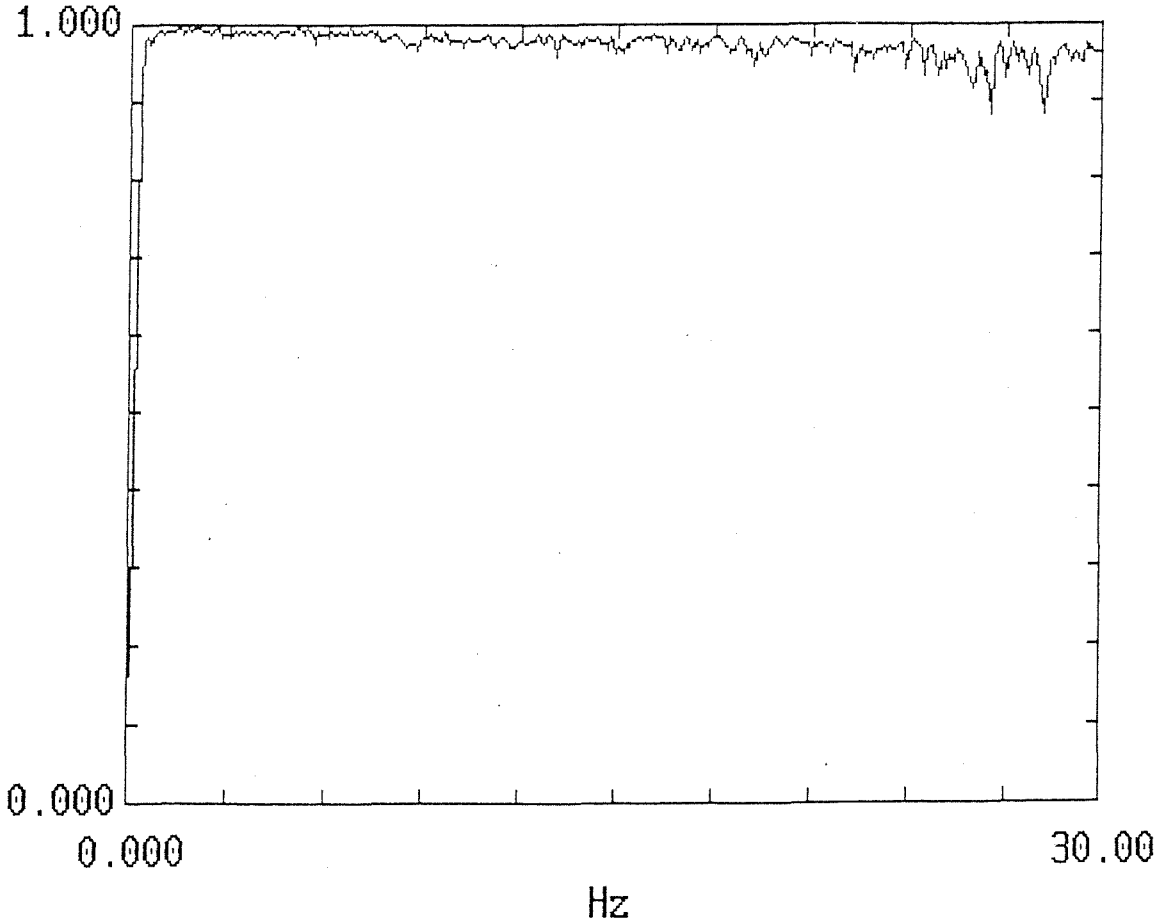

Figure A5.10 Coherency (Seat z to Head z), Std Mk VI Helmet

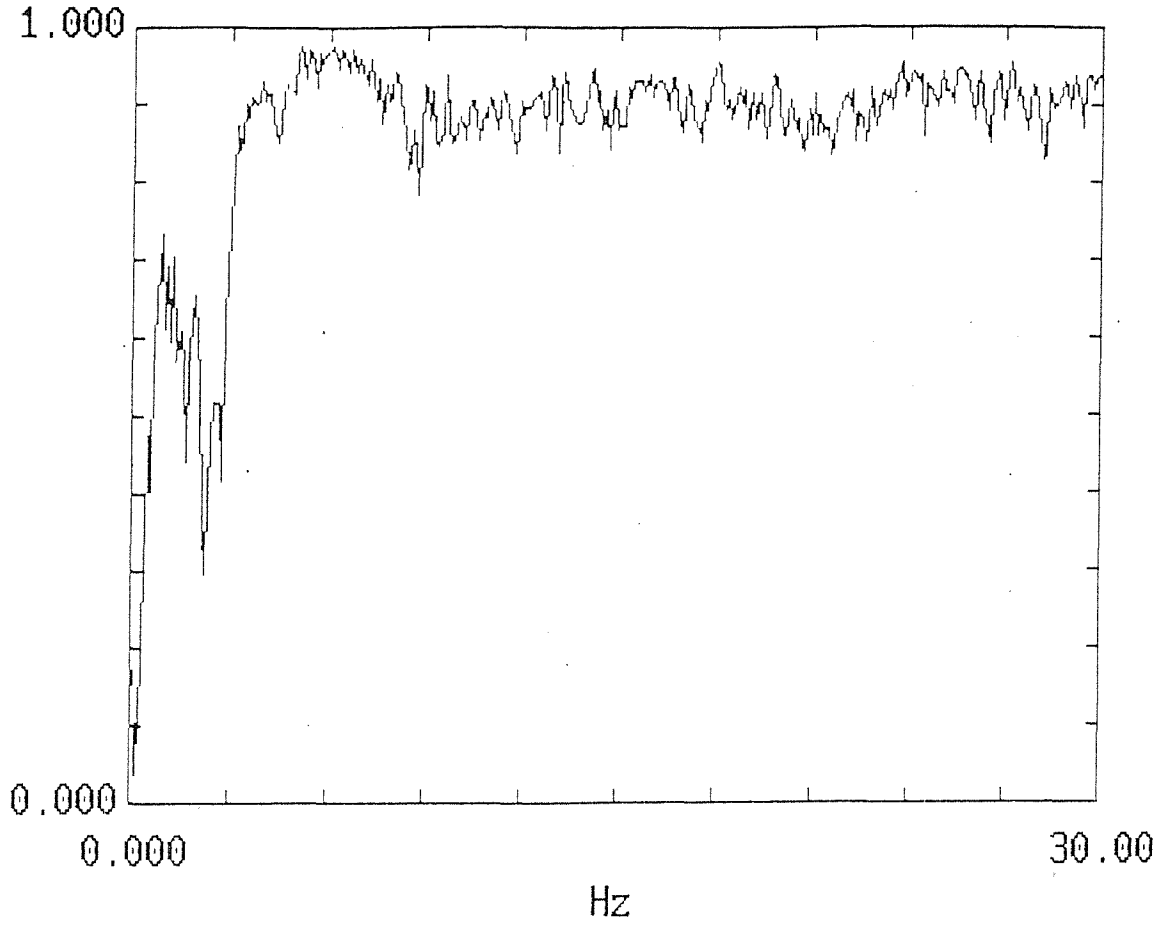

Figure A5.11 Coherency (Seat z to Helmet x), Std Mk VI Helmet

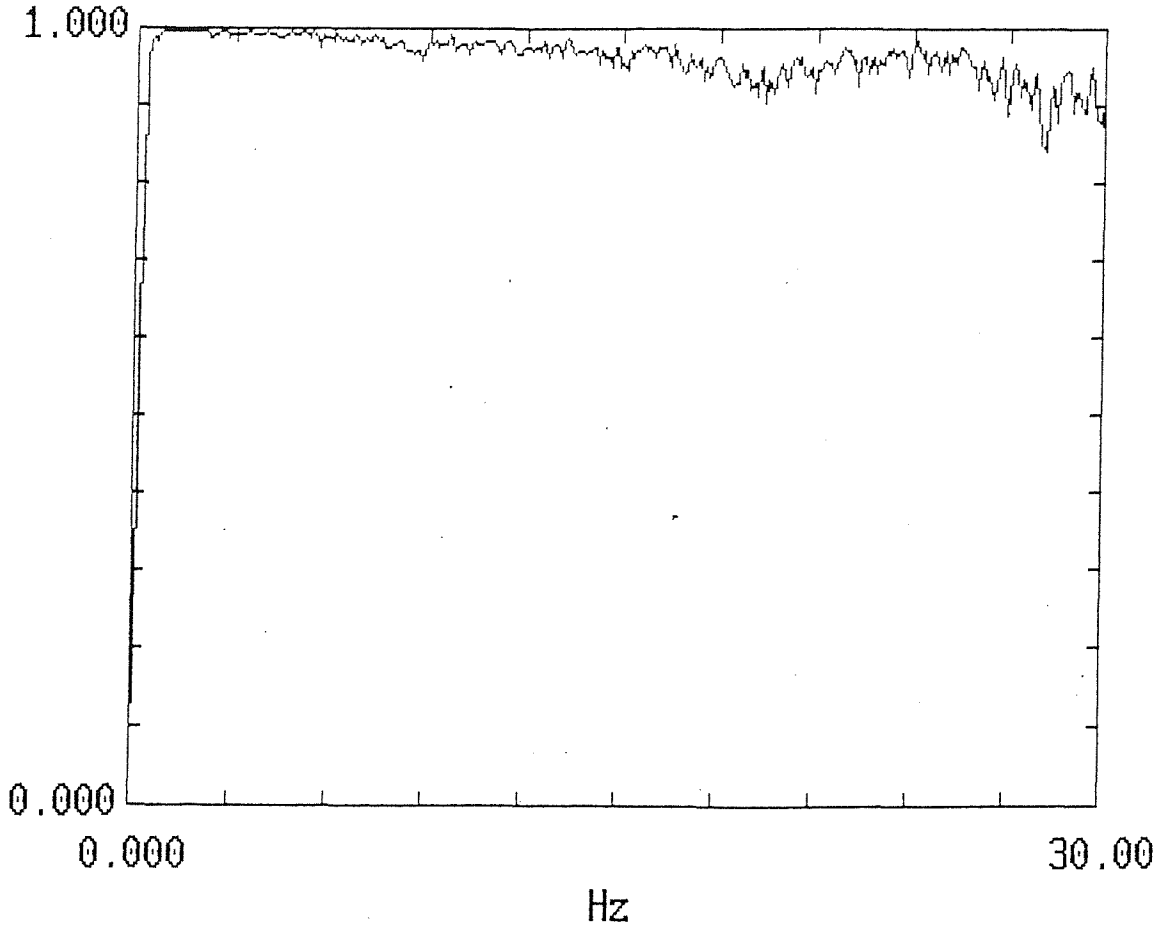

Figure A5.12 Coherency (Seat z to Helmet z), Std Mk VI Helmet

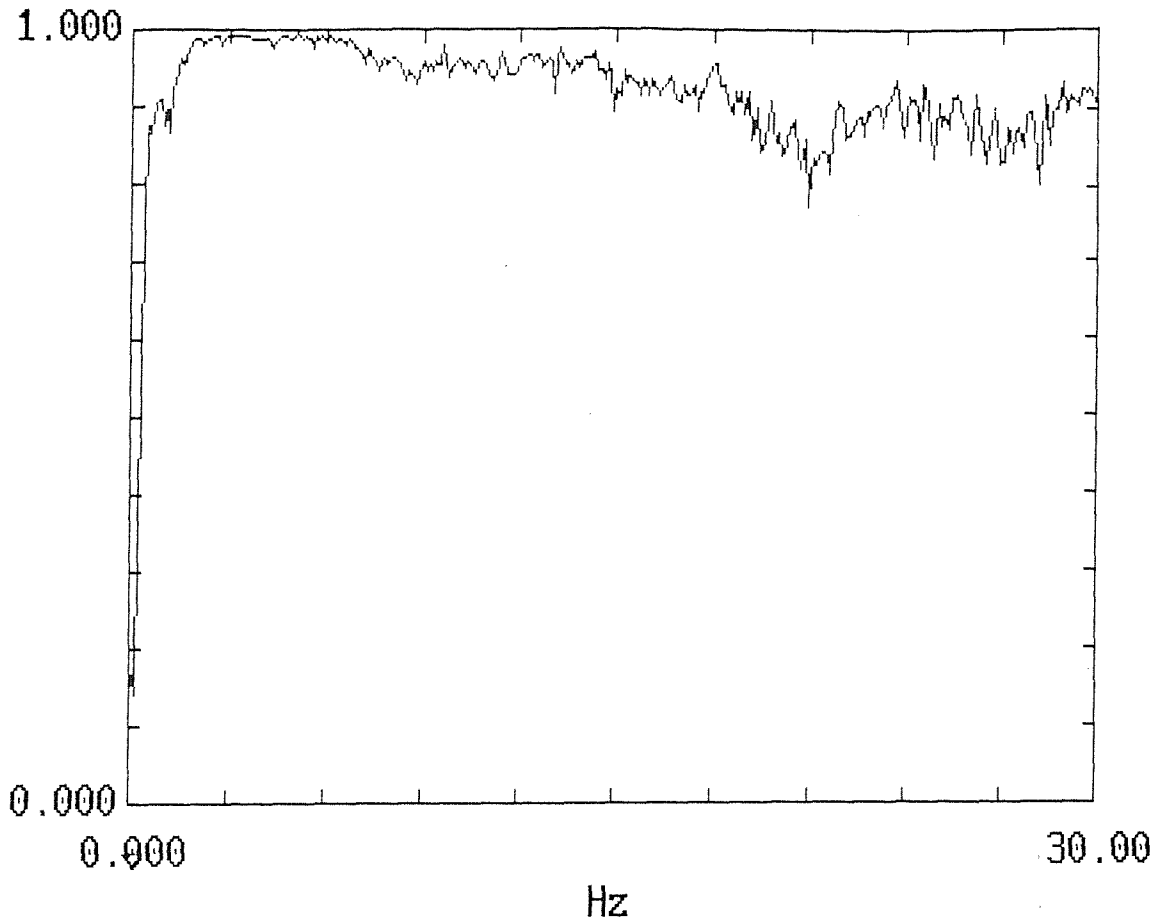

Figure A5.13 Coherency (Seat z to Neck x), Std Mk VI Helmet

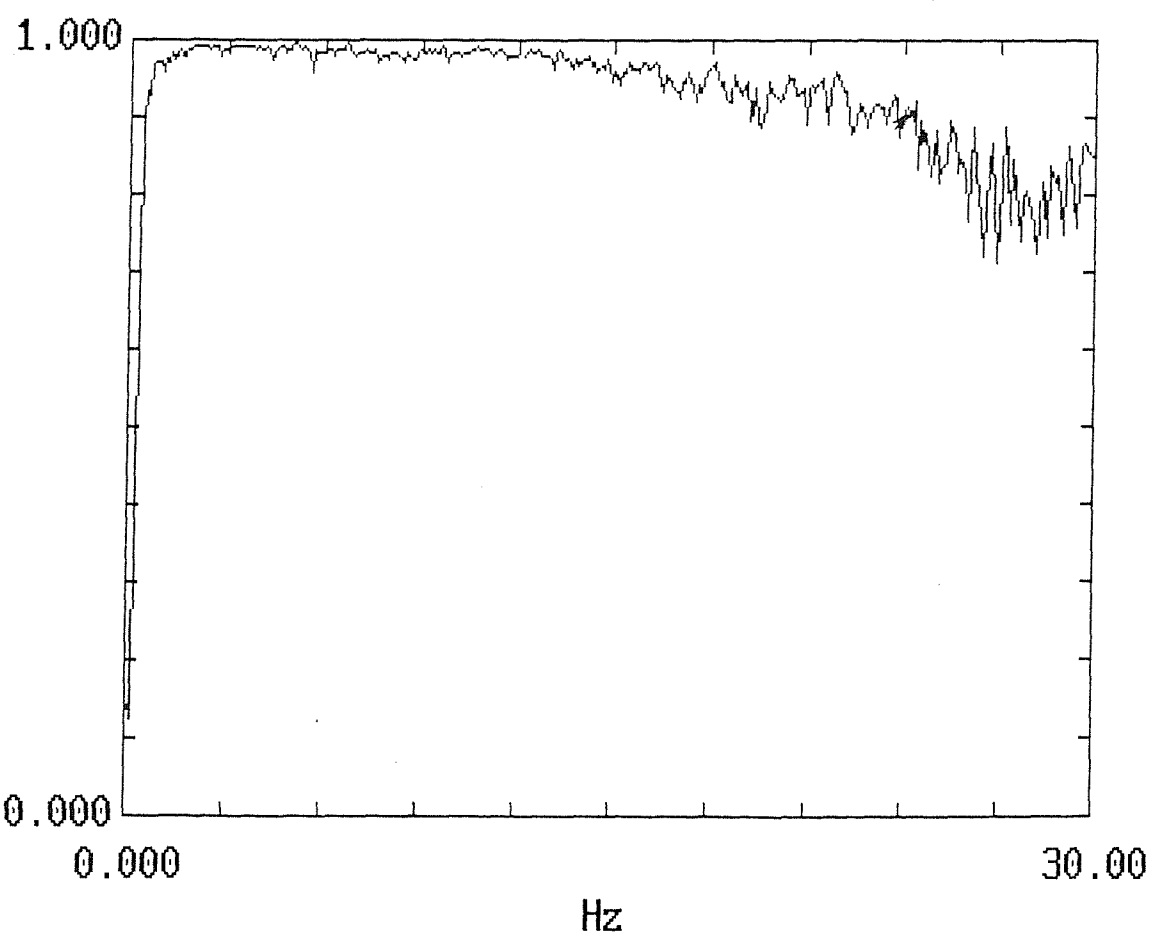

Figure A5.14 Coherency (Seat z to Neck z), Std Mk VI Helmet

REFERENCES

Anton, D. J. (1987). The biodynamic implications of helmet mounted devices. *Proceedings of the Royal Aeronautical Society, Feb 1987, Paper 15.*

Bartz, J. A. (1972). Validation of a three-dimensional mathematical model of the crash victim. *Proceedings of a symposium on Human Impact and Response, Warren, Michigan, 1973.*

Beier, G., Schuck, M., Schuller, E., Spann, W. (1979). Determination of physical data of the head I. Center of gravity and moments of inertia of human heads. *Office of Naval Research, Contract N 000 14-75-C-0486. Prepared by Institute of Forensic Medicine, University of Munich, West Germany.*

Bendat and Piersol (1986). Random data: analysis and measurement procedures. *2nd Edition, J Wiley and sons, 1986*

Belytschko, T., Privitzer, E. (1978). Refinement and validation of a three-dimensional head-spine model. *Aerospace Medical Research Laboratory, Wright-Patterson Air Force Base, Ohio, AMRL-TR-78-7.*

Belytschko, T., Schwer, L., Schultz, A. (1976) A model for analytic investigation of three-dimensional spine-head dynamics. *Aerospace Medical Research Laboratory, Wright-Patterson Air Force Base, Ohio. Report No. AMRL-TR-76-10.*

Berme, N., Capozzo, A., Figura, F.(1984). Loading of the spine during dynamic physical exercises. *Proceedings of the 4th European Conference on Biomaterials, Leuven, Belgium.*

Bhattacharya, A., McCutcheon, E. P., Shvartz, E., Greenlead, E. J. (1980). Body acceleration distribution and 02 uptake in humans during running and jumping. *Journal of Applied Physiology, Respirator Environment Exercise Philosophy, 49(5), pp 881- 887.*

BS6841: 1987. Measurement and evaluation of human exposure to whole-body mechanical vibration and repeated shock. British Standards Institution, 1987.

Cappozzo, A. (1982). Low frequency self-generated vibration during ambulation in normal men. *Journal of Biomechanics, 15(8), pp 599- 609.*

Chandler, R. F., M_cCanville, C. E.., Reynolds, H. M., Yang, J. W. (1975). Investigation of Inertial Properties of the Human Body. *Final Report, Apr. 1, 1972-Dec. 1974. MRL-TR-69-70., Aerospace Medical Research Laboratories, Wright-Patterson Air-Force Base, Dayton, Ohio.*

Clauser, C. E., M_cConville, J. T., Young, J. W. (1969) Weight, volume and centre of mass of segments of the human body. *AMRL-TR-69-70.*

Das, V. E., Zivotofsky, A. Z., DiScenna, A. O., Leigh, R. J. (1995). Head pertubations during walking while viewing a head-fixed target. *Aviation, Space and Environmental Medicine 66, (8), pp 728- 732.*

Dijke, H, V., G. A., Snijders, C. J., Roosch, E. R., Burgers, P. I. C. J. (1993) Analysis of biomechanical and ergonomic aspects of the cervical spine in F-16 flight situations.

Freivalds A., McCauley, D. S. (1990). Biodynamic simulations of helmet mass and center-of-gravity effects. *Journal of Safety Research, Vol. 21, pp141-148, 1990.*

Griffin, M. J. (1975) Vertical vibration of seated subjects: effects of posture, vibration level and frequency. *Aviation, Space and Environmental Medicine,. March, 1975.*

Griffin, M. J., Lewis, C. H., Pasons, K. C., Whitham, E. M. (1978). Studies of the biodynamic response to vibration. *Paper presented at the United Kingdom Group Conference on Human Response to Vibration, NAIE/NCAW Silso, Beds, September 1978.*

Griffin, M. J. (1990). Handbook of human vibration. Academic Press, 1990.

Gunther, R. (1969). Impact vibrations in human walking. *Int. Z angew. Physiol. Arbeitsphysiol 25 pp. 130-141 (1968).*

Harvey, A. K. (1990a). Development of a model of the transmission of vibration through the human body. *Presented at the United Kingdom Informal Group Meeting on Human Response to Vibration, Leeds University.*

Harvey, A. K. (1990b). Dynamics of the Head-Neck System During Exposure to Vibration. *Paper presented at the United Kingdom Informal Group Meeting on Human Response to Vibration held at Leeds University 20-21st September 1997.*

Hoek Van Dijke, G. A., Snijders, C. J., Roosch, E. R., Burgers, P. I. C. J. (1993). Analysis of biomechanical and ergonomic aspects of the cervical spine in F-16 flight situations. *Journal of Biomechanics Vol.26, No 9 pp 1017-1025.*

Huston, R. L., Sears, J. (1981). Effect of protective helmet mass on head/ neck dynamics. *Journal of Biomechanical Engineering, Vol 103, pp18-23.*

Johnson, G. R. (1986). The effect of spectral analysis to assess the performance of shock absorbing footwear. *Engineering in Medicine 15, pp 117 –122.*

Kim, E. Y., Goel, V. K. (1970). Effect of testing mode on the biomechanical response of a spinal motion segment. *Journal of Biomechanics. Vol. 23, No. 3, pp 289-291, 1990.*

Kitazaki, S. (1991) Modelling and analysis of the head-spine dynamics. *Proceedings of the United Kingdom Informal Group Meeting on Human Response to Vibration held at HSE, Buxton.*

Kitazaki, S. (1992). Application of experimental modal analysis to human whole-body vibration. *Proceedings of the United Kingdom Meeting on Human Response to Vibration, University of Southampton, 28-30 September 1992.*

Kitazaki, S. (1994) Modelling mechanical responses to human whole-body vibration. PhD Thesis, University of Southampton, Oct. 1994.

Kitazaki, S., Griffin, M. J. (1998). Resonance behaviour of the seated human body and effects of posture. *Journal of Biomechanics Vol. 31. pp 143- 149.*

Lafortune, M. A. (1991). Three-dimensional acceleration of the tibia during walking and running. *Journal of Biomechanics Vol. 24, No. 10, pp 877-886, 1991.*

Light, L. H., McLellan, G. E., Klenerman, L. (1979). Skeletal transients on heel strike in normal walking with different footwear. *Journal of Biomechanics Vol. 13, pp 477- 480, 1979.*

Liu, Y.K., Wickstrom, J, K. (1973) Estimation of the inertial property distribution of the human torso from segmented cadavaric data. Perspectives in Biomedical Engineering. *Procedings of Biological Engineering Society Symposium, University of Strathclyde, June 1972, pp 203-213.*

NASA Anthropometric Source Book. *July 1978. NASA reference publication 1024.*

Neary, C., Bate, I. J., Heller, C. F., Wiliiams., P. J. (1993). Helmet slippage during visual tracking: The effect of voluntary head movements. *Aviation, Space and Environmental Medicine, 64, (7), pp 623- 630.*

Orne, D. and Liu, Y. K. (1971). A mathematical mode of spinal response to impact. *Journal of Biomechanics, Vol 4. pp 49-71.*

Ozguven, H. N., Berme, N. (1988). An experimental and analytical study of impact forces during human jumping. *Journal of Biomechanics Vol. 21. No 12, pp 1061- 1066, 1988.*

Paddan, G. S. (1984). Translational and rotational head motion produced by vertical seat vibration. *Proceedings of the UK Informal Group Meeting on Human Response to Vibration. Herriot-Watt University, Edinburgh, 21- 22 September*

Paddan, G. S., (1986). Transmission of seat-to-head vibration in a military vehicle. *Presented at the United Kingdom Informal Group Meeting on Human Response to Vibration, 22-23 September, 1986.*

Paddan, G. S.(1990) Effect of centre of rotation on the transmission of roll and pitch vibration to the head for a seated subject. *Presented at the United Kingdom Informal Group Meeting on Human Response to Vibration, Rheumatology and Rehabilitation Research Unit, University of Leeds.*

Paddan, G. S., Griffin, M.J. (1988). The transmission of translational seat vibration to the head- I vertical seat vibration. *Journal of Biomechanics Vol. 21, No. 3. pp191- 197.*

Paddan, G. S., Griffin, M. J. (1992). The transmission of translational seat vibration to the head: the effect of measurement position at the head. *Procedings of the Institute of Mechanical Engineers Vol. 206, pp 159- 168, 1992.*

Pernica, G. (1990). Dynamic load factors for pedestrian movements and rhythmic exercises. *Canadian Acoustics 18, (2), pp 3- 18.*

Prasad, P., King, A. I. (1974). An experimentally Validated Dynamic Model of the pine. *Transactions of the American Society of Mechanical Engineers, Journal of Applied Mechanics, 41(3) pp546-550.*

Privitzer, E., Belytschko, T.. (1980). Impedance model of a three dimensional head-spine model. *Mathematical Modelling Vol. 1 pp 189-209.*

Privitzer, E., Kaleps, I. (1990). Effects of Head- Mounted Devices on Head-Neck Dynamic Response to +G Accelerations. *Agard Conference Proceedings CP-471.*

Privitzer, E., Settecerri, J. J. (1987). Dynamic Analysis of Inertial Loading Effects of Head Mounted Systems. *SAFE Journal- volume 17 no 2, pp 16-22.*

Rao, B. K. N., Jones, B. (1974). Some studies on human response to walking and riding in vehicles. *Procedings of the Human Response to Vibration Conference at Westland Helicopters Ltd, Yeovil, 17- 18 September 1974.*

Rao, B. K. N.,.Jones, B (1975). Some studies on the measurement of head and shoulder vibration during walking. *Ergonomics Vol. 18, No. 5, pp 555-566, 1975.*

Sandover J. (1975). Vibration and ambulation. Procedings of the Human Response to Vibration Conference at Westland Helicopters Ltd, Yeovil, 17- 18 September 1974.

Schultz, A. B., Galante, J. O. (1970). A mathematical model for the study of the mechanics of the human vertebral column. *Journal of Biomechanics (3), pp 405-416.*

Settecerri, J. J., McKenzie, J., Privitzer, E., Beecher, R. M. (1987). Mass properties and inertial loading effects of head encumbering devices. *Proceedings of the 25th SAFE Symposium, Las Vegas, 1987.*

Simic, D. (1970). Acceleration analysis by walking process. *Paper presented at the United Kingdom Group Meeting on the Human Response to Vibration, UOP Bostrom, Northampton, September 7-9, 1977.*

Tortora, G. J., Anagnostakos, N. P.(1990). Principles of anatomy and physiology (sixth edition). *Harper & Row Publishers, New York, ISBN 0-06-046694-4.*

Toth, R. (1966). Multiple Degree-of-Freedom Nonlinear Spinal Model. *Engineering in Medicine and Sinology, Proceedings of the 9th Annual Conference, 1966.*

Vogt, H. L., Coermann, R. R., Fust, H. D. (1968). The effects of simulated buffeting on the internal pressure of man. *Human Factors 4:pp 275-290.*

Voloshin, A., Wosk, J. (1982). An *IN VIVO* study of low back pain and shock absoprtion in the human locomotor system. *Journal of Biomechanics Vol. 15. No 1, pp 21- 27, 1982.*

Walker, L.B., Harris, E. H. and Pontius, V. R. (1973). Mass, volume, centre of mass and mass moment of inertia of the head and neck of the human body. *Final report. Tulane Univ., New Orleans, La (AD-762581).*

Walters, R. L., Morris, J., Perry, J. (1973) Translational motion of the head and truck during normal walking. *Journal of Biomechanics Vol 6, pp 167- 172.*

Wells, M. J. (1982) Helicopter and pilot vibration. *Proceedings of the United Kingdom Informal Group Meeting on Human Response to Vibration, HSE, Cricklewood, London, 16-17 September 1982.*

Wells, M. J., Griffin, M. J. (1984). Benefits of helmet-mounted display image stabilisation under whole-body vibration. *Aviation, Space and Environmental Medicine Vol 55(1) 13-18.*

Woodman, P. W. (1994). Developing a model of the neck-head-helmet system. *Procedings of the United Kingdom Informal Group Meeting on Human Response to Vibration, Institute of Naval Medicine, Gosport, 19 –21 September 1994.*

Woodman, P. W. (1995a) Helmet Movement: Ambulation and Visual Displays, Progress Report 1. *Report prepared for Defence Clothing and Textiles Agency on Agreement Number NNR/2040/08 by Human Factors Research Unit, Institute of Sound and Vibration Research, University of Southampton. H.F.R.U. 95/43 November 1995.*

Woodman, P. D. (1995b). The influence of skin tissue on the relative motion between the head and a helmet. *Proceedings of the United Kingdom Informal Group Meeting on Human Response to Vibration, Wrest Park, Silsoe, 18-20 September 1995.*

Woodman, P. D., Griffin, M. J. (1993) The effect of helmet mass on the transmission of seat vibration to the head and helmet. *Presented at a seminar entitled 'New Developments in Mechanics, Biomechanics and Design Aspects of Military Helmets' held at flight Systems Department, Defence Research Agency.*

Woodman, P. D., Griffin, M. J. (1995) Modelling the effects of helmet mass and moment of inertia on the relative motion between head and helmet. *Presented at the UK Informal Group Meeting on Human Response to Vibration, Silsoe, September 1995.*

Woodman, P. W., Griffin, M. J. (1996). Six axes of head acceleration during ambulation. *Proceedings of Internoise 96, Liverpool, 1996.*